

DISSERTATION

IMMUNE MODULATORY AND ANTIMICROBIAL PROPERTIES OF CANINE AND
HUMAN MESENCHYMAL STEM CELLS

Submitted by

Lyndah Chow

Graduate Degree Program in Cell and Molecular Biology

In partial fulfillments of the requirements

For the Degree of Doctor of Philosophy

Colorado State University

Fort Collins, Colorado

Fall 2018

Doctoral Committee:

Advisor: Steven Dow

Peter Koch
Mark Zabel
Ron Tjalkens

Copyright by Lyndah Chow 2018

All Rights Reserved

ABSTRACT

IMMUNE MODULATORY AND ANTIMICROBIAL PROPERTIES OF CANINE AND HUMAN MESENCHYMAL STEM CELLS

Mesenchymal stem cells (MSC) are multipotent stem cells derived from primary tissue. The immune modulation ability of MSCs is well known in clinical models such as autoimmune disease, graft versus host disease (GVHD), osteoarthritis (OA), rheumatoid arthritis (RA), multiple sclerosis (MS), inflammatory bowel disease (IBD), and various inflammatory pulmonary diseases. Primary mechanisms for immune suppression involve the production of soluble factors to effect innate and adaptive immune cells. However, there exist not only species differences in mechanisms but also donor variability and phenotypical differences due to culture conditions. Although there have been thousands of clinical trials globally, MSCs have yet to be put to general use due to in part, to the lack of standardization, and also extreme differences in patient responses. Due to these inconsistencies, a better model is needed to discover in depth mechanisms and biomarkers that would improve the outcome of stem therapy and provide additional quality control to determine the characteristics of an optimal stem cell donor. Therefore, we decided to delve into the mechanisms of how stem cells interact with immune cells to generate a suppressive, anti-inflammatory, or stimulatory environment.

Dogs develop many of the same inflammatory and autoimmune diseases as humans, with similarities in symptoms, pathology, and also responses to medication. Clinical studies in the canine model can be extremely informative with respect to stem cell mechanisms, safety and potential efficacy. Canine physiology is also much more similar to humans than laboratory mice,

and companion animals are exposed to many of the same environmental risk factors; thus, a valuable large animal model for stem cell therapy. The most common types of stem cells used in clinical trials are derived from adipose or bone marrow, consequently we decided to first compare the mechanisms of immune suppression between canine adipose and bone marrow derived MSCs (Ad-MSC, BM-MSC) in Chapter 2. *In vitro* assays were first used to compare phenotype, transcriptome and differentiation ability of Ad-MSC and BM-MSC, and then co-culture assays were used to investigate the differences in pathways utilized for T cell suppression. Results of these studies demonstrate that even though Ad-MSC and BM-MSC exhibit morphological differences, they are almost identical in their phenotypes and differentiation abilities. The differences become more apparent when in depth transcriptome analysis is performed, with approximately a 6% of genes whose expression is more than 2-fold significantly different. Using several pathway inhibitors, we were also able to discover several differences in T cell suppression pathways. The predominate pathways utilized by Ad-MSCs were limited to the TGF β pathway and the adenosine pathway, while BM-MSCs also utilize the cyclo-oxygenase (COX) pathway for T cell suppression. In addition, canine MSCs also cause T cell necrosis; taken together, this information is a critical component to understanding how patients respond to stem cell therapy, and hopefully will serve to facilitate additional studies for MSC based therapies in spontaneous models of canine disease.

While primary tissue derived MSCs from young and healthy donors is an attractive source of stem cells in that they are easy to culture and possess heightened immunomodulatory properties, there are still many variables such as donor disparities, expansion limitations and possible alloimmune rejection. A new cell type developed in 2006 from skin fibroblasts designated as “induced pluripotent stem cell” (iPSC), is a artificially generated cell type with properties that

resemble embryonic stem cells. These iPS cells are capable of unlimited expansion and can differentiate into cell types from all three germ lines, including MSCs. Using iPS cell derived MSCs can potentially circumvent many of the disadvantages that come from using primary cell derived MSCs. Therefore, we generated iPSC derived MSCs (iMSCs) using a one-step protocol previously published, from a canine iPS line for the purpose of use in ongoing inflammatory disease trials. Results from the studies in Chapter 3 demonstrate that iMSC share phenotypic markers with canine AD-MSC and BM-MSC and will readily differentiate into multiple lineages. Upon comparing immune modulation potency, iMSCs suppress T cell proliferation, IFN- γ production, and also dendritic cell maturation and activation, further substantiating their potential to replace primary cell derived MSCs. Most importantly, array data shows iMSCs up-regulate immune suppressive cytokine genes compared to Ad-MSC or BM-MSC and exhibit an overall more immune suppressive pattern of gene expression. Since one of the major concerns of using iPS cell derived products *in vivo* is tumor formation following systemic administration, we also performed preliminary testing in research beagles. The CT scans from three months after intravenous iMSC injection showed no abnormalities, nor the presence of tumor nodules; which further advocates the use of iMSC in clinical trials.

In addition to their use in inflammatory diseases, MSCs can also be used to ameliorate antibiotic resistant bacterial infections. Previously published clinical studies in our lab have shown that canine MSCs are effective at clearing bacteria in infected joints, soft tissue, and implant when given intravenously combined with antibiotic treatment. With the success of this large animal clinical trial, consequently we decided to pursue mechanistic studies using human bone marrow derived MSCs to investigate their ability to kill bacteria. As discussed in Chapter 4, part of how MSCs clear bacterial infection is due to indirect mechanisms through soluble factors

that act on immune cells such as macrophages and neutrophils. Although there is published data on the effectiveness of human MSCs in mouse models of infections, there is limited mechanistic data on how the MSCs are clearing bacteria *in vivo*. The results presented in Chapter 4 first show that factors produced by human BM-MSCs work through direct mechanisms to kill gram-negative and gram-positive bacteria *in vitro* and inhibit biofilm formation. Moreover, there is synergistic interaction *in vitro* between commonly used antibiotics and BM-MSCs, which could cause changes in bacterial membranes that allow previously ineffective antibiotic treatment to aid in infection clearing. Indirect mechanisms employed by MSCs include producing soluble factors that cause increases in neutrophil phagocytosis, bacterial killing and also the production of neutrophil extracellular traps (NETs); all of which contribute to the efficacy of clearing antibiotic resistant infections or biofilms.

In conclusion, these studies describe the immune modulation properties of canine adipose and bone marrow derived stem cells, as well as transcriptomic studies that provide valuable information on the differences and similarities between stem cell populations. Furthermore, we describe the first canine iPSC line generated without using viral transfection, as well as much-needed functional assays performed with MSCs derived from this canine iPS line. Finally, based on canine clinical trials we explore novel mechanisms of antibacterial activity using human BM-MSCs, which paves the way for clinical trials in patients with chronic infections who have exhausted all other therapies.

ACKNOWLEDGEMENTS

I would first like to thank my mentor Dr. Steven Dow; I will be forever indebted to you for believing in my competency to complete a doctoral program in research. You have provided support and encouragement throughout my time at CSU, and you are a constant fountain of knowledge and wisdom for both academic and personal hardships. I thank you for being always patient and willing to listen and accept my suggestions. No matter where the future taking me, I will always be grateful for the invaluable opportunity and of the profound impact your mentorship has had on my career and personal development.

I would also like to thank my committee members, Drs Mark Zabel, Peter Koch, and Ron Tjalkens for being gracious and available to answer questions, and for their help in aiding my degree completion. Especially to Dr. Peter Koch for generating the canine iPS line that is essential to this body of work. I also owe many thanks to Dr. Valerie Johnson for providing much needed clinical and stem cell related education, and for taking time in her busy schedule to assist with experiments. I am also grateful to Dr. Amanda Guth for her support and suggestions when I first decided to embark on this journey, and lastly Dr. Dan Regan, who is a walking Wikipedia of immunological knowledge and is always willing help with the many difficulties I have encountered in completing all the studies presented in this dissertation.

I would also like to thank the other members and support staff in the Dow lab, without your help and administrative support I would never have completed all of the repetitious experiments presented here. I would also like to acknowledge former members of the Dow lab including my best and longtime friend Dr. Alita Caldwell, thank you for giving me the courage

to take on the unexpected; and Jonathan Coy, for providing valuable algorithms that saved me a great deal of time.

Finally, I would not have made it without the unwavering support and love of my family. To my soon to be husband Jeff Egan; thank you for holding my hand through hard times, and always being my strong foundation. Thank you Papa for believing that I could always achieve greater things, and for providing the financial support I needed to concentrate on my research. I would never be where I am today without my sweet Mom, who is constantly the family mediator and always has words of encouragement, and my brother Enoch who is my sounding board and inspiration, and David and Danny who have each succeeded beyond expectations and continue to motivate me to achieve my maximum potential.

TABLE OF CONTENTS

ABSTRACT	ii
ACKNOWLEDGMENTS	vi
Chapter 1: Review of the Literature	1
Introduction to induced pluripotent stem cells	1
Introduction to mesenchymal stem cells	2
Immune modulation properties of MSCs	3
Induced pluripotent stem cells derived mesenchymal stem cells	6
Properties of iPSC derived MSC	7
Human iPSC derived MSC in animal disease models.....	9
Bactericidal activity of MSCs.....	11
References	14
Chapter 2: Mechanisms of Immune Suppression Utilized by Canine Adipose and Bone Marrow Derived Mesenchymal Stem Cells	25
Summary.....	25
Background.....	26
Materials and Methods	29
Results	36
Discussion.....	53

References	58
Chapter 3: Safety and Immune Regulatory Properties of Canine Induced Pluripotent Stem Cell-derived mesenchymal stem cells	65
Summary.....	65
Background.....	66
Materials and Methods	68
Results	80
Discussion.....	98
References	102
Chapter 4: Direct and Indirect Antimicrobial Activity of Human Mesenchymal Stem Cells....	106
Summary.....	106
Background.....	107
Materials and Methods	109
Results	116
Discussion.....	129
References	132
Chapter 5: Final Conclusions and Future Directions.....	135
References	144

CHAPTER 1

Review of the Literature

Introduction to Induced Pluripotent Stem Cells

Induced pluripotent stem cells (iPSCs) are stem cells derived from adult somatic cells by reprogramming through transient expression of specific transcription factors¹. Like embryonic stem cells, iPSC are capable of unlimited expansion, and can potentially differentiate into any cell type in the body. Using artificially generated pluripotent stem cells eliminates the need for harvesting embryos, bypassing the ethical arguments and regulations that surround the controversy of human embryonic stem cell research². The reprogramming technology for generating iPSC from mouse and human somatic cells was first developed in the mid-2000's³ and rapid progress has been made to use iPSCs and their differentiated progeny to study diseases, test drugs, and to utilize for stem cell therapy in experimental animal models^{1,4-9}.

At present, iPSC are commonly generated from adult skin fibroblasts using 4 reprogramming factors (Oct3/4, SOX2, Klf4, and c-Myc); together these 4 factors are commonly referred to as OSKM^{1,10-13}. Reprogramming of adult cells is initiated by the binding of these OSKM factors to the regulatory elements of many genes, thereby changing the cell state¹⁴. Many reprogramming methods have since been published after the original discovery¹⁵. Delivery of the OSKM factors is no longer limited to retroviral transduction; methods such as episomal plasmids¹⁶, minicircle DNA vectors¹⁷, non integrating RNA viruses¹⁸, mRNA¹⁹ and micro RNAs²⁰ have produced iPSC cells with efficiencies ranging from 0.002% to 0.2%¹⁵. Choosing a reprogramming method depends on the purpose of derivation and also the starting somatic cell type.

iPSCs develop as flattened colonies that contain multiple nuclei, and express pluripotency markers such as Oct3/4, NANOG, SSEA1, and TRA1-60/TRA1-81^{3,13}. The initial selection of an iPSC colony is by morphology or live fluorescent staining²¹. Cells that have been successfully reprogramed are then chosen for single clone expansion in defined media commonly containing basic fibroblast growth factor (bFGF) for human iPSC or leukemia inhibitory factor (LIF) for mouse iPSC²². The use of a feeder layer consisting of inactivated fibroblast, or a substrate such as matrigel or geltrex²³ is also necessary to propagate the reprogrammed cells²². In addition, iPSC are characterized by the ability to undergo induced formation of embryoid bodies, cell structures that contain precursors to endoderm, mesoderm, and ectoderm^{3,6,24,25}. The final confirmatory assays for iPSC generation involve *in vivo* evaluation for teratoma formation following inoculation of cells in highly immune deficient mice^{3,26,27}. The presence of teratomas is confirmed by histological evaluation and verification of pluripotent differentiation for the 3 germ lines endoderm, mesoderm and ectoderm^{27,28}.

Introduction to Mesenchymal Stem Cells

Stem cells from different sources possess variable potency and differentiation abilities. Unlike pluripotent iPSCs that can differentiate into all 3 germ line lineages, mesenchymal stem cells (MSC) are multipotent cells that can differentiate into limited types of cells²⁹. The minimal criteria for defining a MSC population is the ability to adhere to plastic, expression of surface markers CD73, CD90, and CD105, lack of expression of CD34, CD45 and human leucocyte antigen-DR (HLA-DR), and also be able to differentiate into adipocytes, chondrocytes and osteocytes³⁰. Human MSCs have been successfully derived from multiple tissue types such as the most commonly used adult adipose or bone marrow²⁹; and also peripheral blood³¹, as well

as neonatal birth associated tissues such as placenta, umbilical cord and cord blood³². Other sites such as dental pulp³³ have also been investigated as a potential source of MSCs.

Immune Modulation Properties of Mesenchymal Stem Cells

Cellular therapy with MSC offers a promising new option for non-pharmacologic management of inflammatory diseases. There are currently over 500 clinical trials employing MSC worldwide, and positive results from early studies have been reported using MSC for treatment of systemic lupus erythematosus, graft-versus-host disease, rheumatoid arthritis, and inflammatory bowel disease in humans³⁴⁻³⁸. In these studies, MSCs have been shown to lower transplant related mortality in graft versus host disease (GVHD)³⁹, lower inflammation in Crohn's disease⁴⁰, and improve cartilage quality in osteoarthritic patients⁴¹. MSCs have also been used in large animal clinical trials, in naturally occurring immune mediated diseases such as canine osteoarthritis^{42, 43}, in which pain is lessened and movement range are improved in the Ad-MSC treated group. Also canine inflammatory bowel diseases⁴³, in which Ad-MSC treatment significantly improved clinical scoring and remission occurred in 80% of the dogs treated⁴⁴. Promising results were also seen in an equine degenerative joint disease study using peripheral blood derived MSCs; MSC treatment significantly improved clinical lameness for up to 12 months, and the treated joints showed sustained functionality^{45, 46}.

Most clinical studies use MSCs derived from adipose or bone marrow, these MSCs are known to interact with the innate and adaptive immune system to suppress overall inflammatory responses⁴⁷⁻⁵⁴. MSCs are able influence the polarization of naïve macrophages to an anti-inflammatory phenotype by the production of Prostaglandin E2 (PGE₂). Activated macrophages exposed to MSC or MSC conditioned media are prone to increasing IL-10 production, become

more phagocytic, and during an infection, MSC conditioned macrophages exhibit metabolic shifts that increase migration and bacterial killing ability ⁵⁵ through a NADPH oxidase dependent mechanism ⁵⁶ ; they also have decreased TNF α and IL-6 production ⁵⁵. MSCs also inhibit dendritic cell (DC) and natural killer cell activation and proliferation, as well as prevent neutrophil apoptosis ⁵⁷. When peripheral blood DCs are exposed to MSC or MSC conditioned media, they exhibit an anti-inflammatory phenotype ⁵⁸, MSCs also inhibit DC differentiation, shown by a decrease in activation markers such as MHCII, CD40, CD80 and CD86 ⁵⁹. Studies have also shown that MSCs inhibit DC generation from both bone marrow and CD34+ cells ⁶⁰, and also impair the ability of DCs to stimulate T cells. The mechanisms of DC inhibition by MSCs is related to production of soluble factors such as Prostaglandin E2 (PGE₂) ⁶¹ or IL-6 ⁶², and also by secretion of microRNA to block the NF- κ B pathway ⁶³; there are also contact dependent mechanisms that prevent DCs from forming active immune synapses with T cells ⁶⁴.

Neutrophils are also important phagocytic cell of the innate immune system; MSCs have been shown to protect neutrophils from apoptosis ⁶⁵ and reactive oxygen species (ROS) production. Soluble factors have been reported to play a role in MSC effect on neutrophils such as IL-6 ⁶⁶; IL-8 and IFN- β have been shown specifically to regulate neutrophil activation and migration ⁶⁷. Ad-MSCs have also been shown to decrease PMA (phorbol 12-myristate 13-acetate) induced neutrophil extracellular trap (NET) formation or NETosis, by dampening the oxidative burst response ⁶⁸ and engulfing apoptotic neutrophils. However, MSCs have not been reported to have any direct effect on neutrophil phagocytosis, which is an important consideration for efficient clearing of infections ⁶⁹. In some cases, the effector molecules produced by neutrophils can cause collateral damage to inflamed tissue. Murine MSCs have been shown to inhibit neutrophil infiltration by the production of TNF- α -stimulated gene 6 protein

(TSG-6) in an ocular inflammation model ⁷⁰, which is in line with the anti-inflammatory effects of MSC on other immune cell types.

Also important for wound healing, bacterial clearance, and tumoricidal activity are natural killer (NK) cells; MSC influence on NK cells depend on the culture time and activation signals received by the NK cells ⁵⁷. Limited data is available, but the consensus is that MSCs inhibit NK cell activation, proliferation and pro-inflammatory cytokine production ⁷¹. Soluble factors that mediate this response include indoleamine-2,3-dioxygenase (IDO), transforming growth factor- β (TGF- β), PGE₂ and also cell to cell contact ^{72, 73}.

MSCs also are able to suppress the adaptive immune system by producing soluble factors to inhibit B cell activity ⁷⁴, and suppress T cell proliferation ⁵⁷. Inhibition of B cell activity happens through the arrest of the cell cycle checkpoint from G₀ to G₁ ⁷⁵; contact with MSCs causes a depletion of antibody production by B cells, decrease in chemokine receptors CXCR4, CXCR5, CCR7, and chemotaxis to CXCL12 ⁷⁴. Interestingly, the cell cycle arrest does not effect cellular viability ⁵⁴. The mechanisms and soluble factors of which MSCs suppress B cells remain under investigation, however priming MSCs with toll-like receptor (TLR) ligands such as poly I:C seem to play an important role in B cell modulation ⁷⁶.

The effect of MSCs on T cells makes them a prime candidate to treat immune mediated diseases. MSCs inhibit both CD4⁺ and CD8⁺ T cell proliferation, and IFN γ secretion by T_H1 cells ⁵⁸. IL-1 β conditioned MSCs are able to enhance T_H17 responses ⁷⁷, but also increase T regulatory cells (Treg) population in culture ^{78, 79}, and maintain Treg suppressive capacity and FOXP3 expression. Known mechanisms that influence these various populations of T cells include production of IDO (indoleamine 2,3-dioxygenase), and secretion of growth factors such as hepatocyte growth factor (HGF), TGF- β , PGE₂ ^{57, 80, 81}, as well as programmed death ligand PD-

L1 and PD-L2⁸². MSCs also secrete galectin 9, which binds to TIM3 receptor in activated TH1 and Th17 cells, causing apoptotic cell death⁸³. This is similar to the cascade caused by PDL1 binding, which inhibits the phosphorylation of NF- κ B causing apoptosis of T cell subsets⁸⁴.

Induced Pluripotent Stem Cells Derived Mesenchymal Stem Cells

Although the use of MSC for immune modulation as a cellular therapy is proven to be safe and shows promise in clinical trials⁸⁵, results from clinical trials are varied⁸⁶. The use of MSC for cellular therapy poses several challenges. For one, autologous MSC are difficult to generate from older patients, and their functionality is often impaired compared to MSC generated from young individuals^{87,88}. Use of allogeneic MSC derived from young donors offers a means of overcoming the limitations of autologous MSC, but introduces new problems, including donor-to-donor variability, risk of iatrogenically introduced infectious agents, and the potential for alloimmune rejection^{89,90}. One means of overcoming the limitations inherent to the use of primary cultured MSC for clinical studies is to use MSC derived from iPSC^{9,91}. iPSC cells can be generated from easily accessible tissues such as blood, skin, and even hair follicle cells⁹². There are many GMP verified iPSC cell lines available for clinical use⁹³, which have been extensively tested for their purity, safety and viability. Using iPSC cells instead of primary tissue derived cells ensures that patients will have an unlimited supply of young, health donor cells, and also creates many opportunities for personalized drug testing, especially when rare genetic mutations are concerned⁹⁴.

As noted previously, iPSC are pluripotent and can be differentiated into all somatic cell derivatives. Many studies have demonstrated that MSCs can also be differentiated from iPSCs; current published methods that have been used to differentiate MSCs from iPSCs are done by

manipulation of the aspects of growth environment such as the substrate or media components. For example, MSCs can be generated by serial passaging iPS cells onto plastic culture flasks for 5 to 10 passages⁹⁵⁻⁹⁷ after removing growth factors specific to iPSC maintenance; or by first generating embryoid bodies containing all 3 germ lines, then selecting for MSC like cells⁹⁸. Lastly, iPS derived MSCs can also be generated by changing the substrate^{99, 100} or by addition of TGF- β pathway inhibitor to initiate rapid Epithelial-to-mesenchymal transition¹⁰¹.

Even though there are many advantages to using iPS derived cells as a cellular therapy, there are concerns such as the potential risk of tumor formation, or single nucleotide and copy number variation¹⁰². There are currently a limited number of clinical trials using iPS derived cells¹⁰³, and although the only published trial showed that iPSC derived retinal pigment epithelial cells are safe to transplant in age related macular degeneration¹⁰⁴ more testing is needed to ensure the safety and efficacy of iPS derived cells.

Properties of Induced Pluripotent Stem Cells Derived Mesenchymal Stem Cells

Most studies of iMSC reported to date have found that the phenotype of iMSC relatively closely resembles that of bone marrow or adipose derived MSC^{91, 97, 99, 105}. Specifically, iMSC were found to express CD73, CD90, CD105, CD146, and CD166 and to lack expression of the hematopoietic markers CD14, CD34, and CD45^{95, 98, 100, 101, 106-108}, a phenotype shared with Ad-MSC and BM-MSC. These studies also found that iMSCs are capable of tri-lineage differentiation^{96, 97, 99, 100, 109}, and using synthetic substrates may increase the efficiency of derivation and differentiation^{99, 100, 110}. Biological characteristics of iMSCs include the evasion of senescence, and phenotypic stability up to much higher passages than primary tissue derived

MSCs ¹¹¹, higher expression of pluripotency transcription factors ¹⁰⁹, and also the maintenance of donor cell epigenetic profiles ¹¹².

iMSCs are also thought to possess immune modulation properties that are beneficial to various immune mediated diseases. *In vitro* studies using human iMSCs have shown that iMSCs suppress the proliferation of mixed peripheral blood mononuclear cells (PBMC) stimulated with mitogens ¹⁰⁷, the population of effector T cells (CD3-CD4+) is also decreased, as well as Th1, Th2 and Th17 populations. iMSCs also suppress cytokines produced by activated T cells such as IL-2, IFN- γ , TNF- α , and TGF- β ¹¹³. Human iMSCs also have facilitate the induction of increased amounts and differentiation of FoxP3+ CD4+ Treg cells ¹¹³, which has important implications for autoimmune diseases, infections and also cancer ¹¹⁴. The modulation of these various T cell populations is thought to be through factors secreted by iMSCs such as IDO, but other mechanisms have not been thoroughly explored as of yet. iMSCs, like primary tissue derived MSCs also inhibit proliferation of NK cells *in vitro*. iMSCs do this by inhibiting NK cell ERK1/2 signaling and also the expression of activation markers such as granzyme B and IFN- γ secretion ¹¹¹. Although soluble factors such as IDO, PGE₂, and HLA-G are involved in the suppression, inhibition of these factors does not completely reverse the suppression of NK cells, suggesting the involvement in multiple pathways not yet explored ¹¹¹. DCs are important antigen presenting cells that interact with T and B cells to initiate adaptive immune responses. When iMSCs are cultured with monocytes *in vitro*, they inhibit the differentiation into DCs, but do not effect the maturation of DCs when cultured with immature DCs ¹¹⁵. Even though iMSCs do not inhibit phenotypic maturation of DCD, they will effect DC function. When contacting iMSCs, mature DCs showed increased phagocytic ability, but also lost lymphocyte-stimulating ability. This effect is thought to be dependent on cell to cell contact between iMSC-DC and also the

production of IL-10¹¹⁵. Taken together, the *in vitro* data suggests that iMSCs have the potential to be used in immune mediated diseases and may have similar effects as primary tissue derived MSCs.

Human Induced Pluripotent Stem Cells Derived Mesenchymal Stem Cells in animal disease models

Since iPS cells have yet to be tested in human disease models (other than previously mentioned AMD trial¹⁰⁴), testing on iMSC is limited to mouse and large animal models¹¹⁶. The osteogenic ability of iMSCs has been used in various cases to repair experimental bone defects in mice and rats. Using synthetic scaffold implants, human iMSCs have been shown to form new bone when transplanted into mice with calvarial defects⁹⁹, mineralize in subcutaneous injuries^{95, 96}, and also regenerate nonunion radial fractures¹¹⁷. Also important for healing of bone injuries is the vascularization that delivers oxygen and nutrition supply to healing tissue; iMSCs have been shown to increase angiogenesis of endothelial cells *in vitro*¹¹⁸, and also form micro capillary structures and new bone deposits in rat cranial defects¹¹⁹. Vascularization is also important to ameliorate tissue ischemia; human iMSCs also have been shown to decrease necrosis, prevent limb loss and muscle degeneration in a mouse model of critical limb ischemia¹⁰⁹.

Primary cell derived MSCs have been explored to treat chronic kidney disease (CKD) and acute kidney injuries on patients awaiting stem cell transplant¹²⁰. To explore more accessible cells, human iMSCs were used in a mouse CKD model¹⁰⁵. The results showed that iMSCs prevent apoptosis of tubular cells, and in the long term, iMSCs had an anti-fibrotic effect which was attributed to the inhibition of hedgehog signaling¹⁰⁵. Recent studies have also yielded

important information on the advantages of iMSCs to treat chronic obstructive pulmonary disease (COPD), emphysema and other cardiac diseases. Using a rat model for cigarette smoke induced cardiac damage, Liang et al.¹²¹ showed that i.v injected human iMSCs increase ventricular ejection fraction, reversed cardiac lipid metabolism abnormalities, and decreased oxidative stress markers. iMSCs also affected the cytokine balance, reducing pro-inflammatory TNF- α , and increasing anti-inflammatory markers IL-10 and adiponectin. Another study also found that iMSC injections decreased smoke induced infiltration of macrophages and neutrophils in the lung, and decreased apoptosis of lung epithelium¹²². Proposed mechanism of MSC healing in these airway damage models include the inhibition of the NF- κ B pathway in cardiomyocytes¹²¹ and also the secretion of stem cell factor (SCF)¹²².

Due to the enhanced osteogenic and anti inflammatory ability of iMSC, their efficacy has been explored in rat models of periodontitis¹²³. Similar to the bone injury models, iMSCs were found to limit alveolar bone loss¹²⁴, and increase mineralization¹²⁵. iMSCs also reduced the inflammatory immune response against the biofilms formed on the surface of teeth in acute periodontitis models¹²³ by decreasing CXCL1, and also serum levels of pro-inflammatory cytokines IL-1 β and TNF- α . In addition to bone, kidney and lung injury; iMSCs have also been explored for cellular therapy in spinal cord injuries (SCI)¹²⁶. Current patients suffering debilitating SCI are limited to surgical intervention to decompress spinal cord and remove damaged tissue, or the only FDA approved corticosteroid methyl-prednisolone (MP)¹²⁷. Stem cells are an attractive alternative or addition to these treatments because of their regenerative and anti-inflammatory properties that would serve to increase axonal growth, increase myelination and decrease local pro-inflammatory cytokine secretion that further exacerbates injury. Although there are no current animal trials using iMSCs, in vitro data shows that iMSC secrete various

factors that are beneficial to healing such as brain derived neurotrophic factor (BDNF), IL-6 leukemia inhibitory factor (LIF), osteopontin, and osteonectin¹²⁶. iMSCs also increase the extension of dorsal root ganglia (DRG) neurites in co-culture systems¹²⁶.

Lastly, the utility of iMSCs have been briefly explored in models of corneal injury⁵¹. The corneal injury model offers a unique opportunity to study immune privileged sites, Yum et al. found that iMSCs have the same ability as BM-MSCs to reduce swelling, inflammatory cell infiltrate and inflammatory cytokines TNF- α , IL-1 β and IL-6. The mechanism is in part based on the production of protein TSG-6 by iMSCs, which is a protein that has protective and anti-inflammatory effects and is stimulated by signaling molecules such as TNF- α and IL-1.

Bactericidal Activity of Mesenchymal Stem Cells

In addition to their immune modulatory properties, primary cell derived MSCs also have direct and indirect antimicrobial properties. One of the proposed mechanisms for direct bacterial killing ability is thought to be the production of antimicrobial peptides (AMP). Human BM-MSCs are known to produce LL-37¹²⁸ (a cathelicidin family AMP), as well as Hepsidin¹²⁹, β -defensin 2 (hBD2), and lipocalin 2 (Lcn-2)¹³⁰. LL-37 produced by MSCs was found to be a major player in a mouse *E. coli* pneumonia model; although the authors found that LL-37 was only produced after bacterial stimulation, neutralization of LL-37 in conditioned media produced by BM-MSCs ameliorated the ability of MSCs to kill *P. aeruginosa*, *E. coli* and *S. aureus* *in vitro*. Further studies in the *ex vivo* human lung *E. coli* pneumonia model showed that in addition to AMPs, keratinocyte growth factor secreted by the instilled MSCs increased bacterial killing by the alveolar macrophages, and also prevented translocation of the bacteria into the blood stream

¹³¹.

Human BM-MSCs are also able to eliminate *P. aeruginosa* induced peritoneal sepsis in mice through indirect mechanisms. By influencing phagocytic activity of blood monocytes, the MSC treated mice showed increased survival and significantly reducing the bacterial load in peripheral blood stream and spleen ¹³². Further studies in mouse sepsis models as well as in vitro work with macrophages isolated from patients found that PGE₂ produced by the MSCs is responsible for an increase in phagocyte NADPH oxidase (NOX2) activity ⁵⁶.

BM-MSCs also produce factors that enhance antibiotic sensitivity, such as the production of aforementioned LL-37 which weakens the bacterial membrane enough for the antibiotics to take effect ¹³³, or by slowing bacterial growth resulting in a decreased bacterial burden which allows for antibiotics to become more effective. Human BM-MSC have also been tested in a cystic fibrosis transmembrane regulator (CFTR) mutant mouse model of *P. aeruginosa* lung infection, mimicking infection susceptibility in human cystic fibrosis patients ¹³⁴. In this model, the authors report that BM-MSCs utilize direct mechanisms such as the secretion of LL-37, and also indirect mechanisms that influence macrophage recruitment and decrease inflammatory cytokine production in airway epithelial cells; resulting in resolution of infection and decreased clinical scoring.

To date there are only a few studies investigating the ability of MSCs to clear infections in a large animal model. The first study published in 2014 was aimed at resolving bacterial infection after acute lung injury (ALI) in sheep ¹³⁵. After being exposed to smoke induced lung injury, their lungs were instilled with *P. aeruginosa*, and physiological measurements analogous to what is seen in human ALI patients were taken such as blood gas, airway pressures, fluid flux, and vascular resistance. Although the results successfully demonstrated the safety of injecting BM-MSC in a large animal ALI model, there were no significant improvements in bacterial

clearance or neutrophil invasion in the lungs. However, improved oxygenation and decreased pulmonary edema was observed suggesting the potential for MSC therapy that perhaps may take greater effect after the initial 24 hour time point that this study was designed on. Another more recent pre clinical study published in 2017 investigated the effect of toll-like receptor agonist 3 (TLR-3) activated canine adipose derived MSCs on spontaneously-occurring, multi-drug resistant (MDR) infections in pet dogs ¹³⁶. This study combined antibiotic therapy with an intravenous infusion of activated Ad-MSC every 2 weeks for a total of 3 treatments. The infections initially persisted in various sites such as joint, soft tissue and also implants. The results were very promising in that the bacteria present in the wounds including *P. aeruginosa*, *E. coli*, methicillin resistant *S. pseudointermedius*, *Corynebacterium* and *Klebsiella* sp. was completely eliminated (or significantly decreased in one case), and clinical response was unanimously improved. Although the study was not placebo controlled, the results speak strongly to the possible advantages of implant infections commonly seen in a clinical setting, and also the possible clearance of biofilms which frequently evade antibiotic treatments. In conclusion, current published mechanisms of bactericidal activity include direct effects such as the production of antimicrobial peptide LL37, and indirect effects including the influence on macrophages and neutrophils. More controlled clinical trials are needed to fully explain all the soluble cytokines produced by MSCs that kill bacteria, and also how the MSCs affect the gene expression profile of immune cells.

REFERENCES

1. Takahashi K, Yamanaka S. A decade of transcription factor-mediated reprogramming to pluripotency. *Nat Rev Mol Cell Biol.* 2016;17:183-193.
2. Zacharias DG, Nelson TJ, Mueller PS, et al. The science and ethics of induced pluripotency: What will become of embryonic stem cells? *Mayo Clinic Proceedings.* 2011;86:634-640.
3. Takahashi K, Yamanaka S. Induction of pluripotent stem cells from mouse embryonic and adult fibroblast cultures by defined factors. *Cell.* 2006;126:663-676.
4. Yamanaka S. Induced pluripotent stem cells: Past, present, and future. *Cell stem cell.* 2012;10:678-684.
5. Avior Y, Sagi I, Benvenisty N. Pluripotent stem cells in disease modelling and drug discovery. *Nat Rev Mol Cell Biol.* 2016;17:170-182.
6. Ohnuki M, Takahashi K, Fau - Yamanaka S, Yamanaka S. Generation and characterization of human induced pluripotent stem cells. *Curr Protoc Stem Cell, Biol.* 2009
7. Ebert AD, Liang P, Fau - Wu JC, Wu JC. Induced pluripotent stem cells as a disease modeling and drug screening platform. *J. Cardiovasc Pharmacol.* 2012
8. Harding J, Mirochnitchenko O. Preclinical studies for induced pluripotent stem cell-based therapeutics. *The Journal of biological chemistry.* 2014;289:4585-4593.
9. Kimbrel EA, Lanza R. Current status of pluripotent stem cells: Moving the first therapies to the clinic. *Nat Rev Drug Discov.* 2015;14:681-692.
10. Schlaeger TM, Daheron L, Brickler TR, et al. A comparison of non-integrating reprogramming methods. *Nat Biotech.* 2015;33:58-63.
11. Hu K. All roads lead to induced pluripotent stem cells: The technologies of ipsc generation. *Stem cells and development.* 2014;23:1285-1300.
12. Shi Y, Inoue H, Wu JC, et al. Induced pluripotent stem cell technology: A decade of progress. *Nat Rev Drug, Discov.* 2016.
13. Okita K, Yamanaka S. Induction of pluripotency by defined factors. *Exp Cell, Res.* 2010.
14. Bilic J, Belmonte Juan Carlos I. Concise review: Induced pluripotent stem cells versus embryonic stem cells: Close enough or yet too far apart? *Stem cells.* 2011;30:33-41.
15. Malik N, Rao MS. A review of the methods for human ipsc derivation. *Methods in molecular biology (Clifton, N.J.).* 2013;997:23-33.

16. Okita K, Matsumura Y Fau - Sato Y, Sato Y Fau - Okada A, et al. A more efficient method to generate integration-free human ips cells. *Nat, Methods*. 2011.
17. Narsinh KH, Jia F, Robbins RC, et al. Generation of adult human induced pluripotent stem cells using non-viral minicircle DNA vectors. *Nature protocols*. 2011;6:78-88.
18. Ban H, Nishishita N Fau - Fusaki N, Fusaki N Fau - Tabata T, et al. Efficient generation of transgene-free human induced pluripotent stem cells (ipscs) by temperature-sensitive sendai virus vectors. *Proc Natl Acad Sci, U. S. A.* 2011.
19. Warren L, Manos Pd Fau - Ahfeldt T, Ahfeldt T Fau - Loh Y-H, et al. Highly efficient reprogramming to pluripotency and directed differentiation of human cells with synthetic modified mrna. *Cell Stem, Cell*. 2010.
20. Miyoshi N, Ishii H Fau - Nagano H, Nagano H Fau - Haraguchi N, et al. Reprogramming of mouse and human cells to pluripotency using mature micornas. *Cell Stem, Cell*. 2011.
21. Abujarour R, Valamehr B, Robinson M, et al. Optimized surface markers for the prospective isolation of high-quality hipscs using flow cytometry selection. *Scientific reports*. 2013;3:1179.
22. Chen KG, Mallon BS, McKay RDG, et al. Human pluripotent stem cell culture: Considerations for maintenance, expansion, and therapeutics. *Cell stem cell*. 2014;14:13-26.
23. Wagner K, Welch D. Feeder-free adaptation, culture and passaging of human ips cells using complete knockout serum replacement feeder-free medium. *Journal of Visualized Experiments : JoVE*. 2010:2236.
24. Martí M, Mulero L, Pardo C, et al. Characterization of pluripotent stem cells. *Nat. Protocols*. 2013;8:223-253.
25. Okita K, Ichisaka T Fau - Yamanaka S, Yamanaka S. Generation of germline-competent induced pluripotent stem cells. *Nature*. 2007.
26. Hentze H, Soong PL, Wang ST, et al. Teratoma formation by human embryonic stem cells: Evaluation of essential parameters for future safety studies. *Stem Cell Research*. 2009;2:198-210.
27. Wesselschmidt RL. The teratoma assay: An in vivo assessment of pluripotency. *Methods Mol, Biol*. 2011.
28. Weinberger L, Ayyash M, Novershtern N, et al. Dynamic stem cell states: Naive to primed pluripotency in rodents and humans. *Nat Rev Mol Cell Biol*. 2016;17:155-169.
29. Hass R, Kasper C, Böhm S, et al. Different populations and sources of human mesenchymal stem cells (msc): A comparison of adult and neonatal tissue-derived msc. *Cell Communication and Signaling : CCS*. 2011;9:12-12.

30. Dominici M, Blanc K, Mueller I, et al. Minimal criteria for defining multipotent mesenchymal stromal cells. The international society for cellular therapy position statement. *Cytherapy*. 2006;8.
31. Li S, Huang K-J, Wu J-C, et al. Peripheral blood-derived mesenchymal stem cells: Candidate cells responsible for healing critical-sized calvarial bone defects. *Stem Cells Translational Medicine*. 2015;4:359-368.
32. Ullah I, Subbarao Raghavendra B, Rho Gyu J. Human mesenchymal stem cells - current trends and future prospective. *Bioscience Reports*. 2015;35:e00191.
33. Stanko P, Kaiserova K Fau - Altanerova V, Altanerova V Fau - Altaner C, et al. Comparison of human mesenchymal stem cells derived from dental pulp, bone marrow, adipose tissue, and umbilical cord tissue by gene expression. 2014.
34. Gu F, Wang D, Zhang H, et al. Allogeneic mesenchymal stem cell transplantation for lupus nephritis patients refractory to conventional therapy. *Clin Rheumatol*. 2014;33:1611-1619.
35. Sun L, Wang D, Liang J, et al. Umbilical cord mesenchymal stem cell transplantation in severe and refractory systemic lupus erythematosus. *Arthritis Rheum*. 2010;62:2467-2475.
36. Wang D, Zhang H, Liang J, et al. Allogeneic mesenchymal stem cell transplantation in severe and refractory systemic lupus erythematosus: 4 years of experience. *Cell Transplant*. 2013;22:2267-2277.
37. Tyndall A. Mesenchymal stromal cells and rheumatic disorders. *Immunol Lett*. 2015;168:201-207.
38. Tyndall A, van Laar JM. Stem cells in the treatment of inflammatory arthritis. *Best Pract Res Clin Rheumatol*. 2010;24:565-574.
39. Prasad VK, Lucas KG, Kleiner GI, et al. Efficacy and safety of ex vivo cultured adult human mesenchymal stem cells (prochymal) in pediatric patients with severe refractory acute graft-versus-host disease in a compassionate use study. *Biol Blood Marrow Transplant*. 2011;17.
40. Forbes GM, Sturm MJ, Leong RW, et al. A phase 2 study of allogeneic mesenchymal stromal cells for luminal crohn's disease refractory to biologic therapy. *Clin Gastroenterol Hepatol*. 2014;12:64-71.
41. Park YB, Ha CW, Lee CH, et al. Cartilage regeneration in osteoarthritic patients by a composite of allogeneic umbilical cord blood-derived mesenchymal stem cells and hyaluronate hydrogel: Results from a clinical trial for safety and proof-of-concept with 7 years of extended follow-up. 2016.

42. Cuervo B, Rubio M, Sopena J, et al. Hip osteoarthritis in dogs: A randomized study using mesenchymal stem cells from adipose tissue and plasma rich in growth factors. *Int J Mol Sci.* 2014;15:13437-13460.
43. Hoffman AM, Dow SW. Concise review: Stem cell trials using companion animal disease models. *Stem, Cells.* 2016.
44. Perez-Merino EM, Uson-Casaus JM, Zaragoza-Bayle C, et al. Safety and efficacy of allogeneic adipose tissue-derived mesenchymal stem cells for treatment of dogs with inflammatory bowel disease: Clinical and laboratory outcomes. *Vet, J.* 2015.
45. De Schauwer C, Van de Walle Gr Fau - Van Soom A, Van Soom A Fau - Meyer E, et al. Mesenchymal stem cell therapy in horses: Useful beyond orthopedic injuries? *Vet, Q.* 2013.
46. Broeckx S, Zimmerman M, Crocetti S, et al. Regenerative therapies for equine degenerative joint disease: A preliminary study. *PloS one.* 2014;9:e85917.
47. Semon Ja Fau - Maness C, Maness C Fau - Zhang X, Zhang X Fau - Sharkey SA, et al. Comparison of human adult stem cells from adipose tissue and bone marrow in the treatment of experimental autoimmune encephalomyelitis. *Stem Cell Res, Ther.* 2014.
48. Li X, Bai J, Ji X, et al. Comprehensive characterization of four different populations of human mesenchymal stem cells as regards their immune properties, proliferation and differentiation. *International Journal of Molecular Medicine.* 2014;34:695-704.
49. Carrade DD, Borjesson DL. Immunomodulation by mesenchymal stem cells in veterinary species. *Comparative Medicine.* 2013;63:207-217.
50. Klinker MW, Wei C-H. Mesenchymal stem cells in the treatment of inflammatory and autoimmune diseases in experimental animal models. *World Journal of Stem Cells.* 2015;7:556-567.
51. Yun YI, Park SY, Lee HJ, et al. Comparison of the anti-inflammatory effects of induced pluripotent stem cell-derived and bone marrow-derived mesenchymal stromal cells in a murine model of corneal injury. *Cytherapy.* 2017;19:28-35.
52. Zhao Q, Ren H, Han Z. Mesenchymal stem cells: Immunomodulatory capability and clinical potential in immune diseases. *Journal of Cellular Immunotherapy.* 2016;2:3-20.
53. Carrade DD, Lame Mw Fau - Kent MS, Kent Ms Fau - Clark KC, et al. Comparative analysis of the immunomodulatory properties of equine adult-derived mesenchymal stem cells. *Cell, Med.* 2012.
54. Gao F, Chiu SM, Motan DA, et al. Mesenchymal stem cells and immunomodulation: Current status and future prospects. *Cell Death, Dis.* 2016.

55. Vasandan AB, Jahnavi S, Shashank C, et al. Human mesenchymal stem cells program macrophage plasticity by altering their metabolic status via a pge2-dependent mechanism. 2016.
56. Rabani R, Volchuk A, Jerkic M, et al. Mesenchymal stem cells enhance nox2-dependent reactive oxygen species production and bacterial killing in macrophages during sepsis. *European Respiratory Journal*. 2018;51.
57. Glenn JD, Whartenby KA. Mesenchymal stem cells: Emerging mechanisms of immunomodulation and therapy. *World Journal of Stem Cells*. 2014;6:526-539.
58. Aggarwal S, Pittenger MF. Human mesenchymal stem cells modulate allogeneic immune cell responses. 2005.
59. Spaggiari GM, Moretta L. Interactions between mesenchymal stem cells and dendritic cells. In: Weyand B, Dominici M, Hass R, Jacobs R, Kasper C, eds. *Mesenchymal stem cells - basics and clinical application ii*. Berlin, Heidelberg: Springer Berlin Heidelberg; 2013:199-208.
60. Nauta AJ, Kruisselbrink Ab Fau - Lurvink E, Lurvink E Fau - Willemze R, et al. Mesenchymal stem cells inhibit generation and function of both cd34+-derived and monocyte-derived dendritic cells. *J. Immunol*. 2006.
61. Spaggiari GM, Abdelrazik H, Becchetti F, et al. Mscs inhibit monocyte-derived dc maturation and function by selectively interfering with the generation of immature dcs: Central role of msc-derived prostaglandin e2. *Blood*. 2009;113:6576-6583.
62. Djouad F, Charbonnier LM, Bouffi C, et al. Mesenchymal stem cells inhibit the differentiation of dendritic cells through an interleukin-6-dependent mechanism. *Stem cells*. 2007;25:2025-2032.
63. Wu J, Ji C, Cao F, et al. Bone marrow mesenchymal stem cells inhibit dendritic cells differentiation and maturation by microrna-23b. *Biosci, Rep*. 2017.
64. Aldinucci A, Rizzetto L Fau - Pieri L, Pieri L Fau - Nosi D, et al. Inhibition of immune synapse by altered dendritic cell actin distribution: A new pathway of mesenchymal stem cell immune regulation. *J. Immunol*. 2010.
65. Maqbool M, Vidyadaran S Fau - George E, George E Fau - Ramasamy R, et al. Human mesenchymal stem cells protect neutrophils from serum-deprived cell death. 2011.
66. Raffaghello L, Bianchi G Fau - Bertolotto M, Bertolotto M Fau - Montecucco F, et al. Human mesenchymal stem cells inhibit neutrophil apoptosis: A model for neutrophil preservation in the bone marrow niche. *Stem, Cells*. 2008.
67. Lundahl J, Jacobson Sh Fau - Paulsson JM, Paulsson JM. Il-8 from local subcutaneous wounds regulates cd11b activation. *Scand, J. Immunol*. 2012.

68. Jiang D, Muschhammer J, Qi Y, et al. Suppression of neutrophil-mediated tissue damage—a novel skill of mesenchymal stem cells. *Stem cells (Dayton, Ohio)*. 2016;34:2393-2406.
69. Wilgus TA, Roy S, McDaniel JC. Neutrophils and wound repair: Positive actions and negative reactions. *Advances in Wound Care*. 2013;2:379-388.
70. Mittal SK, Mashaghi A, Amouzegar A, et al. Mesenchymal stromal cells inhibit neutrophil effector functions in a murine model of ocular inflammation. *Investigative Ophthalmology & Visual Science*. 2018;59:1191-1198.
71. Sotiropoulou PA, Perez SA, Gritzapis AD, et al. Interactions between human mesenchymal stem cells and natural killer cells. *Stem cells*. 2006;24:74-85.
72. Yagi H, Soto-Gutierrez A, Parekkadan B, et al. Mesenchymal stem cells: Mechanisms of immunomodulation and homing. *Cell Transplant*. 2010;19:667-679.
73. Chabannes D, Hill M, Merieau E, et al. A role for heme oxygenase-1 in the immunosuppressive effect of adult rat and human mesenchymal stem cells. *Blood*. 2007;110:3691-3694.
74. Corcione A, Benvenuto F, Ferretti E, et al. Human mesenchymal stem cells modulate b-cell functions. *Blood*. 2006;107:367-372.
75. Franquesa M, Hoogduijn MJ, Bestard O, et al. Immunomodulatory effect of mesenchymal stem cells on b cells. *Frontiers in Immunology*. 2012;3:212.
76. Najar M, Krayem M, Meuleman N, et al. Mesenchymal stromal cells and toll-like receptor priming: A critical review. *Immune Network*. 2017;17:89-102.
77. Rozenberg A, Rezk A, Boivin M-N, et al. Human mesenchymal stem cells impact th17 and th1 responses through a prostaglandin e2 and myeloid-dependent mechanism. *Stem Cells Translational Medicine*. 2016;5:1506-1514.
78. Luz-Crawford P, Kurte M, Bravo-Alegría J, et al. Mesenchymal stem cells generate a cd4(+)cd25(+)foxp3(+) regulatory t cell population during the differentiation process of th1 and th17 cells. *Stem cell research & therapy*. 2013;4:65-65.
79. Engela AU, Baan CC, Dor FJMF, et al. On the interactions between mesenchymal stem cells and regulatory t cells for immunomodulation in transplantation. *Frontiers in Immunology*. 2012;3:126.
80. Haddad R, Saldanha-Araujo F. Mechanisms of t-cell immunosuppression by mesenchymal stromal cells: What do we know so far? *BioMed Research International*. 2014;2014:14.
81. Ren G, Su J, Zhang L, et al. Species variation in the mechanisms of mesenchymal stem cell-mediated immunosuppression. *Stem cells*. 2009;27:1954-1962.

82. Davies Lindsay C, Heldring N, Kadri N, et al. Mesenchymal stromal cell secretion of programmed death - 1 ligands regulates t cell mediated immunosuppression. *Stem cells*. 2016;35:766-776.
83. Kim S-n, Lee H-J, Jeon M-S, et al. Galectin-9 is involved in immunosuppression mediated by human bone marrow-derived clonal mesenchymal stem cells. *Immune Network*. 2015;15:241-251.
84. Zhou K, Guo S, Tong S, et al. Immunosuppression of human adipose-derived stem cells on t-cell subsets via the reduction of nf-kappab activation mediated by pd-11/pd-1 and gal-9/tim-3 pathways. *Stem Cells, Dev*. 2018.
85. Borakati A, Mafi R, Mafi P, et al. A systematic review and meta-analysis of clinical trials of mesenchymal stem cell therapy for cartilage repair. *Curr Stem Cell Res, Ther*. 2018.
86. Panes J, Garcia-Olmo D, Van Assche G, et al. Expanded allogeneic adipose-derived mesenchymal stem cells (cx601) for complex perianal fistulas in crohn's disease: A phase 3 randomised, double-blind controlled trial. *Lancet*. 2016.
87. Mohd Ali N, Boo L, Yeap SK, et al. Probable impact of age and hypoxia on proliferation and microrna expression profile of bone marrow-derived human mesenchymal stem cells. *PeerJ*. 2016;4:e1536.
88. Choudhery Ms Fau - Badowski M, Badowski M Fau - Muise A, Muise A Fau - Pierce J, et al. Donor age negatively impacts adipose tissue-derived mesenchymal stem cell expansion and differentiation. *J. Transl Med*. 2014.
89. Zhang J, Huang X, Wang H, et al. The challenges and promises of allogeneic mesenchymal stem cells for use as a cell-based therapy. *Stem cell research & therapy*. 2015;6:234.
90. Reinders MEJ, Dreyer GJ, Bank JR, et al. Safety of allogeneic bone marrow derived mesenchymal stromal cell therapy in renal transplant recipients: The neptune study. *Journal of Translational Medicine*. 2015;13:344.
91. Jung Y, Bauer G, Nolta JA. Concise review: Induced pluripotent stem cell-derived mesenchymal stem cells: Progress toward safe clinical products. *Stem cells (Dayton, Ohio)*. 2012;30:42-47.
92. Lim SJ, Ho SC, Mok PL, et al. Induced pluripotent stem cells from human hair follicle keratinocytes as a potential source for in vitro hair follicle cloning. *PeerJ*. 2016;4:e2695.
93. Baghbaderani Behnam A, Tian X, Neo Boon H, et al. Cgmp-manufactured human induced pluripotent stem cells are available for pre-clinical and clinical applications. *Stem Cell Reports*. 2015;5:647-659.
94. Ferreira LM, Mostajo-Radji MA. How induced pluripotent stem cells are redefining personalized medicine. *Gene Ther*. 2013.

95. Hynes Kim MD, Mrozik Krzysztof, Gronthos Stan, and Bartold P. Mark. Generation of functional mesenchymal stem cells from different induced pluripotent stem cell lines. *Stem cells and development*. 2014;23:1084-1096.
96. Zou L, Luo Y, Chen M, et al. A simple method for deriving functional mscs and applied for osteogenesis in 3d scaffolds. *Scientific reports*. 2013;3:2243.
97. Kang R, Zhou Y, Tan S, et al. Mesenchymal stem cells derived from human induced pluripotent stem cells retain adequate osteogenicity and chondrogenicity but less adipogenicity. *Stem Cell Res, Ther*. 2015.
98. Frobel J, Hemeda H, Lenz M, et al. Epigenetic rejuvenation of mesenchymal stromal cells derived from induced pluripotent stem cells. *Stem Cell Reports*. 2014;3:414-422.
99. Villa-Diaz LG, Brown Se Fau - Liu Y, Liu Y Fau - Ross AM, et al. Derivation of mesenchymal stem cells from human induced pluripotent stem cells cultured on synthetic substrates. *Stem, Cells*. 2012.
100. Liu Y, Goldberg Aj Fau - Dennis JE, Dennis Je Fau - Gronowicz GA, et al. One-step derivation of mesenchymal stem cell (msc)-like cells from human pluripotent stem cells on a fibrillar collagen coating. *PloS one*. 2012.
101. Chen YS, Pelekanos Ra Fau - Ellis RL, Ellis Rl Fau - Horne R, et al. Small molecule mesengenic induction of human induced pluripotent stem cells to generate mesenchymal stem/stromal cells. *Stem Cells Transl, Med*. 2012.
102. Harding J, Roberts RM, Mirochnitchenko O. Large animal models for stem cell therapy. *Stem cell research & therapy*. 2013;4:23.
103. Ohnuki M, Takahashi K. Present and future challenges of induced pluripotent stem cells. *Philosophical Transactions of the Royal Society B: Biological Sciences*. 2015;370:20140367.
104. Mandai M, Watanabe A, Kurimoto Y, et al. Autologous induced stem-cell-derived retinal cells for macular degeneration. *New England Journal of Medicine*. 2017;376:1038-1046.
105. Wu HJ, Yiu WH, Wong DWL, et al. Human induced pluripotent stem cell-derived mesenchymal stem cells prevent adriamycin nephropathy in mice. *Oncotarget*. 2017;8:103640-103656.
106. Obara C, Takizawa K, Tomiyama K, et al. Differentiation and molecular properties of mesenchymal stem cells derived from murine induced pluripotent stem cells derived on gelatin or collagen. *Stem Cells International*. 2016;2016:9013089.
107. Ng J, Hynes K, White G, et al. Immunomodulatory properties of induced pluripotent stem cell - derived mesenchymal cells. *Journal of Cellular Biochemistry*. 2016;117:2844-2853.

108. Soontararak S, Chow L, Johnson V, et al. Mesenchymal stem cells (msc) derived from induced pluripotent stem cells (ipsc) equivalent to adipose-derived msc in promoting intestinal healing and microbiome normalization in mouse inflammatory bowel disease model. *Stem Cells Transl, Med.* 2018.
109. Lian Q, Zhang Y, Fau - Zhang J, Zhang J, Fau - Zhang HK, et al. Functional mesenchymal stem cells derived from human induced pluripotent stem cells attenuate limb ischemia in mice. *Circulation.* 2010.
110. TheinHan W, Liu J, Tang M, et al. Induced pluripotent stem cell-derived mesenchymal stem cell seeding on biofunctionalized calcium phosphate cements. *Bone Research.* 2013;1:371.
111. Giuliani M, Oudrhiri N, Noman ZM, et al. Human mesenchymal stem cells derived from induced pluripotent stem cells down-regulate nk-cell cytolytic machinery. *Blood.* 2011;118:3254.
112. Shao K, Koch C, Gupta MK, et al. Induced pluripotent mesenchymal stromal cell clones retain donor-derived differences in DNA methylation profiles. *Molecular Therapy.* 2013;21:240-250.
113. Roux C, Saviane G, Pini J, et al. Immunosuppressive mesenchymal stromal cells derived from human-induced pluripotent stem cells induce human regulatory t cells in vitro and in vivo. *Frontiers in Immunology.* 2017;8:1991.
114. Chapman NM, Chi H. Mtor signaling, tregs and immune modulation. *Immunotherapy.* 2014;6:1295-1311.
115. Gao W-X, Sun Y-Q, Shi J, et al. Effects of mesenchymal stem cells from human induced pluripotent stem cells on differentiation, maturation, and function of dendritic cells. *Stem cell research & therapy.* 2017;8:48.
116. Sabapathy V, Kumar S. Hipsc - derived imscs: Nextgen mscs as an advanced therapeutically active cell resource for regenerative medicine. *Journal of Cellular and Molecular Medicine.* 2016;20:1571-1588.
117. Sheyn D, Ben-David S, Shapiro G, et al. Human ipscs differentiate into functional mscs and repair bone defects. *Stem Cells Transl, Med.* 2016.
118. Chen W, Liu X, Chen Q, et al. Angiogenic and osteogenic regeneration in rats via calcium phosphate scaffold and endothelial cell co - culture with human bone marrow mesenchymal stem cells (mscs), human umbilical cord mscs, human induced pluripotent stem cell - derived mscs and human embryonic stem cell - derived mscs. *Journal of Tissue Engineering and Regenerative Medicine.* 2017;12:191-203.
119. Liu X, Chen W, Zhang C, et al. Co-seeding human endothelial cells with human-induced pluripotent stem cell-derived mesenchymal stem cells on calcium phosphate scaffold enhances osteogenesis and vascularization in rats. *Tissue Eng Part, A.* 2017.

120. Peired AJ, Sisti A, Romagnani P. Mesenchymal stem cell-based therapy for kidney disease: A review of clinical evidence. *Stem Cells International*. 2016;2016:4798639.
121. Liang Y, Li X, Zhang Y, et al. Induced pluripotent stem cells-derived mesenchymal stem cells attenuate cigarette smoke-induced cardiac remodeling and dysfunction. *Frontiers in Pharmacology*. 2017;8:501.
122. Li X, Zhang Y, Liang Y, et al. Ipsc - derived mesenchymal stem cells exert scf- dependent recovery of cigarette smoke - induced apoptosis/proliferation imbalance in airway cells. *Journal of Cellular and Molecular Medicine*. 2017;21:265-277.
123. Hynes K, Bright R, Marino V, et al. Potential of ipsc-derived mesenchymal stromal cells for treating periodontal disease. *Stem Cells International*. 2018;2018:12.
124. Yang H, Aprecio RM, Zhou X, et al. Therapeutic effect of tsg-6 engineered ipsc-derived mscs on experimental periodontitis in rats: A pilot study. *PloS one*. 2014;9:e100285.
125. Hynes K, Menicanin D Fau - Han J, Han J Fau - Marino V, et al. Mesenchymal stem cells from ips cells facilitate periodontal regeneration. 2013.
126. Brick RM, Sun AX, Tuan RS. Neurotrophically induced mesenchymal progenitor cells derived from induced pluripotent stem cells enhance neuritogenesis via neurotrophin and cytokine production. *Stem Cells Translational Medicine*. 2018;7:45-58.
127. Vismara I, Papa S, Rossi F, et al. Current options for cell therapy in spinal cord injury. *Trends in Molecular Medicine*. 2017;23:831-849.
128. Krasnodembskaya A, Song Y, Fang X, et al. Antibacterial effect of human mesenchymal stem cells is mediated in part from secretion of the antimicrobial peptide ll-37. *Stem cells*. 2010;28:2229-2238.
129. Alcayaga-Miranda F, Cuenca J, Martin A, et al. Combination therapy of menstrual derived mesenchymal stem cells and antibiotics ameliorates survival in sepsis. *Stem cell research & therapy*. 2015;6:199.
130. Gupta N, Krasnodembskaya A, Kapetanaki M, et al. Mesenchymal stem cells enhance survival and bacterial clearance in murine escherichia coli pneumonia. *Thorax*. 2012;67:533-539.
131. Lee JW, Krasnodembskaya A, McKenna DH, et al. Therapeutic effects of human mesenchymal stem cells in ex vivo human lungs injured with live bacteria. *American Journal of Respiratory and Critical Care Medicine*. 2013;187:751-760.
132. Krasnodembskaya A, Samarani G, Song Y, et al. Human mesenchymal stem cells reduce mortality and bacteremia in gram-negative sepsis in mice in part by enhancing the phagocytic activity of blood monocytes. *American Journal of Physiology - Lung Cellular and Molecular Physiology*. 2012;302:L1003-L1013.

133. Sutton MT, Fletcher D, Ghosh SK, et al. Antimicrobial properties of mesenchymal stem cells: Therapeutic potential for cystic fibrosis infection, and treatment; 2016: 12.
134. Bonfield TL, Lennon D, Ghosh SK, et al. Cell based therapy aides in infection and inflammation resolution in the murine model of cystic fibrosis lung disease. *Stem Cell Discovery*. 2013;Vol.03No.02:15.
135. Asmussen S, Ito H, Traber DL, et al. Human mesenchymal stem cells reduce the severity of acute lung injury in a sheep model of bacterial pneumonia. *Thorax*. 2014;69:819-825.
136. Johnson V, Webb T, Norman A, et al. Activated mesenchymal stem cells interact with antibiotics and host innate immune responses to control chronic bacterial infections. *Sci, Rep*. 2017.

CHAPTER 2

Mechanisms of Immune Suppression Utilized by Canine Adipose and Bone Marrow-Derived Mesenchymal Stem Cells

Summary

Mesenchymal stem cells (MSC) from rodents and humans have been shown to suppress T cells by distinct primary pathways, with NO-dependent pathways dominating in rodents and IDO-dependent pathways dominating in humans. However, the immune suppressive pathways utilized by canine MSC have not been as thoroughly studied, nor have BM-MSC and Ad-MSC been directly compared for their immune modulatory potency or pathway utilization. Therefore, **these studies were designed to investigate the hypothesis that MSCs from different tissue origins will utilize different pathways for immune suppression.** First, canine BM-MSC and Ad-MSC were generated *in vitro* and then their potency in suppressing T cell proliferation and cytokine production were compared, as well as differential gene expression. Mechanisms of T cells suppression were also investigated for both MSC types. We found that BM-MSC and Ad-MSC were roughly equivalent in terms of their ability to suppress T cell activation. However, the two MSC types used both shared and distinct biochemical pathways to suppress T cell activation. Adipose-derived MSC utilized, TGF- β signaling pathways and adenosine signaling to suppress T cell activation, whereas BM-MSC used cyclooxygenase, TGF- β , and adenosine signaling pathways to suppress T cell activation. These results indicate that canine MSC are distinct from human and rodent MSC in terms of their immune suppressive pathways, relying primarily on cyclooxygenase and TGF- β pathways for T cell suppression, rather than on NO or IDO-mediated pathways.

Background

Cellular therapy with MSC offers a promising new option for non-pharmacologic management of inflammatory diseases. There are currently over 400 clinical trials employing MSC worldwide, and positive results from early studies have been reported using MSC for treatment of systemic lupus erythematosus, graft-versus-host disease, rheumatoid arthritis, and inflammatory bowel disease in humans¹⁻⁵. Pet dogs develop many of the same immune-mediated diseases as humans and can thus serve as a valuable spontaneous animal model for evaluating stem cell therapeutics, as reviewed recently (Hoffman A and Dow S, manuscript in press). Thus, for effective utilization of the canine spontaneous disease model, it is important to gain a better understanding of the mechanism(s) of action of immune modulation by canine MSC in order to properly design *in vivo* studies and interpret *in vitro* assays.

Mesenchymal stem cells interact with both the innate and adaptive immune systems, generally leading to abatement of ongoing inflammatory responses, though in some cases MSC may also upregulate immune responses^{6,7}. The immune modulatory properties of MSC have been employed extensively for suppression of inflammation in a number of different immune-mediated, inflammatory disease models in rodents⁸. For example, MSC derived from adipose tissues or bone marrow have been used to treat experimental allergic encephalitis, inflammatory bowel disease, immune-mediated arthritis, airway inflammation, and graft versus host disease in rodent models^{1,9-12}. In addition, human MSC have been administered to rodent models of inflammatory diseases¹³⁻¹⁷. Thus, it is apparent that the immune modulatory properties of MSC can be utilized therapeutically in a number of different diseases settings.

Numerous studies have investigated the underlying mechanisms that drive the immune modulatory properties of both human and mouse MSC^{16,18-20}. In human MSC, the reported

pathways of immune suppression by MSC include the indoleamine 2,3-deoxygenase (IDO)^{21, 22}, cyclooxygenase²³⁻²⁵, TGF- β ²⁶, soluble IL-1Ra^{27, 28}, soluble MHC^{29, 30}, and the PD-L1 pathways^{31, 32}. In general however, the IDO-dependent pathway is considered the primary mechanism of human MSC suppression of activated immune effector cells²¹. For rodent MSC, the nitric oxide (NO) dependent immune suppressive pathways predominate³³, though other pathways including TGF- β and IL-10 have been reported³⁴. It is also important to note that these immune modulatory pathways typically only become operative after the MSC have first been activated immunologically, typically by pro-inflammatory cytokines such as IFN- γ , TNF- α , IL-1 β , or IL-17, or by certain TLR ligands³⁵⁻³⁷. Thus, in the most assays used to evaluate MSC immune suppressive pathways, activated T cells are co-cultured with MSC, and in these assays the activated T cells provide the source of MSC-activating cytokines. In studies with suppression of innate immune effector cells such as DC, the requirement for addition of MSC-activating cytokines such as IFN- γ is more apparent³⁸⁻⁴⁰

Mesenchymal stem cells derived from bone marrow or adipose tissues of dogs also exhibit immune modulatory activity. For example, it was reported recently that intrathecal injection of MSC in dogs with idiopathic meningoencephalitis resulted in clinical improvement⁴¹. Local injection of MSC has also been used in the management of keratoconjunctivitis sicca in dogs, an immune mediated disorder that results in loss of tear production⁴². Human embryonic stem cell derived MSC were also reported recently to suppress inflammation associated with furunculosis in dogs, an inflammatory disease of the peri-rectal tissues of canines⁴³. Mesenchymal stem cells have also been widely used for treatment of osteoarthritis in dogs, a progressive degenerative condition that also has an associated inflammatory component. Studies of canine Ad-MSC and BM-MSC injected into the elbow and hip joints of dogs with

osteoarthritis produced positive results in terms of improvement in clinical measures of osteoarthritis reported in most investigations⁴⁴⁻⁴⁹.

Previously it was reported that various different sources of canine MSC modulate immune responses *in vitro*^{12, 50-54}. In the study by Lee et al, which utilized canine bone marrow MSC, PGE2 was identified as the primary MSC factor that suppressed T cell proliferation^{12, 54}. Kang et al identified PGE2 as an important T cell suppressive factor secreted by canine Ad-MSC, and also found that IDO production played an important role in T cell suppression⁵⁰. Thus, the cyclooxygenase pathway appears to be a major pathway in canine MSC suppression, though relatively few other pathways have been investigated.

Therefore, we sought in the present study to better define the functional immune modulatory properties of canine MSC, and to determine whether there were important differences between Ad-MSC and BM-MSC in terms of either their potency or the pathways utilized for T cell suppression. To address these questions, Ad-MSC and BM-MSC were generated and their immune modulatory properties evaluated using *in vitro* assays and T cells obtained from unrelated animals. These studies revealed that canine Ad-MSC and BM-MSC were similar in terms of their surface phenotype and overall immune modulatory potency. However, several important differences in the pathways of immune suppression utilized by each cell type were discovered. In addition, our results indicated that canine MSC did not utilize either the IDO or NO pathways as their predominant mechanisms for T cell suppression. Thus, canine MSC appear to be distinct from human and rodent MSC in terms of their utilization of major immune suppression pathways.

Materials and Methods

Culture medium for MSC and T cells.

Bone marrow and adipose-derived MSC were cultured in DMEM low glucose supplemented with essential and non-essential amino acids, Glutamax 1% penicillin-streptomycin (all from Life Technologies Corp. Grand Island NY) and 10% fetal bovine serum (FBS) (VWR Life Science, Radnor, PA). Canine T cells were cultured in the same media with the addition of 55uM 2-Mercaptoethanol (Life Technologies Corp. Grand Island NY)

Biochemical reagents.

Aminoguanidine and meclofenamic acid (MFA) were purchased from (Sigma-Aldrich, St. Louis MO), L-NMMA acetate, indomethacin, SB431542, LY364947, 1-MT (1-Methyl-D-tryptophan), ZM 241385, and CSC (8-(3-chlorostyryl) caffeine) were all purchased from Tocris (Bristol, UK). CAY 10581 was purchased from Santa Cruz Biotechnology, Inc. (Dallas, TX). Biochemical reagents were prepared as working solutions according to manufacturer directions and once reconstituted, all were stored at -20C prior to use.

Generation of canine Ad-MSC and BM-MSC.

All procedures involving live animals were approved by the Institutional Animal Care and Use Committee at Colorado State University. Adipose and bone marrow were each collected from 3 unrelated, healthy adult dogs. Canine adipose tissue (0.5g) was collected from using an 8 mm skin punch biopsy instrument, following sterile prep of the skin surface. The collected tissue was washed with sterile PBS and then cut into small pieces with scalpel blades. The minced tissues were then placed into a 50 mL conical and digested with 1mg/mL of collagenase type I (Sigma-Aldrich, St. Louis MO), for 30 min at 37°C. After 30 min of enzymatic digestion, MSC complete growth medium was added to inactivate collagenase. The

digested cells were then collected by centrifugation and plated in T75 cell culture flask (Corning Inc. Corning, NY) and allowed to adhere for 72 hours. All non-adherent cells were then removed at the first medium change at 72 hours and the adherent cells were re-fed with media. Media was then changed every 72h thereafter, and cells were passaged by trypsinization once Ad-MSc reached approximately 80% confluence.

Bone marrow aspirates were collected by bone marrow needles from the proximal humerus of dogs that were anesthetized or heavily sedated. The bone marrow samples were further minced *in vitro* and washed twice with PBS. Bone marrow samples were then placed into 50 mL conical tubes and digested with 1mg/mL of collagenase type 1 for 45 min at 37°C. The single cell suspensions were pelleted after digestion by centrifugation, washed twice in PBS, then resuspended in complete medium and plated in T-75 flasks with complete MSC medium and allowed to adhere for 72 hours. All non-adherent cells were then removed at the first medium change at 72 hours and adherent cells were re-fed with medium. Medium was then changed every 72h thereafter, and cells were passaged by trypsinization once BM-MSc reached approximately 80% confluence.

Tri-lineage differentiation.

Tri lineage differentiation for both Ad-MSc and BM-MSc was performed between passages 2 and 3, using the StemPro Adipogenesis Differentiation Kit, the Chondrogenesis Differentiation Kit, and the Osteogenesis Differentiation Kit (Life Technologies Corp. Grand Island NY), according to manufacturer's instructions. At the completion of the differentiation protocol for each cell lineage, cells were incubated with appropriate stains and photographed, using an Olympus CKX41 light microscope and attached SC30 digital camera. Images were captured using getIT software v5.2 (Olympus Soft Imaging Solutions).

MSC and T cell co-culture assays.

Canine peripheral blood mononuclear cells (PBMC) were prepared from EDTA-anticoagulated whole blood collected from the jugular vein of dogs. To prepare PBMC, anticoagulated blood was separated over a Ficoll gradient using lymphocyte separation medium (LSM; MP Biomedicals Inc, Santa Ana, CA), according to manufacturer's instructions. To assess T cell proliferation, the purified PBMC were labeled with carboxyfluorescein succinimidyl ester (CFSE) (ThermoFisher, Waltham, MA), according to manufacturer's directions. The CFSE stained cells were then plated in triplicate wells of a 96-well, flat bottom plate in 100 ul MSC medium containing 55 uM β -mercaptoethanol at a density of 5×10^5 cells per well. Activation of T cell proliferation was initiated by addition of Concavalin A (ConA) (Sigma-Aldrich, St. Louis, MO) at a concentration of 10 ug/mL. The effects of Ad-MSC and BM-MSC on T cell proliferation and cytokine production were assessed by adding unlabeled Ad-MSC or BM-MSC to PBMC cultures at ratios of 1:10 (MSC:PBMC), in a final volume of 200 ul per well of triplicate wells of 96-well plates. Co-cultures of MSC and T cells in contact were maintained for 96 hours, at which point the supernatant was collected (and stored frozen) for cytokine analysis, and the non-adherent cells were collected for flow cytometric analysis (see below).

T cell proliferation analysis

T cell proliferation with the addition of inhibitors was analyzed using EDU (5-ethynyl-2'-deoxyuridine) staining. EDU (Life Technologies Corp. Grand Island, NY) 3uM. was added to co-culture at 48 hours after plating. At 96 hours non adherent cells were collected and surfaced stained for detection of canine CD5⁺ cells, using an anti canine CD5-Alexa Fluor®488 (clone YKIX322.3, ABD Serotech. Raleigh, NC). After surface staining, cells were fixed with 4% PFA (Affymetrix Inc. Cleveland, OH) and permeabilized with saponin-based permeabilization and

wash reagent (Life Technologies Corp. Grand Island, NY). 50 uL of reaction cocktail mixed in PBS containing Copper(II) sulfate pentahydrate ($\text{CuSO}_4 \cdot 5\text{H}_2\text{O}$) 1mM, L-Ascorbic acid 50mM (Sigma-Aldrich, St. Louis MO). Sulfo-Cyanine5 (Cy5) azide 1 uM (Lumiprobe Corporation, Hallandale Beach, FL). Was then added, after 30 minutes incubation at room temperature, cells were washed with PBS and analyzed by flow cytometry. T cell proliferation was measured as the percent Edu (Cy5) positive within the gated CD5+ population of cells. T cell proliferation index was calculated as the proliferation percentage normalized to the value for stimulated PBMC+MSC, which was assigned a value of 1.

Flow cytometry.

For analysis of the surface phenotype of Ad-MSC and BM-MSC, cells were harvested by trypsinization and resuspended at a concentration of 1×10^6 cell/mL in FACS buffer (PBS, 2% FBS, and 0.1% sodium azide) on ice. Cells (1×10^5 /well) were immunostained in 96-well polystyrene round bottom plates. Non-specific staining was blocked with normal dog serum, then MSC were then incubated with primary antibodies for 30 minutes at room temperature. The primary antibodies used in these studies were: CD34-FITC (clone 1H6 serotech, Raleigh, NC), CD44-FITC (clone 1M7 eBioscience Inc. San Diego CA), CD45-FITC (clone YKIX716.13, Serotech. Raleigh, NC), CD73-biotin (clone TY/11.8, Biolegend. San Diego CA), CD90-APC (clone YKIX337.217, eBioscience Inc, San Diego CA), and unconjugated CD105 (clone 8A1, Abcam. Cambridge, MA). After primary antibody incubation, cells were washed with FACS buffer, then analyzed using a Beckman-Coulter Gallios flow cytometer. Samples stained with anti CD105 were incubated with additional donkey anti mouse IgG –FITC (Jackson ImmunoResearch Laboratories, Inc. West Grove, PA), Data analysis was done using FlowJo 9.0.8 software. In histogram plots of MSC phenotype (see Figure 1), the x-axis represented

fluorescence intensity and the y-axis represented cell count. Red histograms depict isotype staining, while blue histograms represent staining intensity using the specific antibody.

For analysis of T cell proliferation, non-adherent CFSE-labeled cells were collected from each well at 96 hours, and then immunostained for detection of canine CD5⁺ cells, using an anti canine CD5-APC (clone YKIX322.3, ABD Serotech, Raleigh, NC). After 30 min incubation with CD5 antibody, the cells were washed with FACS buffer and re-suspended in 200ul and then analyzed by flow cytometry. Histograms were generated using FlowJo 9.0.8 software. The CD5⁺ population of cells was first gated, and then the proliferation percent measured as the frequency of dividing cells that had reduced CFSE fluorescence compared to un-stimulated, CFSE-labeled CD5⁺ T cells. T cell proliferation index was calculated as the proliferation percentage normalized to the value for stimulated PBMC+MSC, which was assigned a value of 1

IFN- γ ELISA

Supernatants were collected from 96 hour co-cultures of T cells and MSC and stored at -20°C prior to analysis. Concentrations of IFN- γ in supernatants was determined using a canine IFN- γ specific ELISA (R&D Systems, Minneapolis, MN), according to the manufacturer's directions. A cytokine stimulation index (S.I) was calculated as the IFN- γ concentration (pg/ml) from the test sample normalized to the mean IFN- γ concentration present in supernatants from activated PBMC co-cultured with MSC.

Neutralization of IFN- γ

IFN- γ present in T cell and MSC co-cultures was neutralized using an anti-canine IFN- γ antibody (R&D Systems Minneapolis, MN) at a concentration 10 ng/mL. At 48h, an additional 5 ng/mL of the anti-IFN- γ antibody was added to co-cultures to assure complete neutralization. T cell proliferation was analyzed as previously described above.

Immunocytochemistry

Expression of intracellular stem cell antigens by Ad-MSC and BM-MSC was determined by plating cells on glass coverslips in 24-well cell culture plates and allowing the cells to adhere for 24 hours. Cells were fixed with 4% PFA for 10 min at room temperature, then washed in PBS and permeabilized with 0.1% Triton-X. Non-specific binding was minimized by incubation with 10% secondary antibody species serum plus 0.1% Triton for 1 hour prior to application of primary antibody. Each well was incubated with primary antibody overnight at 4°C. Primary antibodies used are as follows: Oct3/4 (clone H134, Santa Cruz Biotechnology, Inc. Dallas, TX) and vimentin (clone V9, Merck Millipore, Billerica, MA). Corresponding rabbit and mouse IgG irrelevant isotype antibodies were used at concentrations matching the primary antibodies (eBioscience Inc, San Diego CA). Cells were washed with PBS with 0.05% Tween and then incubated with secondary antibodies (donkey anti mouse IgG or donkey anti rabbit IgG; Jackson ImmunoResearch Laboratories, Inc. West Grove, PA), then washed and mounted with DAPI counter stain. Visualization of fluorescence staining was performed using an Olympus IX83 confocal microscope. Images were imported as Tiff files to Photoshop CC 2015, and adjusted with high definition resolution (HDR) toning. For each antibody, adjusted HDR toning was saved as preset values and applied to corresponding isotype control stains as well.

T cell apoptosis and cell death measurement in co-cultures

Co-cultures of MSC and PBMC were prepared as noted above, except that the activated T cells were not labeled with CFSE. After culture for 24 hour, 48 hour, 72 hour and 96 hours, non-adherent cells (primarily CD5⁺ T cells) were collected and prepared for analysis of apoptosis and cell death. Cells were immunostained for CD5 (eBiosciences), and for Annexin V expression (V405 Annexin V, Life Technologies Corp. Grand Island, NY). Assessment of cell

death was done by adding 7-AAD viability stain (eBiosciences Inc) to cells immediately before flow cytometric analysis. Histograms were generated with Flowjo 9.0.8 software, and CD5⁺ cells were evaluated for expression of Annexin V and 7-AAD.

Comparison of gene expression profiles by microarray analysis

Triplicate, independent cultures of Ad-MSC and BM-MSC, were established as previously described above and cellular RNA collected from semi-confluent cultures using Qiagen RNeasy mini kit. The RNA was then labeled and hybridized to Canine Gene 1.0 ST Arrays (Affymetrix, Santa Clara, CA) using standard Affymetrix protocols. Image files were converted to log₂ expression values with RMA (Robust Multiarray Average) background correction and quantile normalization, as implemented by a statistical/visualization package (Partek Genomics Suite v6.6; St Louis, MO). The normalized expression values used in the statistical and bioinformatics analysis for these studies, as well as the original raw visual data used to calculate these values, have been deposited in the publicly accessible database Gene Expression Omnibus (<http://www.ncbi.nlm.nih.gov/geo/>) under the accession number (GSE90449). We used a one-way ANOVA model to compute fold-change and p-values, comparing expression levels for 32,391 transcripts from triplicate cultures of Ad-MSC and BM-MSC, measured with the gene arrays. The statistical/fold change results, along with the individual log₂ expression values for the top 100 over-expressed and 100 under-expressed genes for Ad-MSC vs. BM-MSC is provided in Supplementary Figure 1.

The Ingenuity Pathway Analysis (IPA) platform (Ingenuity, Redwood City, CA) was used to perform systems analysis on the top 5% of genes that were significantly differentially expressed between Ad-MSC and BM-MSC. The IPA software uses Fisher's exact test to identify over-represented and connected biological units in a defined set of genes, which can

include pathways, cellular functions, or known targets of regulatory genes. In some cases, a confidence or z score was generated based on the activation state of the pathway (or upstream regulators of the pathway) or based on the expression pattern of the associated genes. The IPA software was also used to group transcripts into gene-limited networks (containing 35 genes at most) based on evidence of direct or indirect relationships between molecules according to the IPA Knowledge Base.

Statistical analysis.

Statistical comparisons between data sets with two treatment groups were done using an unpaired T test. Comparisons between 3 or more groups were done using ANOVA, followed by Tukey multiple means comparison post-test. Analyses were done using Prism 6 software (GraphPad, La Jolla, CA). For all analyses, statistical significance was determined for $p < 0.05$.

Results.

Phenotypic comparison of Ad-MSC and BM-MSC.

The surface phenotypes of canine Ad-MSC and BM-MSC were compared, using flow cytometry to quantitate expression of stem cell surface markers, as reported in earlier studies of canine MSC^{12, 50, 55}. We found that both types of MSC were very similar in terms of their surface phenotypes, inasmuch as each cell type expressed high levels of CD44, CD90 and CD105, but were negative for expression of the hematopoietic stem cell antigens CD45 and CD34 (**Figure 2.1**). Notably, neither MSC cell type expressed surface marker CD73, though this molecule has been reported to be expressed by canine MSC in other studies⁵⁰. We did however observe CD73 expression using the same antibody by MSC derived from canine iPSC (Chow, et al, manuscript in preparation), indicating that in some instances surface marker CD73 can be expressed by canine MSC. Ad-MSC and BM-MSC derived from additional, unrelated dogs in

the study all displayed a very similar surface phenotype (data not shown). MSC were also evaluated by immunocytological staining for expression of intracellular proteins associated with MSC in other species (**Figure 2.2**). Both Ad-MSC and BM-MSC expressed high levels of the mesenchymal cytoskeletal intermediate filament protein vimentin (**Figure 2.2A, 2.2B**). Both cell types were also positive for intra-nuclear expression of the nuclear transcription factor OCT3/4 (**Figure 2.2C, 2.2D**). However, the two cell types did exhibit morphological differences, with Ad-MSC being more elongated, versus the flattened and oblong BM-MSC (not shown). These findings are consistent with the previously reported phenotypes of both human and rodent MSC^{56 57}

Tri-lineage differentiation.

The ability of Ad-MSC and BM-MSC to undergo tri-lineage differentiation, an important property of MSC, was assessed next. Using standard differentiation induction conditions, Ad-MSC and BM-MSC both readily differentiated into cells with properties consistent with chondrocytes, adipocytes, and osteoblasts (*data not shown*). Thus, tri-lineage differentiation properties were equally shared by the two MSC types.

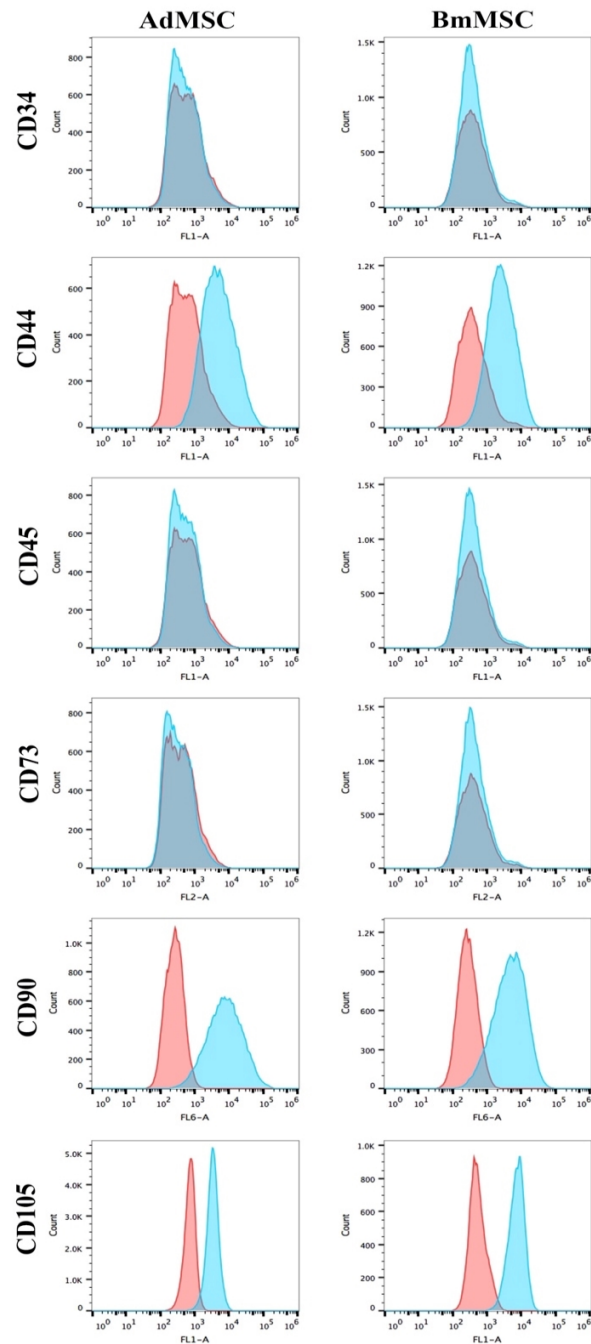


Figure 2.1. Immunophenotypic characterization of canine Ad-MSC and BM-MSC by flow cytometry. Canine Ad-MSC (left column) and BM-MSC (right column) at passage 2 to 3 were immunostained with antibodies to stem cell surface markers CD34, CD44, CD45, CD73, CD90 (or the intracellular marker CD105), and analyzed by flow cytometry using protocols described in Methods. Histograms depict fluorescence intensity on the x-axis and cell count on the y-axis. Red histograms depict isotype antibody staining, while blue histograms depict staining with relevant, directly-conjugated primary mAbs. Each study was repeated at least twice with similar results, including studies with MSC from several unrelated animals

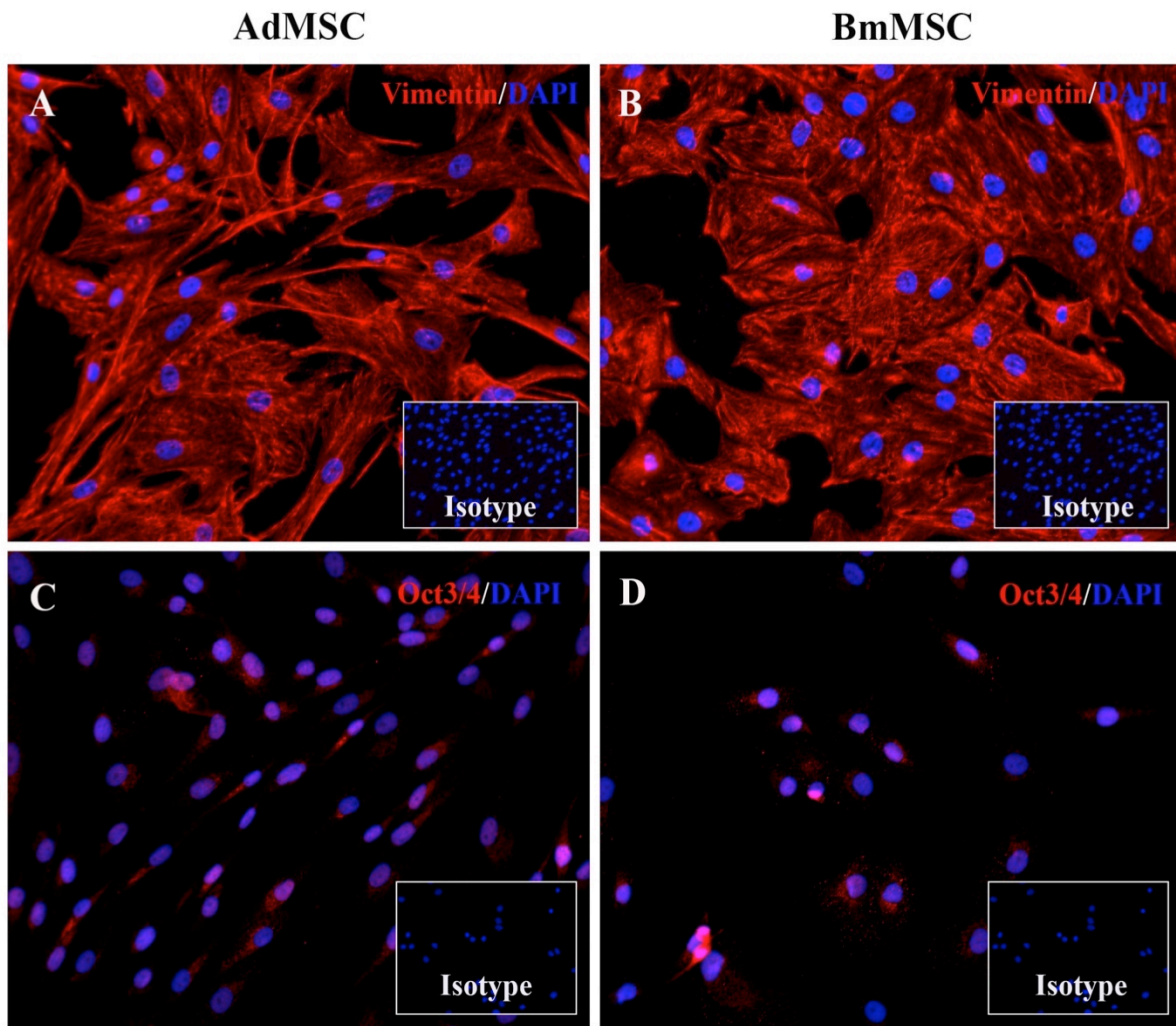


Figure 2.2 Immunocytochemical characterization of Ad-MSC and BM-MSC by immunofluorescence staining. MSC were cultured on glass slides and immunostained for detection of expression of intracellular stem cell antigens, as described in Methods. Slides were counterstained with DAPI for nuclear detection. Inset boxes depict staining with isotype control antibodies. In (2.2 A) and (2.2 B), Ad-MSC and BM-MSC were stained with anti-vimentin antibody, followed by Cy3-conjugated secondary antibody. The expression of vimentin revealed differences in morphology of Ad-MSC versus BM-MSC. In (2C) and (2D), Ad-MSC and BM-MSC were immunostained with anti-Oct3/4 antibody, followed by Cy3-conjugated secondary antibody, revealing extensive Oct3/4 intra-nuclear expression in both populations of MSC

Suppression of T cell proliferation and cytokine release by Ad-MSc and BM-MSc.

The immune modulatory properties of MSC have been widely described, both *in vitro* and *in vivo*, based in large part on assays that assess T cell suppression^{8, 58, 59}. Therefore, we used PBMC obtained from healthy donor dogs (unrelated to the source dog for MSC cultures) and Ad-MSc and BM-MSc to assess and compare immune modulatory properties of each cell type. Triplicate wells of activated T cells were incubated with MSC at an MSC to PBMC ratio of 1:10, for 96 hours. At the initiation of the assays, T cells were activated with ConA (10 µg/ml). To assess proliferation, PBMC were labeled with CFSE, as described in Methods (MSC were unlabeled in these assays). At 96 hours, supernatants were collected for IFN- γ quantitation by ELISA, and T cell proliferation was analyzed by flow cytometry.

T cells were immunostained for CD5 expression and the dilution of CFSE staining intensity of CD5⁺ T cells was assessed as a measure of T cell proliferation (**Figure 2.3**). Both Ad-MSc and BM-MSc significantly suppressed T cell proliferation when incubated with MSC (**Figure 2.3, A-D**). Ad-MSc suppressed proliferation by an average of 88%, compared to 86% suppression for BM-MSc (this difference was not statistically significant).

In addition, co-culture with Ad-MSc and BM-MSc also produced significant suppression of IFN- γ release by activated T cells (**Figure 2.3E**), with 93% suppression of IFN- γ release induced by Ad-MSc and 86% suppression induced by BM-MSc (differences were not statistically significant). These results indicated that canine Ad-MSc and BM-MSc are both capable of inducing significant suppression of T cell function, at roughly equivalent potency.

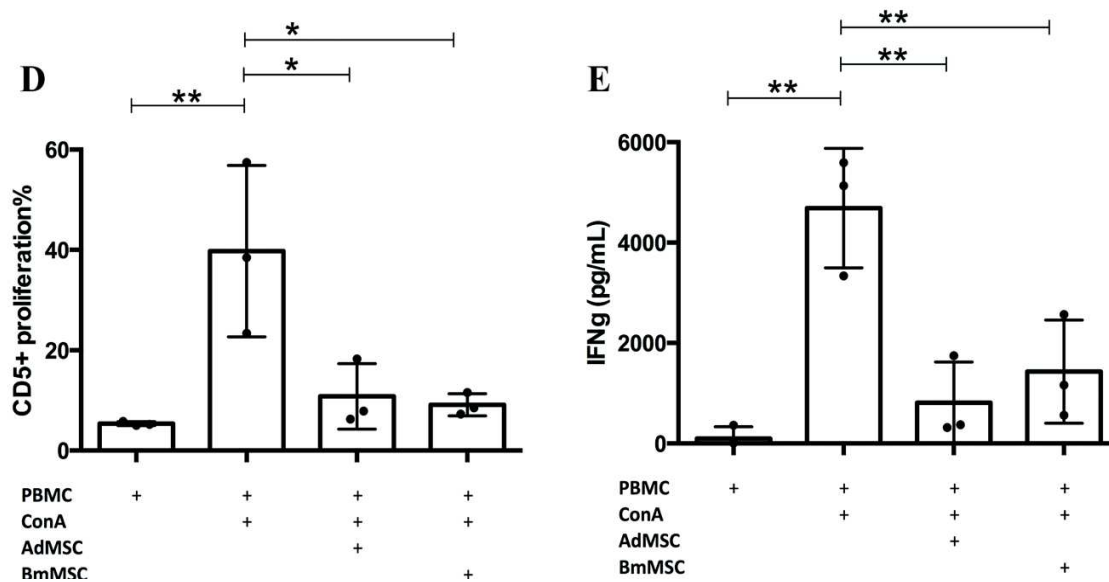
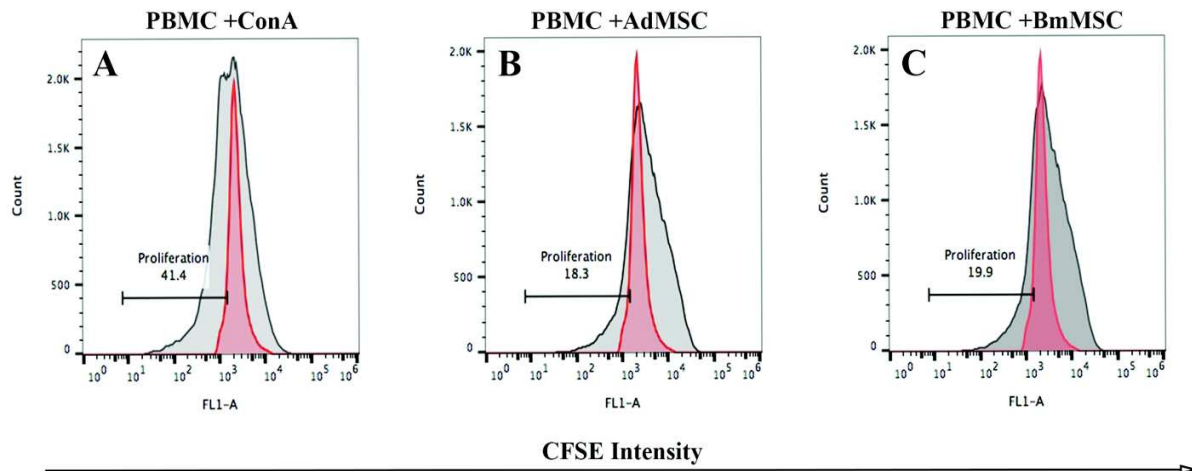


Figure 2.3. Effects of Ad-MSC and BM-MSC on T cell proliferation and IFN- γ production. In panel A-C, representative histograms of proliferating CFSE⁺CD5⁺ T cells are depicted, either of activated T cells alone (2.3A), T cells with Ad-MSC (2.3B), or T cells with BM-MSC (2.3C). The x-axis represents fluorescence intensity of CFSE (FITC), y-axis represents cell count. Unstimulated, CFSE⁺CD5⁺ T cells are depicted in pink shading, while activated CFSE⁺CD5⁺ T cells are depicted in gray shading. In (2.3D), the effect of Ad-MSC and BM-MSC co-cultures at 1:10 ratios (MSC:T cells) on T cell proliferation were presented, using pooled data from 3 separate MSC:T cell co-culture experiments with PBMC obtained from 3 unrelated donor animals. Data points represent mean T cell proliferation from each individual donor dog. Percent CD5⁺ T cell proliferation is depicted on the y-axis. In (2.3E), IFN- γ concentrations were measured in supernatants collected after 96 hours of incubation from co-cultures of MSC and T cells in triplicate wells, in pooled experiments from 3 different donor animals. IFN- γ concentrations were determined using canine IFN- γ ELISA. Significance was calculated using one-way ANOVA, with Tukey's multiple means comparison (* $p < 0.05$, ** $p < 0.01$).

Mechanisms of T cell suppression by MSC.

Studies were conducted next to identify and compare mechanisms of T cell suppression induced by canine MSC (**Figure 2.4**). These studies used both T cell proliferation and IFN- γ production as the primary read-outs (though IFN- γ release proved to be the more sensitive readout for these assays). Inhibitors of most of the major known pathways of MSC suppression of T cells in other species were evaluated, including the following inhibitors and pathways: NO pathway (aminoguanidine, L-NMMA); cyclooxygenase pathway (indomethacin, MFA); TGF- β pathway (SB431542, LY364947); IDO pathway (1-MT, CAY 10581); adenosine receptor pathway (ZM241385, CSC), and checkpoint molecule pathway (blocking antibodies to canine PD-L1). The doses of inhibitors used were determined in most cases by titration studies in our laboratory, or based on inhibitor concentrations used in previous publications.

We found that for suppression of T cell function by canine Ad-MSC, the predominant pathways utilized were the TGF- β pathway and the adenosine pathways, as revealed by significant reversal of inhibition of T cell proliferation and IFN- γ release following incubation with a TGF- β receptor inhibitor (SB431542) or with an adenosine receptor antagonist (ZM241385) (**Figure 2.4A, 2.4B**). In contrast, blocking other signaling pathways using inhibitors or antibodies did not significantly reverse T cell suppression elicited by Ad-MSC (data not shown). TGF- β release in the range of 5-15 ng/mL was also detected in conditioned medium from T cells co-cultured with Ad-MSC (data not shown). It was not possible however to measure adenosine concentrations directly.

For BM-MSC inhibition of T cells, the TGF- β and adenosine pathways were also found to be active (**Figure 2.4C, 2.4D**). In addition, we also identified an important contribution from the cyclooxygenase pathway, inasmuch as significant reversal of suppression occurred following

the addition of indomethacin or MFA to the BM-MSc and T cell co-cultures (**Figure 2.4C, 2.4D**). In addition, BM-MSc co-cultured with T cells led to the secretion of high concentrations of PGE2 and TGF- β (data not shown). Thus, we concluded from these studies that canine Ad-MSc and BM-MSc use two overlapping immune modulatory pathways (TGF- β and adenosine signaling) for T cell suppression, while BM-MSc also utilize the cyclo-oxygenase pathway for T cell suppression.

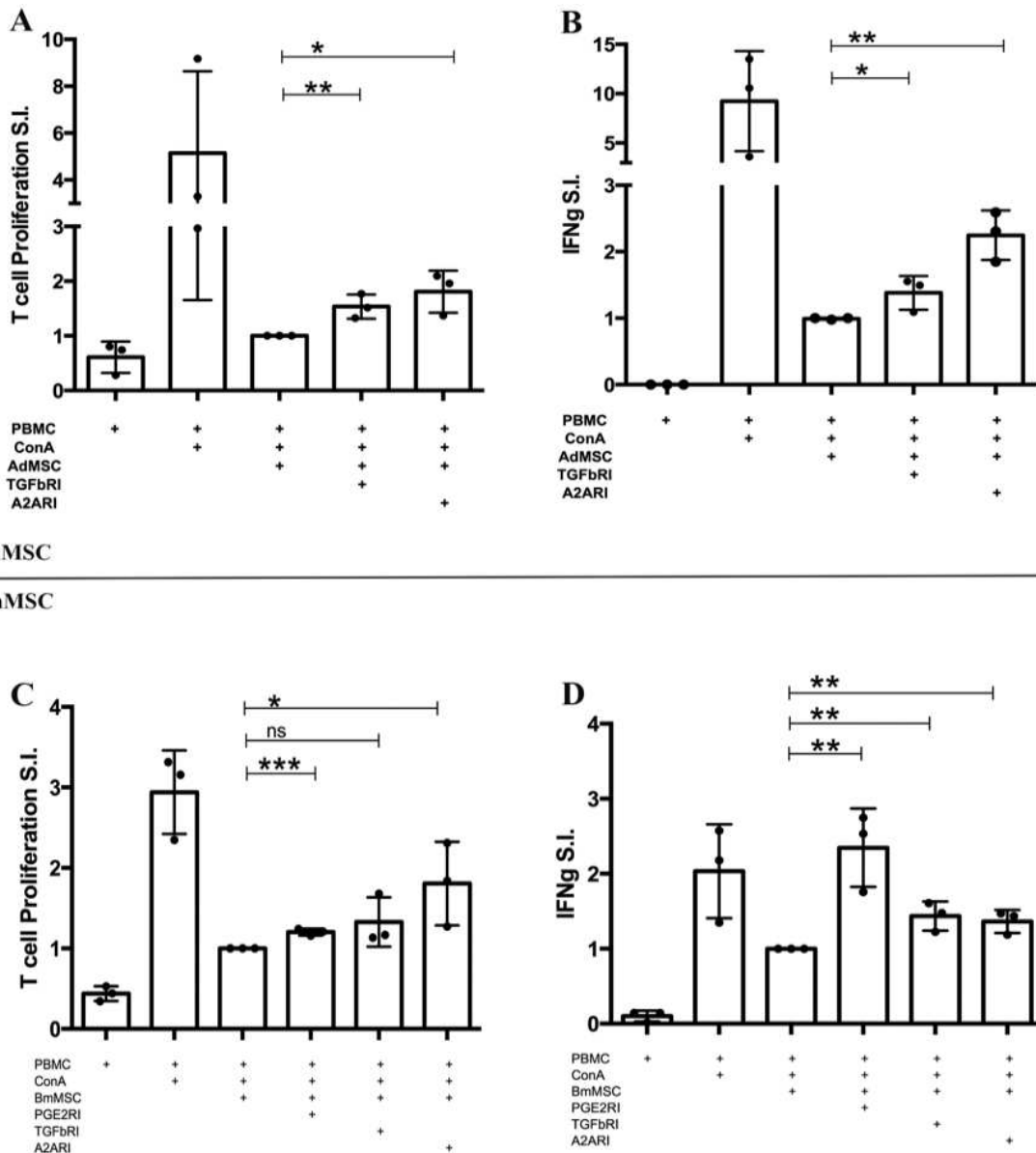


Figure 2.4. Identification of pathways regulating MSC suppression of T cell proliferation and cytokine production

Ad-MSC (2.4A and 2.4B) and BM-MSC (2.4C and 2.4D) were co-cultured with T cells at a 1:10 ratio as described in Methods, with the addition of pathway inhibitors. A T cell proliferation and IFN- γ index was calculated as the proliferation percentage normalized to the value for stimulated PBMC+MSC, which was assigned a value of 1. Addition of TGF β RI and A₂ARI significantly reversed inhibition of T cell proliferation (2.4A) and T cell IFN- γ release (2.4B), while for BM-MSC, TGF β RI, A₂ARI, and COXI all 3 significantly reversed suppression of proliferation (2.4C) and IFN- γ release (2.4D). The effects of pathway inhibitors were compared statistically between MSC:T cell co-cultures without inhibitors and MSC:T cell co-cultures with each specific inhibitor, using one-tailed, unpaired, parametric t-tests. Significance was noted for * p< 0.05, ** p< 0.01, *** p< 0.001, and **** p<0.0001 . These graphs represent pooled data from 3 independent experiments using MSC from 3 unrelated donor animals.

MSC activation by IFN- γ required for full immune suppressive activity.

Several studies have found that in order for MSC to suppress T cells, the MSC must first be activated by pro-inflammatory cytokines^{18, 19, 60, 61}. The major cytokine known to “license” MSC to become immune modulatory has been identified as IFN- γ ^{36, 60}. Therefore, the role of IFN- γ in regulating the T cell suppressive effects of canine MSC was evaluated by neutralizing IFN- γ production during MSC: T cell co-cultures (**Figure 2.5**). These experiments revealed that the ability of MSC to suppress T cell proliferation was significantly attenuated when IFN- γ was neutralized at the initiation of the co-cultures. Therefore, analogous to other species, IFN- γ produced by activated canine T cells also plays a critical role in the early activation of canine MSC, including both Ad-MSC and BM-MSC, resulting in an immunosuppressive phenotype.

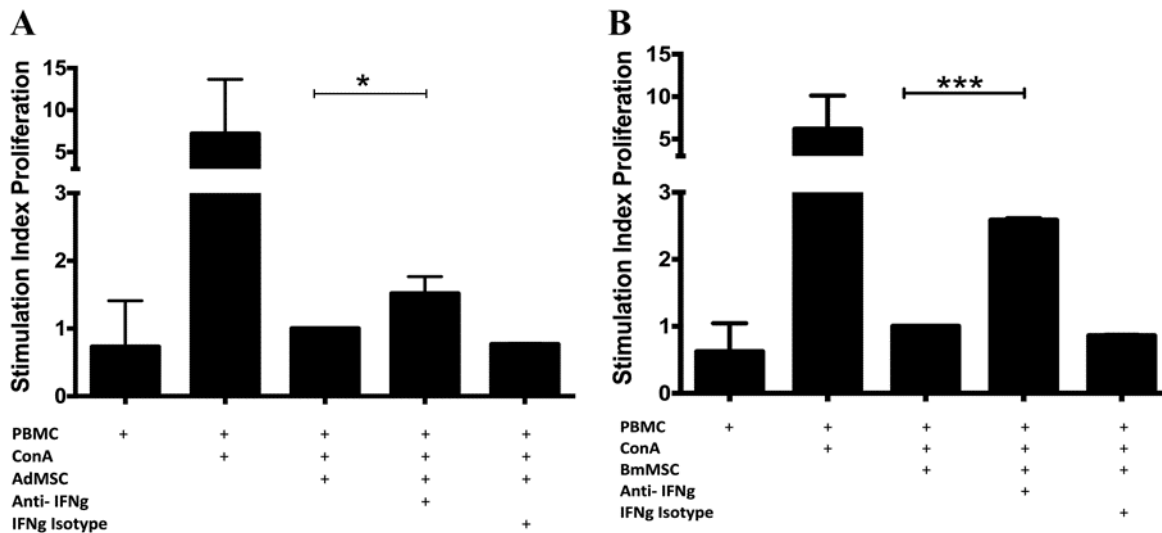


Figure 2.5. Effects of IFN- γ neutralization on MSC suppression of T cell proliferation. Co-cultures of Ad-MSC or BM-MSC and activated T cells were incubated with anti-canine IFN- γ neutralizing antibody (10 ug/ml) added at the initiation of the co-culture, with additional antibody added at 48h at 5 ug/ml. The effects of IFN- γ neutralization on suppression of T cell proliferation by Ad-MSC (**2.5A**) and BM-MSC (**2.5B**) are demonstrated. Addition of anti IFN- γ neutralizing antibody significantly blocked the suppression of T cell proliferation, compared to T cells co-cultured with Ad-MSC alone or with Ad-MSC and an equivalent concentration of an isotype control antibody. Statistical comparison was done using one-tailed, unpaired, parametric t-tests. Significance was noted for * $p < 0.05$, and *** $p < 0.001$.

MSC induce T cell death in co-culture.

Previous reports have suggested that MSC may suppress the function of activated T cells in part by inducing T cell apoptosis⁶²⁻⁶⁴. Therefore, the effects of addition of MSC on apoptosis of activated canine T cells were assessed in co-culture assays, using flow cytometric expression of Annexin V combined with cell membrane permeability changes to detect early and late apoptotic and cell death events in T cells (**Figure 2.6A, 2.6B**). These studies revealed that the presence of MSC in co-cultures with T cells did not significantly influence (either positively or negatively) the number of early or late apoptotic CD5⁺ T cells over a 96-hour period. However, the numbers of dead T cells (7-AAD⁺CD5⁺) increased progressively in co-cultures with both Ad-MSC and BM-MSC, compared to cultures of activated T cells alone, reaching the level of statistical significance at 96 hours (**Figure 2.6C**). For example, co-culture with Ad-MSC increased the percentage of dead T cells to 20% (compared with 9% for activated T cell cultures alone), while co-culture with BM-MSC increased the percentage of dead T cells to 29%. Thus, the presence of canine MSC can decrease the overall viability of activated T cells.

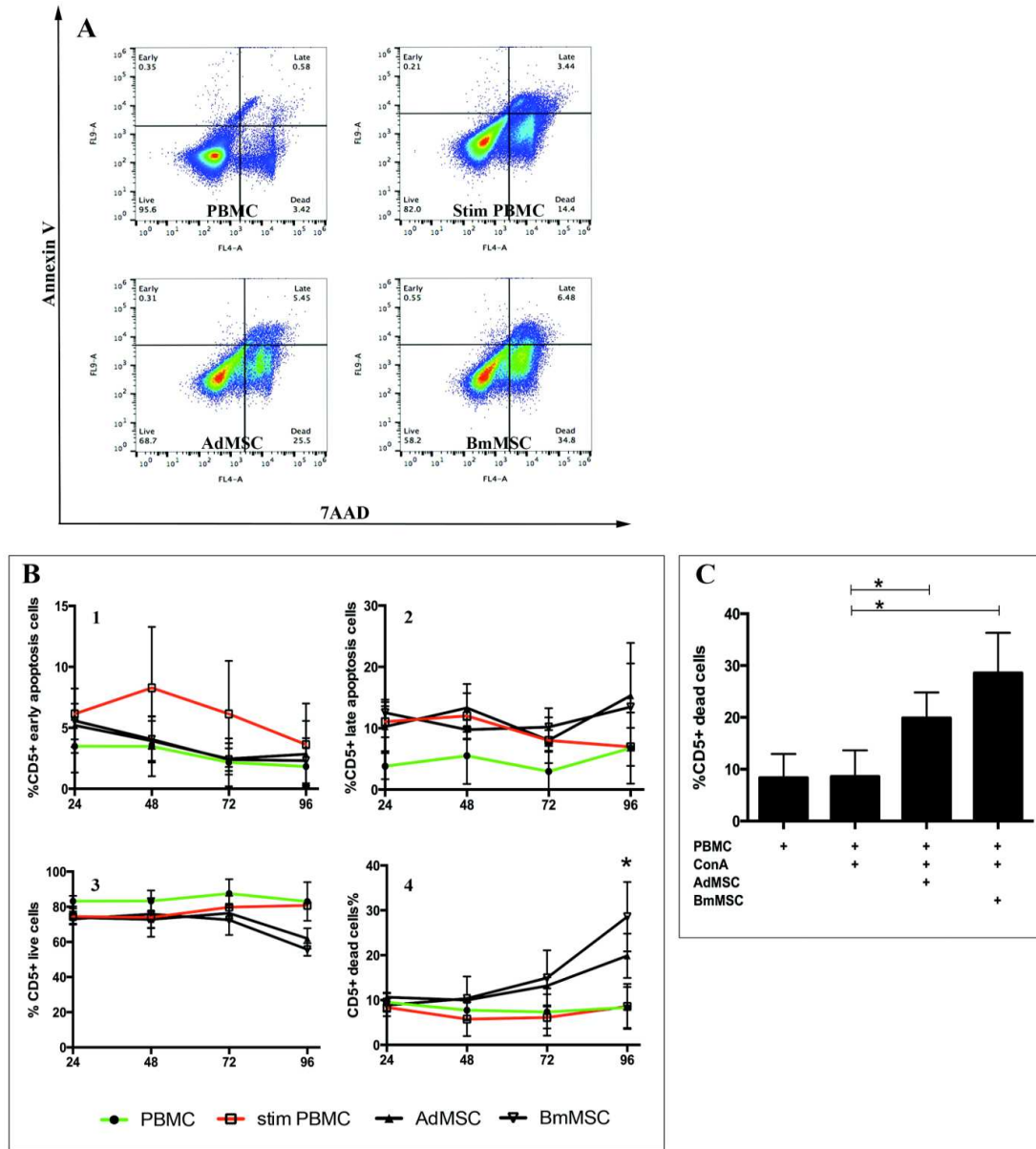


Figure 2.6. Co-culture with MSC induces T cell death. Activated T cells alone, or T cells co-cultured with MSC at a 1:10 ratio (MSC:T cells), were cultured in triplicate. At 24h intervals, the non-adherent cells were collected and immunostained with anti-CD5 antibody, Annexin V for apoptosis detection, and 7-AAD for detection of dead cells. In (2.6A), representative FACS plots of CD5⁺ T cells from unstimulated, stimulated, stimulated + Ad-MSC, and stimulated + BM-MSC cultures following 96-hours in culture. In (2.6B), the mean number of live T cells, early and late apoptotic T cells, and dead T cells from triplicate cultures are plotted over time for T cells from unstimulated cultures, stimulated cultures only, stimulated cultures + Ad-MSC and stimulated cultures + BM-MSC. In (2.6C), the mean percentage of 7-AAD⁺ T cells are plotted for T cells collected at 96 hours. Statistical comparisons were performed with unpaired t-test between stimulated T cells alone and stimulated T cells + Ad-MSC, or between stimulated T cells alone and stimulated T cells + BM-MSC. Significance was noted for * $p < 0.05$.

Gene expression patterns in Ad-MSK and BM-MSK.

To compare the gene expression patterns of Ad-MSK and BM-MSK, microarray studies were done, using Affymetrix canine OST 1.0 chips. (The full array data have been deposited in the Gene Expression Omnibus database online). Differential gene expression analysis showed that 698 genes were up-regulated in Ad-MSK compared to BM-MSK, with a fold change >2 and $p < 0.02$. In addition, 695 genes were down-regulated in Ad-MSK compared to BM-MSK, with a fold change of < -2 (raw data deposited in Gene Expression Omnibus under accession number GSE90449). Principle component analysis (PCA) (**Figure 2.7A**) demonstrated that the biological replicates of the same cell type clustered together, within a standard deviation of 2, with over 74% variance accounted for by cell type. Over 60% of differentially expressed genes with a significance of $p < 0.05$ fell within a -2 to 2 fold difference (**Figure 2.7B**). Using a complete list of immune function related genes from The Immunology Database and Analysis Portal (ImmPort) system (import.niaid.nih.gov) we found only 77 genes out of the 3699 that had a fold change >2 or <-2 with a p -value with FDR <0.02 (**Figure 2.7C**). Because of the effect of soluble molecules produced by MSC on immune cells, we also analyzed cytokine expression using a complete list of 442 cytokines from the ImmPort database, and found 63 genes that were differentially expressed. Concurrent with the finding that MSC induced T cell death in culture, 129 cell death and apoptosis related genes were analyzed from the KEGG pathway database. This analysis revealed only 28 differentially expressed genes with a p -value <0.5 (Figure 7C).

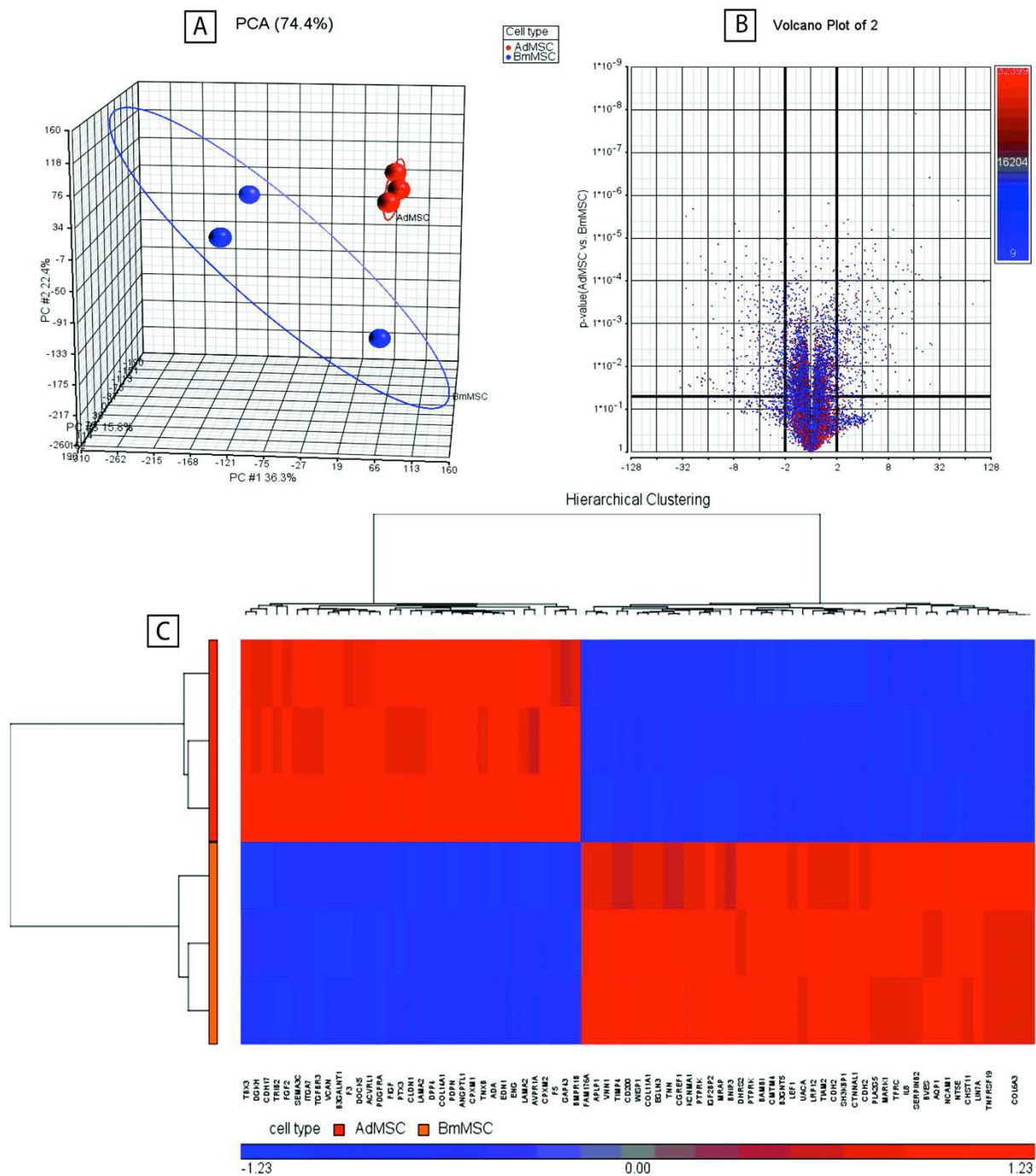


Figure 2.7. Differential gene expression by Ad-MSC vs BM-MSC. The Partek Genomics Suite was used to import microarray data from the canine 1.0 ST Affymatrix chip. **(2.7A)** A principle component analysis plot generated from these data depicts 3 biological replicates of each cell type, with red representing Ad-MSC, and blue representing BM-MSC. An ellipsoid was drawn around cell types using a sample standard deviation of 2. PC1 depicts a variation of 36.3%, PC2 a variation of 22.4%, and PC3 a variation of 5.6%. **(2.7B)** Volcano plot of all differentially expressed genes in the analysis of Ad-MSC vs. BM-MSC. X axis represents fold

change, thick axis lines drawn at fold change -2 and 2. Y axis represents p value, thick axis line marks 0.02. Color code represents column number assigned to each gene location on the Affymetrix chip. **(2.7C)** Cluster analysis and heat map of significant cytokine, apoptosis, and immune function genes in Ad-MSC and BM-MSC. Gene lists were downloaded from databases as described in methods. Red represents a higher expression, and blue represents lower expression with scale bar for each category (Ad-MSC or BM-MSC) on the left side of plots.

Finally, Gene Ontology (GO) Enrichment Analysis and Pathway Enrichment Analysis was also performed using the IPA platform to determine the biological significance of the genes differentially expressed between Ad-MSC and BM-MSC **(Figure 2.8)**, in which the top 25 upregulated and down-regulated bio-functions and pathways are depicted. Ad-MSC have higher expression of genes in the VEGF signaling, G receptor alpha signaling, STAT3 pathways. BM-MSC have higher expression of genes in the corticotropin pathway, the IL-1 pathway, the B cell receptor pathway, and the MAPK signaling pathways. Functional pathways upregulated in Ad-MSC included cardiovascular system development, endothelial cell development, carbohydrate metabolism and other cell growth related functions, while BM-MSC were upregulated in functional genes related to bone and connective tissue development, digestive system and other functions related to cytokinesis **(Figure 2.9)**.

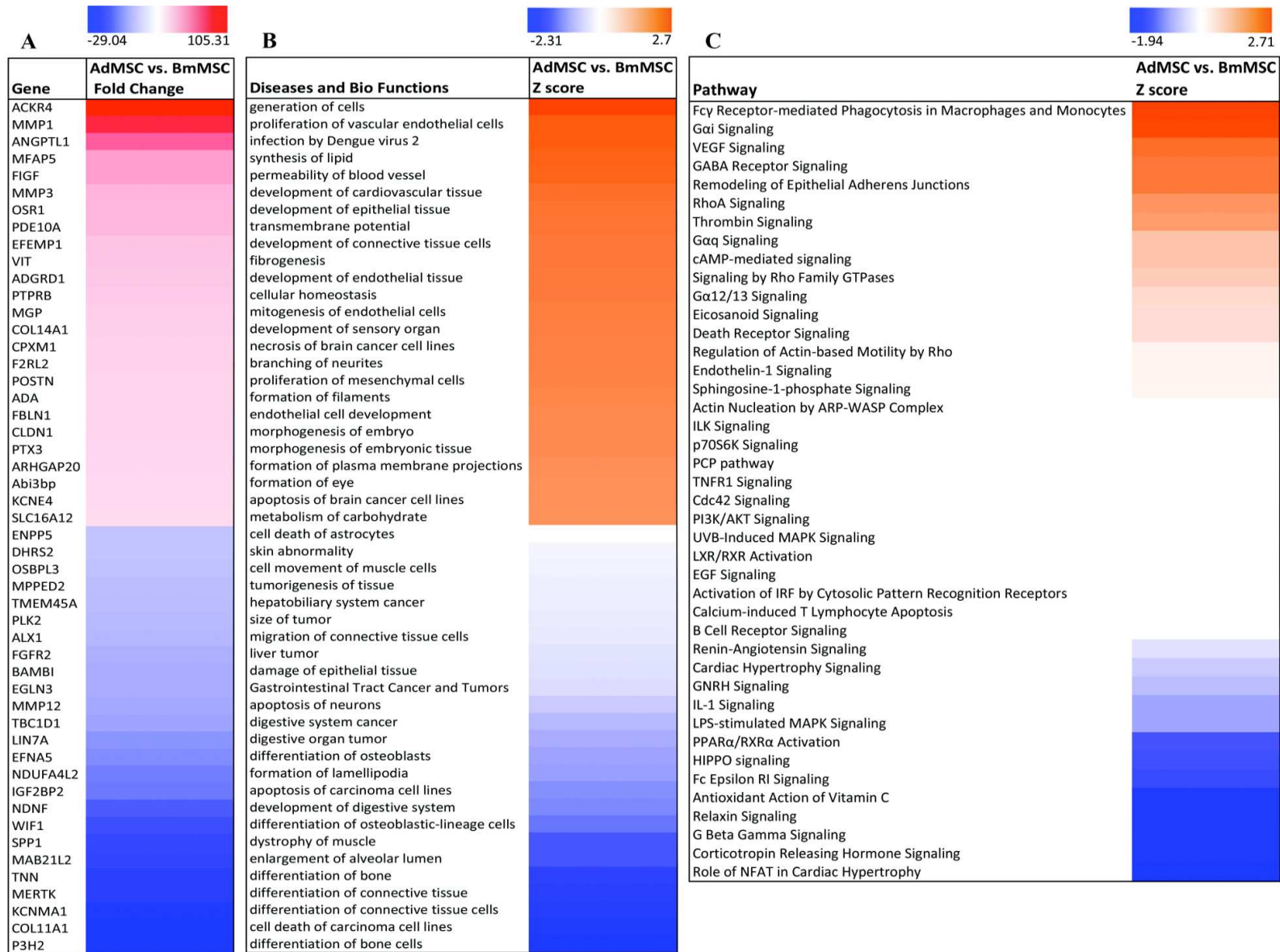
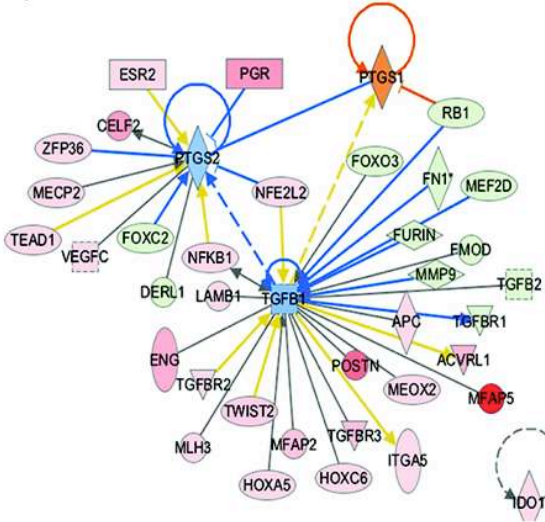


Figure 2.8 Over and under-expressed genes, pathways and functions.

The IPA software was used to determine the biological significance and pathways associated with differentially expressed genes between Ad-MSC and BM-MSC. **(2.8A)** List of top 25 up regulated genes in Ad-MSC vs BM-MSC with red representing a positive fold change, blue representing negative fold change, or higher expression in BM-MSC. **(2.8B)** List of top 50 significant gene functions with $p < 0.02$. Orange represents more enriched functions in Ad-MSC with a high z score of 2.7, functions in blue are downregulated in Ad-MSC with a low Z score of -2.3. **(2.8C)** List of all significant pathways that are over or under-expressed in Ad-MSC vs. BM-MSC; color scale shows overexpressed pathways in orange, with a highest activation z score of 2.71, and lowest in blue with a z score of -1.94.

A) TGF β network interactions Ad-MSC vs. BM-MSC



B) Adenosine network interactions Ad-MSC vs. BM-MSC

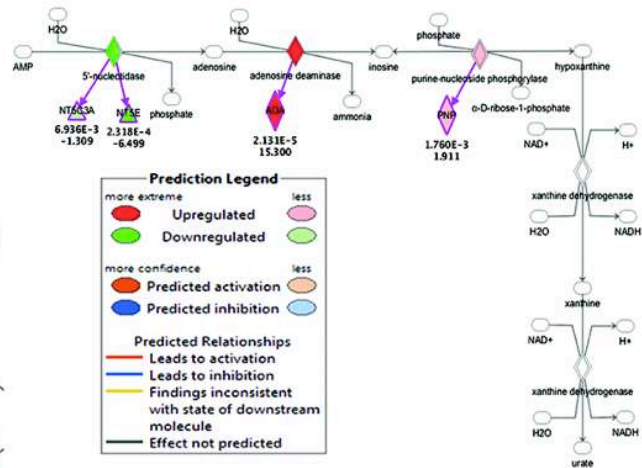


Figure 2.9: TGF- β and adenosine pathway analysis and gene interactions of Ad-MSC vs. BM-MSC. (2.9A) TGF- β network analysis was performed with IPA software, and depicts upregulated and downregulated genes in Ad-MSC vs. BM-MSC, and interactions involved in TGF- β signaling pathways (see prediction legend for color coding). **(2.9B)** Adenosine network analysis performed with IPA software depicts genes upregulated and downregulated in Ad-MSC vs. BM-MSC, and interactions involved in purine biosynthesis.

Discussion.

Studies in spontaneous, large animal disease models can serve as an important role for assessment of stem cell therapies ultimately intended for use in humans. Dogs develop many of the same inflammatory and autoimmune diseases as humans and thus clinical studies of stem cell therapy in these canine models can be particularly informative with respect to safety and potential efficacy, in time frames much accelerated compared to human studies ⁶⁵.

However, it is also known that the mechanism(s) of action of MSC varies amongst species. For example, IDO-dependent mechanisms of immune modulation by MSC dominate in humans, non-human primates, and pigs, whereas in rabbits and rodents NO-dependent mechanisms of immune suppression are much more important ^{20, 34, 66-68}. Therefore, it is useful for evaluating MSC therapy in spontaneous disease models such as dogs to determine which immune modulatory pathways are operative. Based on the studies reported here, we conclude that MSC from dogs utilize different pathways than either humans or rodents, relying primarily on the TGF- β pathway, adenosine pathway, and cyclooxygenase pathways for T cell suppression.

We did not find evidence for utilization of either the NO or IDO pathways by canine MSC. These results differ from those of Kang et al, who reported that the IDO pathway was operative in canine Ad-MSC mediated suppression of T cells ⁵⁰. However, Kang et al also reported that canine co-culture with MSC resulted in an increased production of the inflammatory cytokine IFN γ , rather than suppression as we found in our studies. In their culture system irradiated MSCs were also used, along with multiple growth factors in the culture media; which may have had an effect on cellular responses and signaling. Nonetheless, in our studies we utilized two different inhibitors of the IDO pathway (1-MT and CAY 10581), at previously

published doses^{50, 69, 70}, and failed to find evidence for IDO-dependent T cell suppression by canine MSC. Therefore, while we cannot fully explain the discrepancy between our studies and those of Kang et al, we believe that results are consistent with the conclusion that the IDO pathway does not play an important role in T cell suppression by canine MSC.

Previous studies have revealed important differences between Ad-MSC and BM-MSC with respect to a variety of different properties, including osteogenesis, protection from sepsis, and healing of cardiac infarction⁷¹⁻⁷⁴. Recently, the immune modulatory properties of human Ad-MSC and BM-MSC were compared⁷⁵. In these studies, there were differences in cytokine secretion profiles between the two types of MSC, but when tested for T cell suppression activity, the differences observed were relatively minor. Likewise, our studies also did not detect important differences in potency between canine Ad-MSC and BM-MSC in terms of suppression of T cell activation. Moreover, the pathways used for immune modulation were also similar, with one important exception. In the case of canine BM-MSC, the cyclooxygenase pathway was identified as an important pathway for T cell suppression, in addition to the TGF- β and adenosine receptor-mediated pathways. Identification of the cyclooxygenase pathway for T cell suppression by canine BM-MSC is in agreement with a previous study that also identified PGE2 production as a major mediator of T cell suppression by canine MSC⁷⁶. However, this previous study did not evaluate the activity of other T cell suppression pathways.

It is now accepted that MSC generally do not exert their immune suppressive effects until they are activated to upregulate T cell suppressive pathways by pro-inflammatory cytokines, especially IFN- γ ^{35, 36}. Indeed, several studies have revealed that when MSC are administered in the absence of IFN- γ or other inflammatory signals, they fail to exert significant immune modulatory activity^{35, 77}. Thus, we conducted studies to determine whether MSC activation by

IFN- γ was also required for activity by canine MSC. Thus, we observed that when MSC were co-cultured with activated T cells, and IFN- γ release was neutralized at the initiation of the co-cultures, T cell suppression was also significantly abrogated (**Figure 2.5**). Therefore, it appears that canine MSC, like human and mouse MSC, must also be “licensed” by inflammatory cytokines to become functionally active in immune modulation.

Our studies also investigated other processes by which MSC might elicit immune downmodulation, in addition to suppression of T cell proliferation and reduction in cytokine production. For example, a net loss of activated T cells via increased cell death could over time lead to immune suppression. Thus, we evaluated T cell apoptosis and cell death responses to MSC using *in vitro* co-cultures. Activation of T cells with ConA in itself (without addition of MSC) induced a significant increase in early and late T cell apoptosis, and co-culture with Ad-MSC or BM-MSC did not significantly accelerate this process (see **Figure 2.6**). However, T cell death was significantly increased when activated T cells were co-cultured with MSC, particularly at later time points in culture (see **Figure 2.6**). These findings suggest that MSC may indirectly induce necrotic cell death in activated T cells, an effect that would result in an overall net loss of T cells in inflamed sites or where T cells might be exposed to accumulated MSC, such as the lungs, spleen, or lymph nodes.

The phenotype of canine Ad-MSC and BM-MSC was found to be relatively similar, based on cell surface marker expression, growth characteristics in culture, and expression of certain intracellular stem cell markers, though some morphological differences were noted (see **Figures 2.1 and 2.2**). Gene expression analysis however revealed several important differences in genes related to immunological functions between Ad-MSC and BM-MSC. For example, Gene Ontology (GO) enrichment analysis of differential gene expression (based on $p < 0.05$

differences) revealed a significant enrichment of two genes in the adenosine metabolic process and also in two genes involved in the prostaglandin metabolic process, and enrichment of >5 genes in the TGF- β signaling and binding pathways in Ad-MSc versus BM-MSc (**Figure 2.9**). In Ad-MSc expression of the PLA2G5 gene for phospholipase A2 and the PTGS2 gene (Prostaglandin-Endoperoxide Synthase 2) involved in PGE synthesis were both down regulated, which is consistent with the lack of response of Ad-MSc to PGE2 COX1 and COX2 pathway inhibitors.

Pathway analysis also showed differential expression of genes regulated downstream of the TGF- β receptor (**Figure 2.9**). These findings highlight the complexity of the cell regulatory networks operative in both Ad-MSc and BM-MSc and help explain how blocking TGF- β receptor signaling might have very tissue-specific effects. The adenosine pathway analysis also demonstrated up regulation of the adenosine deaminase (ADA) gene in Ad-MSc, a gene that is involved in purine synthesis (Supplementary Figure 2).

In summary, we found that canine Ad-MSc and BM-MSc were roughly equivalent in terms of their immune modulation potency and their surface phenotypic properties, and they resembled in many respects analogous populations of human and rodent MSC. Overall, relatively minor differences were uncovered in gene expression patterns between Ad-MSc and BM-MSc; with the most notable differences being in the VEGF signaling pathway, which is upregulated in Ad-MSc, and the connective tissue and bone differentiation pathways, which are upregulated in the BM-MSc.

Canine MSC were found to rely on relatively distinct pathways of T cell suppression relative to MSC from humans and rodents, preferentially utilizing TGF- β , Adenosine, and cyclooxygenase pathways to a much greater degree than IDO or NO-dependent pathways.

Induction of T cell necrosis by canine MSC also appeared to be an additional mechanism of immune modulation. These findings help to provide a better understanding of canine MSC biology and will serve to facilitate studies of MSC-based therapies for modulation of inflammatory diseases in spontaneous models of canine disease.

REFERENCES

1. Gu F, Wang D, Zhang H, et al. Allogeneic mesenchymal stem cell transplantation for lupus nephritis patients refractory to conventional therapy. *Clin Rheumatol*. 2014;33:1611-1619.
2. Sun L, Wang D, Liang J, et al. Umbilical cord mesenchymal stem cell transplantation in severe and refractory systemic lupus erythematosus. *Arthritis Rheum*. 2010;62:2467-2475.
3. Wang D, Zhang H, Liang J, et al. Allogeneic mesenchymal stem cell transplantation in severe and refractory systemic lupus erythematosus: 4 years of experience. *Cell Transplant*. 2013;22:2267-2277.
4. Tyndall A. Mesenchymal stromal cells and rheumatic disorders. *Immunol Lett*. 2015;168:201-207.
5. Tyndall A, van Laar JM. Stem cells in the treatment of inflammatory arthritis. *Best Pract Res Clin Rheumatol*. 2010;24:565-574.
6. Waterman RS, Tomchuck SL, Henkle SL, et al. A new mesenchymal stem cell (MSC) paradigm: Polarization into a pro-inflammatory msc1 or an immunosuppressive msc2 phenotype. *PloS one*. 2010;5:e10088.
7. Le Blanc K, Davies LC. Mesenchymal stromal cells and the innate immune response. *Immunology Letters*. 2015;168:140-146.
8. Klinker MW, Wei C-H. Mesenchymal stem cells in the treatment of inflammatory and autoimmune diseases in experimental animal models. *World Journal of Stem Cells*. 2015;7:556-567.
9. Ko IK, Kim B-G, Awadallah A, et al. Targeting improves MSC treatment of inflammatory bowel disease. *Molecular Therapy*. 2010;18:1365-1372.
10. Augello A, Tasso R, Negrini SM, et al. Cell therapy using allogeneic bone marrow mesenchymal stem cells prevents tissue damage in collagen-induced arthritis. *Arthritis & Rheumatism*. 2007;56:1175-1186.
11. Gupta N, Su X Fau - Popov B, Popov B Fau - Lee JW, et al. Intrapulmonary delivery of bone marrow-derived mesenchymal stem cells improves survival and attenuates endotoxin-induced acute lung injury in mice. 2007.
12. Baron F, Storb R. Mesenchymal stromal cells: A new tool against graft-versus-host disease? *Biol Blood Marrow Transplant*. 2012;18:822-840.

13. Bruck F, Belle L, Lechanteur C, et al. Impact of bone marrow-derived mesenchymal stromal cells on experimental xenogeneic graft-versus-host disease. *Cytherapy*. 2013;15:267-279.
14. Gordon D, Pavlovska G, Glover CP, et al. Human mesenchymal stem cells abrogate experimental allergic encephalomyelitis after intraperitoneal injection, and with sparse cns infiltration. *Neuroscience letters*. 2008;448:71-73.
15. Zhou K, Zhang H Fau - Jin O, Jin O Fau - Feng X, et al. Transplantation of human bone marrow mesenchymal stem cell ameliorates the autoimmune pathogenesis in mrl/lpr mice. 2009.
16. Liu Y, Mu R Fau - Wang S, Wang S Fau - Long L, et al. Therapeutic potential of human umbilical cord mesenchymal stem cells in the treatment of rheumatoid arthritis. 2010.
17. Gonzalez MA, Gonzalez-Rey E Fau - Rico L, Rico L Fau - Buscher D, et al. Adipose-derived mesenchymal stem cells alleviate experimental colitis by inhibiting inflammatory and autoimmune responses. 2009.
18. Shi Y, Su J, Roberts AI, et al. How mesenchymal stem cells interact with tissue immune responses. *Trends Immunol*. 2012;33:136-143.
19. Ma S, Xie N, Li W, et al. Immunobiology of mesenchymal stem cells. *Cell Death Differ*. 2014;21:216-225.
20. Hoogduijn MJ, Popp F, Verbeek R, et al. The immunomodulatory properties of mesenchymal stem cells and their use for immunotherapy. *International immunopharmacology*. 2010;10:1496-1500.
21. Su J, Chen X, Huang Y, et al. Phylogenetic distinction of inos and ido function in mesenchymal stem cell-mediated immunosuppression in mammalian species. *Cell Death Differ*. 2014;21:388-396.
22. Ling W, Zhang J Fau - Yuan Z, Yuan Z Fau - Ren G, et al. Mesenchymal stem cells use IDO to regulate immunity in tumor microenvironment. 2014.
23. Aggarwal S, Pittenger MF. Human mesenchymal stem cells modulate allogeneic immune cell responses. 2005.
24. Chen K, Wang D Fau - Du WT, Du Wt Fau - Han Z-B, et al. Human umbilical cord mesenchymal stem cells huc-mscs exert immunosuppressive activities through a pge2-dependent mechanism. 2010.
25. Hegyi B, Kudlik G Fau - Monostori E, Monostori E Fau - Uher F, et al. Activated t-cells and pro-inflammatory cytokines differentially regulate prostaglandin e2 secretion by mesenchymal stem cells. 2012.

26. Xu C, Yu P Fau - Han X, Han X Fau - Du L, et al. TGF-beta promotes immune responses in the presence of mesenchymal stem cells. 2013.
27. Ortiz LA, Dutreil M, Fattman C, et al. Interleukin 1 receptor antagonist mediates the antiinflammatory and antifibrotic effect of mesenchymal stem cells during lung injury. *Proceedings of the National Academy of Sciences of the United States of America*. 2007;104:11002-11007.
28. Juge-Aubry CE, Somm E Fau - Chicheportiche R, Chicheportiche R Fau - Burger D, et al. Regulatory effects of interleukin (IL)-1, interferon-beta, and il-4 on the production of il-1 receptor antagonist by human adipose tissue. 2004.
29. Rizzo R, Campioni D Fau - Stignani M, Stignani M Fau - Melchiorri L, et al. A functional role for soluble HLA-g antigens in immune modulation mediated by mesenchymal stromal cells. 2008.
30. Selmani Z, Naji A Fau - Zidi I, Zidi I Fau - Favier B, et al. Human leukocyte antigen-g5 secretion by human mesenchymal stem cells is required to suppress t lymphocyte and natural killer function and to induce cd4+cd25highfoxp3+ regulatory t cells. 2008.
31. Wang WB, Yen ML, Liu KJ, et al. Interleukin-25 mediates transcriptional control of pd-11 via stat3 in multipotent human mesenchymal stromal cells (hMSCs) to suppress th17 responses. 2015.
32. Gu YZ, Xue Q Fau - Chen Y-j, Chen Yj Fau - Yu G-H, et al. Different roles of pd-11 and FASL in immunomodulation mediated by human placenta-derived mesenchymal stem cells. 2013.
33. Ren G, Zhang L, Zhao X, et al. Mesenchymal stem cell-mediated immunosuppression occurs via concerted action of chemokines and nitric oxide. *Cell stem cell*. 2008;2:141-150.
34. Ren G, Su J, Zhang L, et al. Species variation in the mechanisms of mesenchymal stem cell-mediated immunosuppression. *Stem cells*. 2009;27:1954-1962.
35. Sheng H, Wang Y, Jin Y, et al. A critical role of IFN [gamma] in priming MSC-mediated suppression of t cell proliferation through up-regulation of b7-h1. *Cell Res*. 2008;18:846-857.
36. Krampera M, Cosmi L, Angeli R, et al. Role for interferon-gamma in the immunomodulatory activity of human bone marrow mesenchymal stem cells. *Stem cells*. 2006;24:386-398.
37. Tomchuck SL, Zvezdaryk Kj Fau - Coffelt SB, Coffelt Sb Fau - Waterman RS, et al. Toll-like receptors on human mesenchymal stem cells drive their migration and immunomodulating responses. 2008.

38. Jung YJ, Ju Sy Fau - Yoo ES, Yoo Es Fau - Cho SJ, et al. MSC-dc interactions: MSC inhibit maturation and migration of BM-derived DC. 2007.
39. English K, Barry Fp Fau - Mahon BP, Mahon BP. Murine mesenchymal stem cells suppress dendritic cell migration, maturation and antigen presentation. 2007.
40. Nauta AJ, Kruisselbrink Ab Fau - Lurvink E, Lurvink E Fau - Willemze R, et al. Mesenchymal stem cells inhibit generation and function of both cd34+-derived and monocyte-derived dendritic cells. 2006.
41. Zeira O, Asiag N, Aralla M, et al. Adult autologous mesenchymal stem cells for the treatment of suspected non-infectious inflammatory diseases of the canine central nervous system: Safety, feasibility and preliminary clinical findings. *J Neuroinflammation*. 2015;12:181.
42. Villatoro AJ, Fernandez V, Claros S, et al. Use of adipose-derived mesenchymal stem cells in keratoconjunctivitis sicca in a canine model. *Biomed Res Int*. 2015;2015:527926.
43. Ferrer L, Kimbrel EA, Lam A, et al. Treatment of perianal fistulas with human embryonic stem cell-derived mesenchymal stem cells: A canine model of human fistulizing crohn's disease. *Regen, Med*. 2016.
44. Black LL, Gaynor J, Adams C, et al. Effect of intraarticular injection of autologous adipose-derived mesenchymal stem and regenerative cells on clinical signs of chronic osteoarthritis of the elbow joint in dogs. *Vet Ther*. 2008;9:192-200.
45. Cuervo B, Rubio M, Sopena J, et al. Hip osteoarthritis in dogs: A randomized study using mesenchymal stem cells from adipose tissue and plasma rich in growth factors. *Int J Mol Sci*. 2014;15:13437-13460.
46. Guercio A, Di Marco P, Casella S, et al. Production of canine mesenchymal stem cells from adipose tissue and their application in dogs with chronic osteoarthritis of the humeroradial joints. *Cell Biol Int*. 2012;36:189-194.
47. Hiyama A, Mochida J, Iwashina T, et al. Transplantation of mesenchymal stem cells in a canine disc degeneration model. *J Orthop Res*. 2008;26:589-600.
48. Yun S, Ku SK, Kwon YS. Adipose-derived mesenchymal stem cells and platelet-rich plasma synergistically ameliorate the surgical-induced osteoarthritis in beagle dogs. *J Orthop Surg Res*. 2016;11:9.
49. Whitworth DJ, Banks TA. Stem cell therapies for treating osteoarthritis: Prescient or premature? *Vet J*. 2014;202:416-424.
50. Kang JW, Kang KS, Koo HC, et al. Soluble factors-mediated immunomodulatory effects of canine adipose tissue-derived mesenchymal stem cells. *Stem cells and development*. 2008;17:681-693.

51. Mielcarek M, Storb R, Georges GE, et al. Mesenchymal stromal cells fail to prevent acute graft-versus-host disease and graft rejection after dog-leukocyte-antigen haploidentical bone marrow transplantation. *Biology of blood and marrow transplantation : journal of the American Society for Blood and Marrow Transplantation*. 2011;17:214-225.
52. Kim H-S, Kim K-H, Kim S-H, et al. Immunomodulatory effect of canine periodontal ligament stem cells on allogenic and xenogenic peripheral blood mononuclear cells. *Journal of Periodontal & Implant Science*. 2010;40:265-270.
53. Clark KC, Kol A, Shahbenderian S, et al. Canine and equine mesenchymal stem cells grown in serum free media have altered immunophenotype. *Stem Cell Reviews*. 2016;12:245-256.
54. Lee WS, Suzuki Y, Graves SS, et al. Canine bone marrow derived mesenchymal stromal cells suppress allo-reactive lymphocyte proliferation in vitro but fail to enhance engraftment in canine bone marrow transplantation. *Biology of blood and marrow transplantation : journal of the American Society for Blood and Marrow Transplantation*. 2011;17:465-475.
55. Whitworth DJ, Frith JE, Frith TJ, et al. Derivation of mesenchymal stromal cells from canine induced pluripotent stem cells by inhibition of the TGF beta/activin signaling pathway. *Stem cells and development*. 2014;23:3021-3033.
56. Jiang Y, Jahagirdar BN, Reinhardt RL, et al. Pluripotency of mesenchymal stem cells derived from adult marrow. *Nature*. 2002;418:41-49.
57. Wang X, Dai J. Concise review: Isoforms of oct4 contribute to the confusing diversity in stem cell biology. *Stem Cells (Dayton, Ohio)*. 2010;28:885-893.
58. Glenn JD, Whartenby KA. Mesenchymal stem cells: Emerging mechanisms of immunomodulation and therapy. *World Journal of Stem Cells*. 2014;6:526-539.
59. Kyurkchiev D, Bochev I, Ivanova-Todorova E, et al. Secretion of immunoregulatory cytokines by mesenchymal stem cells. *World Journal of Stem Cells*. 2014;6:552-570.
60. Krampera M. Mesenchymal stromal cell 'licensing': A multistep process. *Leukemia*. 2011;25:1408-1414.
61. Aggarwal S, Pittenger MF. Human mesenchymal stem cells modulate allogeneic immune cell responses. *Blood*. 2005;105:1815-1822.
62. Carrade Holt DD, Wood Ja Fau - Granick JL, Granick JI Fau - Walker NJ, et al. Equine mesenchymal stem cells inhibit t cell proliferation through different mechanisms depending on tissue source. 2014.
63. Plumas J, Chaperot L Fau - Richard MJ, Richard Mj Fau - Molens JP, et al. Mesenchymal stem cells induce apoptosis of activated t cells. 2005.

64. Akiyama K, Chen C, Wang D, et al. Mesenchymal stem cell-induced immunoregulation involves FAS ligand/ FAS-mediated t cell apoptosis. *Cell stem cell*. 2012;10:544-555.
65. Hoffman AM, Dow SW. Concise review: Stem cell trials using companion animal disease models. *STEM CELLS*. 2016;n/a-n/a.
66. Gao F, Chiu SM, Motan DA, et al. Mesenchymal stem cells and immunomodulation: Current status and future prospects. *Cell Death, Dis*. 2015.
67. Ren G, Su J, Zhang L, et al. Species variation in the mechanisms of mesenchymal stem cell-mediated immunosuppression. *Stem cells*. 2009;27:1954-1962.
68. Khatri M, O'Brien TD, Chattha KS, et al. Porcine lung mesenchymal stromal cells possess differentiation and immunoregulatory properties. *Stem cell research & therapy*. 2015;6:222.
69. Yang S-H, Park M-J, Yoon I-H, et al. Soluble mediators from mesenchymal stem cells suppress t cell proliferation by inducing il-10. *Experimental & Molecular Medicine*. 2009;41:315-324.
70. Kuçi Z, Seiberth J, Latifi-Pupovci H, et al. Clonal analysis of multipotent stromal cells derived from cd271(+) bone marrow mononuclear cells: Functional heterogeneity and different mechanisms of allosuppression. *Haematologica*. 2013;98:1609-1616.
71. Elman JS, Li M, Wang F, et al. A comparison of adipose and bone marrow-derived mesenchymal stromal cell secreted factors in the treatment of systemic inflammation. *J Inflamm (Lond)*. 2014;11:1.
72. Liao HT, Chen CT. Osteogenic potential: Comparison between bone marrow and adipose-derived mesenchymal stem cells. *World J Stem Cells*. 2014;6:288-295.
73. Szepes M, Benko Z, Cselenyak A, et al. Comparison of the direct effects of human adipose- and bone-marrow-derived stem cells on postischemic cardiomyoblasts in an in vitro simulated ischemia-reperfusion model. *Stem Cells Int*. 2013;2013:178346.
74. Rasmussen JG, Frobert O, Holst-Hansen C, et al. Comparison of human adipose-derived stem cells and bone marrow-derived stem cells in a myocardial infarction model. *Cell Transplant*. 2014;23:195-206.
75. Ock SA, Baregundi Subbarao R, Lee YM, et al. Comparison of immunomodulation properties of porcine mesenchymal stromal/stem cells derived from the bone marrow, adipose tissue, and dermal skin tissue. *Stem Cells Int*. 2016;2016:9581350.
76. Mielcarek M, Storb R, Georges GE, et al. Mesenchymal stromal cells fail to prevent acute graft-versus-host disease and graft rejection after dog leukocyte antigen-haploidentical bone marrow transplantation. *Biol Blood Marrow Transplant*. 2011;17:214-225.

77. Ren G, Zhang L, Zhao X, et al. Mesenchymal stem cell-mediated immunosuppression occurs via concerted action of chemokines and nitric oxide. *Cell stem cell*. 2008;2:141-150.

CHAPTER 3

Safety and Immune Regulatory Properties of Canine Induced Pluripotent Stem Cell-Derived Mesenchymal Stem Cells

Summary

Mesenchymal stem cells (MSCs) exhibit broad immune modulatory activity *in vivo* and can suppress T cell proliferation and dendritic cell activation *in vitro*. Currently, most MSC for clinical usage are derived from younger donors, due to ease of procurement and to the superior immune modulatory activity. However, the use of MSC from multiple unrelated donors makes it difficult to standardize study results and compare outcomes between different clinical trials. One solution is the use of MSC derived from induced pluripotent stem cells (iPSC); as iPSC-derived MSC have nearly unlimited proliferative potential and exhibit *in vitro* phenotypic stability.

These studies were designed to investigate the hypothesis that MSCs generated from iPSCs have immune modulation properties equivalent to primary tissue derived AD-MSC and BM-MSC, and can be used safely for cellular therapy. We investigated the functional properties of canine iPSC-derived MSC (iMSC), including immune modulatory properties and potential for teratoma formation. We found that canine iMSC downregulated expression of pluripotency genes and appeared morphologically similar to conventional MSC. Importantly, iMSC retained a stable phenotype after multiple passages, did not form teratomas in immune deficient mice, and did not induce tumor formation in dogs following systemic injection. We concluded therefore that iMSC were phenotypically stable, immunologically potent, safe with respect to tumor formation, and represented an important new source of cells for therapeutic modulation of inflammatory disorders.

Background

Induced pluripotent stem cells (iPSCs) are stem cells derived from adult somatic cells by reprogramming through transient expression of specific transcription factors (Oct3/4, SOX2, Klf4, and c-Myc) ¹. Like embryonic stem cells, iPSC are capable of unlimited expansion, and can potentially differentiate into any cell type in the body. At present, most clinical studies of stem cell therapy utilize MSC derived from adipose tissues or bone marrow ². However, the use of MSC for cellular therapy poses several challenges. For one, autologous MSC are difficult to generate from older patients, and their functionality is often impaired compared to MSC generated from young individuals ^{3,4}. Use of allogeneic MSC derived from young donors offers a means of overcoming the limitations of autologous MSC, but introduces new problems, including donor-to-donor variability, risk of iatrogenically introduced infectious agents, and the potential for alloimmune rejection ^{5,6}.

One means of overcoming the limitations inherent to the use of primary cultured MSC for clinical studies is to use MSC derived from iPSC ^{7,8}. For example, MSC generated from iPSC offer several advantages, including unlimited passage potential, uniform cell sourcing and phenotyping, and the ability to select and/or modify iPSC-derived MSC for specific desirable properties ^{9,10}. Therefore, there is increasing interest in the use of uniform source MSC such as iPSC-derived MSC for evaluation in clinical settings.

As noted in a recent review, domestic dogs offer several important advantages as animal models for stem cell therapy evaluation, including the spontaneous development of diseases that closely mimic human disease (e.g. autoimmune diseases, inflammatory bowel disease, neurological disease, and cancer), a shared environment with humans, and the availability of an outbred population with robust immune systems and lifelong exposure to diverse pathogens ¹¹.

Induced pluripotent stem cells have been generated from adult dog fibroblasts, but thus far have only been produced using integrating retroviral gene transduction methodologies¹²⁻²⁰. There are risks however to the use of retroviral gene transduction methodologies, including alterations of the host genome, or neoplasm formation²¹.

In previous studies using rodent models, iMSC have been evaluated as cellular therapy for suppression of inflammatory diseases^{9,22}. The evaluation of human iPSC derived cells for therapy has been subjected to extremely stringent government regulations, and only one study has been conducted so far worldwide²³. Thus, the evaluation of iPSC cellular therapeutics in a large animal model to assess safety and efficacy could significantly advance the field of stem cell therapy and iPS cell based treatments.

Therefore in the current report we evaluated the immune modulatory properties of canine iMSC and compared their efficacy to that of conventional adipose and bone marrow-derived MSC. In addition, we assessed iMSC safety in terms of teratoma and tumor formation, using both immune deficient mouse models and purpose-bred dogs. We report here that canine iMSC were functionally equivalent to or superior to conventional Ad-MSC and BM-MSC in terms of their *in vitro* immune suppressive potency, for both T cell and DC suppression. In addition, while canine iPSC readily induced teratomas in immune deficient mice, canine iMSC did not induce teratoma formation. Most importantly, dogs injected i.v. with canine iMSC did not develop detectable tumors over a 1-year period of observation and imaging. Therefore, we conclude that cellular therapy with allogeneic iMSC holds promise as a well-tolerated and potentially effective new cellular therapy for treatment of inflammatory disorders.

Materials and Methods

Culture medium for MSC, T cells and iPSC.

Ad-MSC, BM-MSC and T cells were cultured in MSC media containing DMEM, Glutamax 1x, Pen/Strep 1x, NEAA 1x, b-mercaptoethanol (ThermoFisher, Waltham, MA), 10% FBS (VWR Life Science, Radnor, PA). iPSC colonies were maintained in iPSC media containing KO-DMEM, Glutamax 1x, Pen/Strep 1x, NEAA 1x, beta-mercaptoethanol 55 μ M (ThermoFisher, Waltham, MA), 20% FBS (VWR Life Science, Radnor, PA) and LIF (human Leukemia inhibitory factor) 1000 U/mL (Merck Millipore, Billerica, MA). iMSC were maintained in MSC media with KO-DMEM.

Generation of canine skin fibroblasts.

All procedures involving live animals were approved by the Institutional Animal Care and Use Committee at Colorado State University. Skin biopsies were obtained from a single healthy adult dog and the adherent adipose tissues were removed from the epidermis by scraping with scalpel blade. Biopsy samples were cut into small sections measuring 2 mm². In each well of a 6-well tissue culture plate in MSC medium with the addition of 1 mM Sodium Pyruvate (ThermoFisher, Waltham, MA), 2-3 biopsy specimens were placed and covered with 22 mm² glass cover slips (ThermoFisher, Waltham, MA). Fibroblast outgrowth was observed after approximately 2 weeks in culture. Once confluent, skin fibroblasts were removed from surrounding edges of biopsy specimen using trypsin EDTA (Life Technologies Corp. Grand Island NY) and frozen at the second passage for further use.

Generation of canine induced pluripotent stem cells.

Canine iPSC were generated by the Colorado University Denver, Charles C. Gates Center for Regenerative Medicine and Stem Cell Biology iPSC Core. Transgene integration-free iPS

cells were generated from canine skin fibroblast using a CytoTune iPS Reprogramming kit (Life Technologies Corp. Grand Island NY). Donor skin biopsy was collected using 6mm skin biopsy punch (Miltex, York, PA) from a 6-year old dog. Donor dog was screened using a complete blood count and serum biochemistry panel, tested negative for Hemoplasma species, Ehrlichia species, Rickettsial species, Bartonella species using PCR, and negative for vector borne diseases using IDEXX 4DX – snap test for companion animals (IDEXX Laboratories, Inc. Westbrook, ME).

Skin fibroblasts from the donor animals were incubated overnight with CytoTune reprogramming vectors, and cultured 7 days before transferring to irradiated MEF (mouse embryonic fibroblasts) feeder cells (Global Stem, Gaithersburg, MD). Flat multinucleated iPSC colonies were observed approximately 14 days after transfection, and each colony was picked manually and expanded individually in a single well on MEF. The iPSC colonies so derived were maintained in iPSC medium and cultured on MEFs. MEFs were plated on a 0.1% gelatin substrate (Merck Millipore, Billerica, MA) at 2×10^4 cells per cm^2 .

Generation of canine adipose-derived MSC (Ad-MSC) and bone marrow derived MSC (BM-MSC).

All procedures involving live animals were approved by the Institutional Animal Care and Use Committee at Colorado State University. To generate Ad-MSC, adipose tissues (0.5g) was collected from single dog using a biopsy tool. Adipose tissue was washed with sterile PBS and minced with scalpel blades. Adipose tissue was then collected into 50 mL conical tubes (ThermoFisher, Waltham, MA) and digested with 1mg/mL of collagenase type I (Sigma-Aldrich, St. Louis MO), for 30 min at 37°C. After 30 min, complete MSC medium was added to inactivate collagenase. Cells were then collected by centrifugation and plated in T75 cell culture

flasks (Corning Inc. Corning, NY). The first media change was performed 3 days after plating, with subsequent media changes every 3 days and passaged when reaching 80% confluency.

Bone marrow aspirates from a single dog was collected by means of bone marrow needles from the proximal humerus of healthy adult dog that was anesthetized. Bone marrow chunks were cut into smaller pieces using sterile scalpels and washed twice with PBS. Bone marrow was then collected into 50 mL conical and digested with 1mg/mL of collagenase for 45 min in 37°C. Cells were pelleted after digestion by centrifugation and plated in T75 flask with MSC media. . Non-adherent cells were removed at the first medium change at 96 hours and the adherent cells were re-fed with MSC medium. Adherent cells with an MSC morphology were detached by brief trypsinization (ThermoFisher, Waltham, MA) and re-plated in fresh flasks, in order to eliminate more tightly adherent monocytes and macrophages from the cultures. Media changes were performed every 3 days and cells were passaged by trypsinization when reaching 80% confluency.

Generation of iPS-derived mesenchymal stem cells (iMSC).

Canine iPS colonies were detached from feeder layers by incubation with 1 U/mL dispase (Stemcell Technologies Cambridge, MA) for 15 min at 37°C. Detached cells were collected and plated on Matrigel (Corning Inc. Corning, NY) coated plates in iPS maintenance media with addition of 10µM Rock Inhibitor (Y-27632) (Tocris Bristol, UK) for the first 24 hours. Media changes were performed daily. When plates reached 70% confluency, culture conditions were changed to generate iMSC. First, the iPSC culture medium was changed to MSC medium with addition of 10 uM TGF-β inhibitor (SB 431542) (Tocris Bristol, UK). The cells were then allowed to differentiate for 10 days with medium changes daily and addition of fresh SB431542. After 10 days, cells were detached and plated at concentration of 40,000 cells/cm² in T-75 cell

culture treated flasks with iMSC medium, which was counted as passage 0 (p0). Cells were grown to confluency and passaged (P1) at 20,000 cells/cm². At P2, the cell number was decreased to 10,000 cells/cm², and at P3 and subsequent passages, the cell number was decreased to 4,000 cells/cm². The iMSC line generated was verified by QC procedures standard to cellular therapies, and tested for sterility by aerobic bacterial and mycoplasma, and fungal culture. **Figure 3.0** details the experimental flow chart for the generation of iMSC.

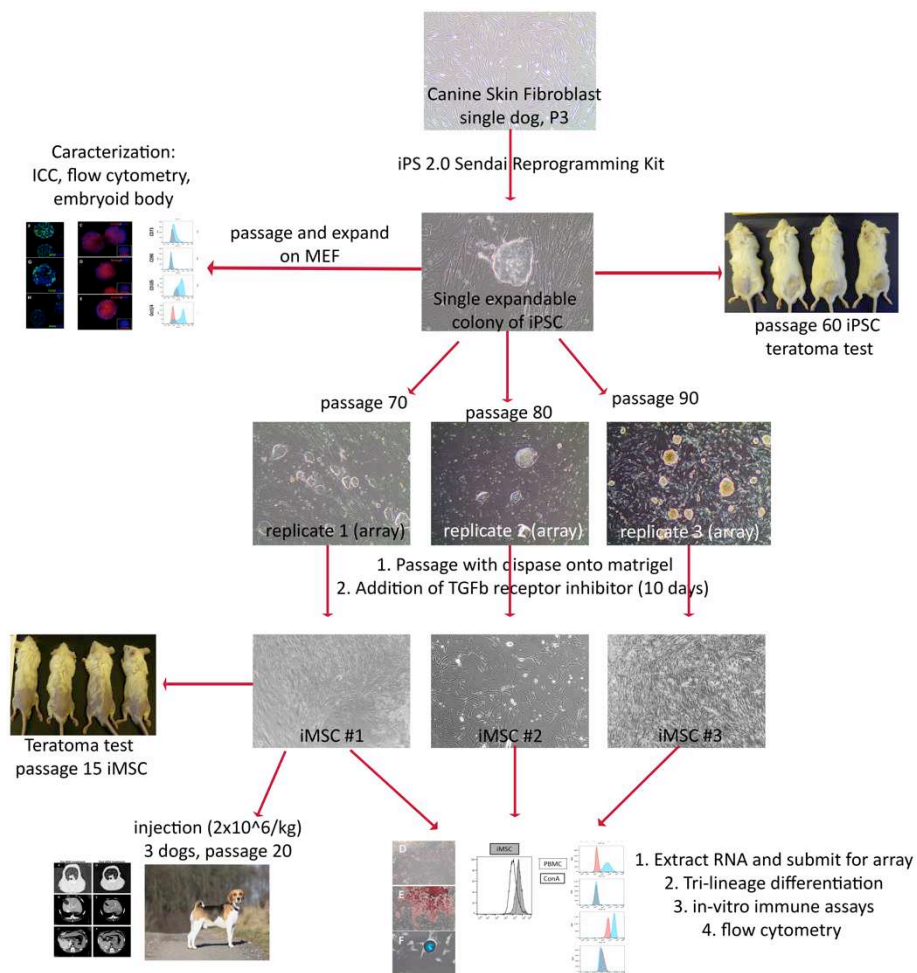


Figure 3.0 Experimental flow chart: generation of single canine iPSC line from skin fibroblast to generation of iMSC.

Bright field microscopy.

Bright field images were taken with an Olympus CKX41 microscope, using standard objective lenses. Digital images were captured using an Olympus SC30 camera and Olympus Soft Imaging getIT software.

Tri-lineage differentiation

Tri-lineage differentiation of iMSC was performed according to manufactures instructions using the StemPro Adipogenesis Differentiation Kit, the Chondrogenesis Differentiation Kit, and the Osteogenesis Differentiation Kit (Life Technologies Corp. Grand Island NY). At the completion of the differentiation protocol for each cell lineage, cells were incubated with appropriate stains: Oil red O for lipids in adipocytes, Alizarin Red calcium stain for osteocytes, and Alcian blue for glycosaminoglycans in chondrocytes. (Sigma-Aldrich, St. Louis, MO). Stained cells were photographed, using an Olympus CKX41 light microscope and attached SC30 digital camera.

Immunocytochemical evaluation of iPS cells.

Canine iPS colonies were lifted from MEF feeder layers by treatment with dispase for 15 min at 37°C. Whole colonies were plated on glass chamber slides (ThermoFisher, Waltham, MA) with addition of 10 μ M Rock Inhibitor (Y-27632) for 24 hours prior to staining. Each chamber was first washed with PBS, then fixed with 4% PFA (Affymetrix Santa Clara, CA) for 10 min at room temperature. Chamber wells were then washed with PBS, and permeabilized with 0.5% tritonX (ThermoFisher, Waltham, MA). Non-specific binding was minimized by incubation with 10% secondary antibody species serum plus 0.1% Triton for 1 hour prior to application of primary antibody. Each well was incubated with primary antibody overnight at 4°C. Primary antibodies used in these studies include: anti-Oct3/4 (clone H134, Santa Cruz

Biotechnology, Inc. Dallas, TX), anti-Nanog (Clone H-155 Santa Cruz Biotechnology Inc. Dallas, TX), and anti-CD105 (clone 8A1 Abcam, Cambridge, MA). Corresponding rabbit and mouse irrelevant isotype antibodies were used at concentrations matching the primary antibodies (eBioscience Inc, San Diego CA). After overnight incubation, cells were washed with PBS 0.05% tween and incubated with secondary antibody conjugated to biotin (donkey anti mouse IgG or donkey anti rabbit IgG; Jackson ImmunoResearch Laboratories, Inc. West Grove, PA). After 30 min incubation at room temperature, cells were washed with PBS 0.05% Tween and incubated another 15 min with Streptavidin conjugated Cy3 (Invitrogen, Carlsbad, CA), followed by DAPI counter stain (Sigma-Aldrich, St. Louis, MO). Visualization of fluorescence staining was performed on Olympus IX83 spinning disk confocal microscope. Images were imported as Tiff files to Photoshop CC 2015, and adjusted with high definition resolution (HDR) toning. For each antibody, adjusted HDR toning was saved as preset values and applied to corresponding isotype control stains as well.

Embryoid body (EB) generation.

Canine iPSC colonies were detached by Accutase (Stemcell Technologies Cambridge, MA) incubation for 15 min at 37°C. Colonies were digested to single cell suspensions and re-suspended in embryoid formation media containing (IMDM Life Technologies Corp. Grand Island NY), 15% FBS, Glutamax, Pen/Strep, NEAA, and 200uM ascorbic acid (Sigma-Aldrich St. Louis, MO), 55µM B-mercaptoethanol and 10µM ROCK inhibitor (Y-27632) (Tocris Bristol, UK) at 10µM. Cells were allowed to aggregate on 100mm Ultra-Low Attachment culture dish (Corning Inc. Corning, NY) for 10~ 12 days, with medium changes every 3 days. Embryoid body (EB) spheroids were then collected and prepared for staining. Prior to staining, EBs were fixed for 30 min in 4% PFA, then placed in serial dilution of PBS-buffered sucrose (Thermo

Fisher Waltham, MA) solutions (10, 20 and 30%, in sequence) at room temperature, each solution replaced every 30 min⁴⁸. Embryoid body spheres were then embedded in OCT (optimal cutting temperature) compound (Scigen Scientific Gardena, CA) and cryosectioned to 5µM thickness on poly-L-Lysine (Sigma-Aldrich, St. Louis, MO) coated slides. Immunocytochemical staining was then performed as previously described with primary antibodies αSMA (smooth muscle actin; clone ab5694 Abcam Cambridge, MA), TUJ1 (beta III tubulin; clone TUJ1 Covance Inc. San Diego, CA), AFP (α-Fetoprotein; clone C3 Sigma-Aldrich, St. Louis, MO). Biotin conjugated secondary antibodies were used followed by streptavidin, Alexa Fluor® 488 conjugate (Life Technologies Corp. Grand Island NY). Visualization of fluorescence staining was performed on Olympus IX83 spinning disk confocal microscope. Images were enhanced using Adobe Photoshop CC 2015 software. For each antibody, adjusted HDR toning was saved as preset values and applied to corresponding isotype control stains.

Teratoma assay for pluripotency verification of iPSC and evaluation of iMSC.

Canine iPSC colonies were detached from feeder layer using 1U/mL Dispase (Stemcell Technologies, Vancouver, BC) incubation for 15 min at 37°C. Cells were then resuspended in 30% Matrigel (Corning Inc. Corning, NY) with PBS at 2×10^7 cells/mL. Next, 100 µL of the cell suspension containing 2×10^6 iPS cells were injected s.c. into the flank of NOD/SCID mice (n = 4 mice per group). After 20 days, when tumor growth exceeded 10 mm diameter, tumors were excised after euthanizing mice. Tumors were fixed by immersion in 10% neutral buffered formalin and processed for standard hematoxylin and eosin (H&E) staining. H&E stained slides were evaluated by a board-certified veterinary pathologist (DR) to determine the presence of histological features consistent with all three germ layers.

The ability of iMSC to induce teratoma formation was evaluated similarly. Briefly, a suspension of 2×10^7 cells/ mL iMSC in 30% Matrigel was prepared, and 100 ul of this cell suspension was injected s.c. in NOD/SCID mice (n = 4 per group) in the flank, which was clipped. Mice were observed for 90 days for teratoma formation at the site of cell injection. At the completion of the study, the mice were euthanized, and tissues at the site of iMSC injection were harvested and fixed and processed for H & E staining and histological evaluation.

Measurement of proliferation using IncuCyte Zoom

To compare proliferation rates, iMSC, Ad-MSC and BM-MSC were plated at 20,000 cells per well in a 12-well cell culture plate (Corning Inc. Corning, NY), and placed in an IncuCyte® instrument (Essen BioScience Inc. Ann Arbor, MI). The default software parameters with IncuCyte phase-only processing module, and the 10X objective was used for imaging. IncuCyte software (Essen BioScience Inc. Ann Arbor, MI) was used to calculate mean confluence of 9 non-overlapping bright phase images per well, with triplicate wells per cell type evaluated. Images were taken every 6 hours over a period of 7 days.

Assessment of tumor formation by iMSC injection in dogs.

Three healthy, purpose-bred, adult Beagle dogs were injected i.v. with 2×10^6 iMSC per kg body weight, and tumor formation was monitored by whole body CT and clinical evaluation. CT evaluations were performed immediately before cell injection, and then repeated at 90 days. In addition, the dogs were monitored by monthly physical examinations for the remainder of 1 year after cell injection. Each of the dogs was placed in a home following study completion, and owners have been contacted to assess health status since the 1-year study was completed.

Flow cytometry for phenotyping

For analysis of the surface phenotype of Ad-MSC, BM-MSC and iMSC, cells were harvested by trypsinization and resuspended at a concentration of 1×10^6 cells/mL in FACS buffer (PBS, 2% FBS, and 0.1% sodium azide) on ice. 1×10^5 cells were plated in 96 well polystyrene round bottom plate and pelleted by centrifugation, then incubated with 5 μ L of dog serum to minimize Non-specific binding. Primary antibodies used for flow cytometry: CD24-PE (clone M1/69 eBioscience Inc. San Diego CA), CD34-FITC (clone 1H6 Serotech, Raleigh, NC), CD44-FITC (clone 1M7 eBioscience Inc. San Diego CA), CD45-FITC (clone YKIX716.13 Serotech, Raleigh, NC), CD73-biotin (clone TY/11.8, Biolegend. San Diego CA), CD90-APC (clone YKIX337.217, eBioscience Inc, San Diego CA), Oct3/4 (clone EM92, eBioscience Inc. San Diego CA), and unconjugated CD105 (clone 8A1, Abcam. Cambridge, MA). After primary antibody incubation, cells were washed and resuspended in FACS buffer for analysis. Samples stained with anti CD105 and Oct3/4 were stained according to eBioscience intracellular protocol prior to addition of primary antibody, with a 30 min pretreatment of fixation/ permeabilization solution (eBioscience Inc, San Diego CA). The secondary donkey anti mouse IgG-FITC (Jackson ImmunoResearch Laboratories, Inc. West Grove, PA) was added to unconjugated primary antibody CD105 stained cells, and Streptavidin FITC (eBioscience Inc, San Diego CA) was added to CD73-biotin stained cells.. Stained cells were then analyzed on Beckman Coulter Gallios flow cytometer. Histograms were generated with Flowjo 9.0.8 software (Tree Star, Ashland, OR)., with the x-axis representing florescence intensity and the y-axis representing cell count.

Flow cytometry of T cell proliferation and inhibition of DC maturation

For analysis of T cell proliferation by flow cytometry, non-adherent CFSE-labeled cells were collected from triplicate or quadruplicate wells at 96 hours, and then immunostained for detection of canine CD5⁺ cells, using an anti-canine CD5-APC (clone YKIX322.3, ABD Serotech, Raleigh, NC) then analyzed by flow cytometry. Histograms were generated using FlowJo 9.0.8 software. The CD5⁺ population of cells was first gated, and then the proliferation percent measured as the frequency of dividing cells that had reduced CFSE fluorescence compared to un-stimulated, CFSE-labeled CD5⁺ T cells. For analysis of canine DC, adherent PBMC were collected after 5 days in culture as described below, then immunostained with primary antibodies for 20 min in FACS buffer following a 5 min incubation with normal dog serum (Jackson ImmunoResearch Laboratories, Inc. West Grove, PA) to block non-specific binding. Antibodies used were as follows: mouse-anti-canine CD11c (clone CA11.6A1, Bio-Rad Hercules, CA) was used followed by a donkey anti-mouse conjugated with either APC or AlexaFluor 488 (Affymetrix-eBioscience, San Diego, CA); FITC-conjugated anti-canine MHCII (clone YKIX334.2 Bio-Rad, Hercules, CA), PE-conjugated anti-human (canine cross-reactive) CD86 (clone IT2.2 eBioscience, San Diego, CA). Stained cells were then analyzed using a Beckman Coulter Gallios flow cytometer (Beckman Coulter, Miami, FL) and data were analyzed using FlowJo software.

T cell inhibition assays.

MSC were collected by trypsinization and plated in triplicate wells in sterile 96-well flat bottom cell culture plates (Corning Inc. Corning, NY) at a density of 5×10^4 cells per well in 100 μ L of MSC medium. MSCs were incubated at 37°C for 1 hour prior to addition of peripheral blood mononuclear cells (PBMCs). For PBMC preparation, peripheral blood was collected from

the jugular or radial vein of healthy adult dogs into Vacutainer® tubes containing EDTA as an anticoagulant. To obtain PBMC, whole blood was diluted with an equal volume of sterile PBS and layered over LSM® (MP Biomedicals Inc. Santa Ana, CA) and centrifuged for 30 minutes. Mononuclear cells were collected and then labeled with CellTrace™ CFSE Cell Proliferation Kit (ThermoFisher, Waltham, MA), according to manufactures instructions. CFSE labeled cells were then plated in 100 ul MSC media at 5×10^5 cells per well to the existing MSCs for a final ratio of 1:10 MSC:PBMC. Activation of T cell proliferation was initiated by addition of Concavalin A (ConA) (Sigma-Aldrich, St. Louis, MO) at a concentration of 10 µg/mL. Cells in co-culture were incubated for 96 hours at 37°C. After 96 hours, the supernatant was collected (and stored frozen) for cytokine analysis and the cells were collected for flow cytometric analysis of proliferation, as noted above.

IFN-γ ELISA.

Supernatants were collected from T cell and MSC co-cultures at 96 hours. Secretion of IFN-γ was quantitated using a canine specific IFN-γ ELISA (R&D Systems, Minneapolis, MN), according to manufactures instructions.

Preparation of monocyte-derived DC.

Whole blood was collected from healthy adult dogs, and PBMC were prepared as noted in a recent report from our lab ²⁶. The PBMC were plated in 24-well plates at a density of $2.5-5 \times 10^6$ cells/well and allowed to adhere to the wells for 3-6 hrs at 37°C. The wells were then subsequently agitated gently with a pipette to remove non-adherent cells. The adherent monocytes were then placed in DC medium containing 50 ng/ml human GM-CSF and 10 ng/ml mouse IL-4 (PeproTech, Rock Hill, NJ). The DC differentiation medium was changed 48-72 hrs and full differentiation of monocytes to DC was apparent between 5 and 7 days as determined by

flow cytometry for expression of CD11c. CD11c^{hi} cells comprised >70% of cells in culture, and greater than 95% of the CD11c⁺ cells expressed MHCII and CD86 and CD40 (not shown). Maturation of immature DCs was achieved by treatment with 50 ng/ml LPS 055:B5 (InVivoGen, San Diego, California) for 24-36 hrs. Activated DCs displayed significant up regulation of surface expression of MHCII, CD86 and CD40 relative to untreated DCs, as assessed by flow cytometric analysis (not shown).

Effects of iMSC on DC maturation.

iMSC were cultured together with DC to assess their effects on DC maturation and activation, as noted previously with canine Ad-MSC and BM-MSC ²⁶. iMSCs were either untreated or treated for 18 hrs with 100 ng/ml canine IFN- γ (R&D Systems, Minneapolis, MN) prior to addition to iMSC cultures. iMSC were added to DCs approximately 30 min prior to stimulation with 50 ng/ml LPS. The ratio of iMSC to DC used was 1:10. The co-cultures were either untreated or treated with 50 ng/ml LPS for 24-36 hr and the loosely adherent DCs were harvested and separated from the tightly adherent MSCs by gentle agitation of the wells via gentle pipetting, which allowed selective harvesting of DC. The DC were immunostained with antibodies to CD11c, MHCII, CD86 and CD40 as noted above, and analyzed by flow cytometry for expression of activation and maturation phenotypes.

Comparison of gene expression profiles of iMSC, iPSC, and Ad-MSC and BM-MSC by microarray analysis.

Triplicate, independent cultures of iPSC, iMSC, Ad-MSC and BM-MSC, all derived from the same adult dog, were established as described above. Cellular RNA collected from semi-confluent cultures at the same time points in culture, using a Qiagen RNeasy mini kit (Qiagen, Hilden, Germany). The RNA was then labeled and hybridized to Canine Gene 1.0 ST

Arrays (Affymetrix, Santa Clara, CA), using standard Affymetrix protocols. Image files were converted to log₂ expression values with RMA (Robust Multiarray Average) background correction and quantile normalization, as implemented by a statistical/visualization package (Partek Genomics Suite v6.6; St Louis, MO). The normalized expression values used in the statistical and bioinformatics analysis for these studies, as well as the original raw visual data used to calculate these values, have been deposited in the publicly accessible database Gene Expression Omnibus (<http://www.ncbi.nlm.nih.gov/geo/>) under the accession number GSE90449 and GSE94081. The Database for Annotation, Visualization and Integrated Discovery (DAVID) v6.8 Beta was used to perform KEGG (Kyoto Encyclopedia of Genes and Genomes) pathway analysis on the significantly different genes, using a previously described protocol⁴⁹. The KEGG pathways were statistically significant at the default p-value <0.1.

Statistical analysis.

Comparisons between 3 or more groups were done using ANOVA, followed by Tukey multiple means post-test. Analyses comparing two groups of data were done using non-parametric t-test (Mann-Whitney). Analyses were done using Prism6 software (GraphPad, La Jolla, CA). For all analyses, statistical significance was determined for p<0.05.

Results

iPSC derived from canine adult fibroblasts demonstrate properties of self-renewal and pluripotency

Transfection of dog adult skin fibroblasts using non-integrating Sendai vectors produced iPSC colonies, though the efficiency of colony generation was very low, with only 2 colonies being produced following multiple attempts at transfection (data not shown). Only one of these colonies was viable for further expansion. Successfully transduced iPSC cells appeared as small

colonies with a characteristic appearance of ES cell colonies with defined borders and multinucleated centers (**Figure 3.1**). A single canine iPSC line was further characterized to assure a normal canine chromosomal ploidy and was shown to be free of mycoplasma infection and other adventitious agents (data not shown). The iPSC line could be passaged for at least 6 months and up to 100 passages in cell culture, which provided evidence of their sustained proliferative capacity.

iPSC colonies were assessed for expression of the pluripotency markers Oct3/4 and Nanog, using immunocytochemical staining (ICC). These assays revealed that the canine iPSC colonies expressed high levels of both endogenous transcription factors, and also high expression of CD105, a glycoprotein transmembrane TGF- β receptor (**Figure 3.1C-E**). To verify the *in vitro* differentiation potential of the canine iPSC line, the embryoid body formation assay was used²⁷. Following culture under EB conditions, the resulting spheroids showed positive ICC staining for markers specific for 3 developmental germ layers, including alpha-fetoprotein (endoderm), β -tubulin (ectoderm), and smooth muscle actin (mesoderm) (**Figure 3.1F-H**).

To assess pluripotency *in vivo*, the teratoma assay was performed using s.c. injection of canine iPS cells imbedded in Matrigel²⁸. Within 20 days of injection, NOD/SCID mice (n = 4) all developed teratomas >10 mm diameter (**Figure 3.1J**). The NOD/SCID mice were sacrificed at day 20, and the tumors were dissected, fixed, and evaluated by hematoxylin and eosin stain (Figure 1K). The tumors were found to express all 3 germ layers (**Figure 3.1L-Q**), thereby confirming the full *in vivo* differentiation capacity of the canine iPS cell line.

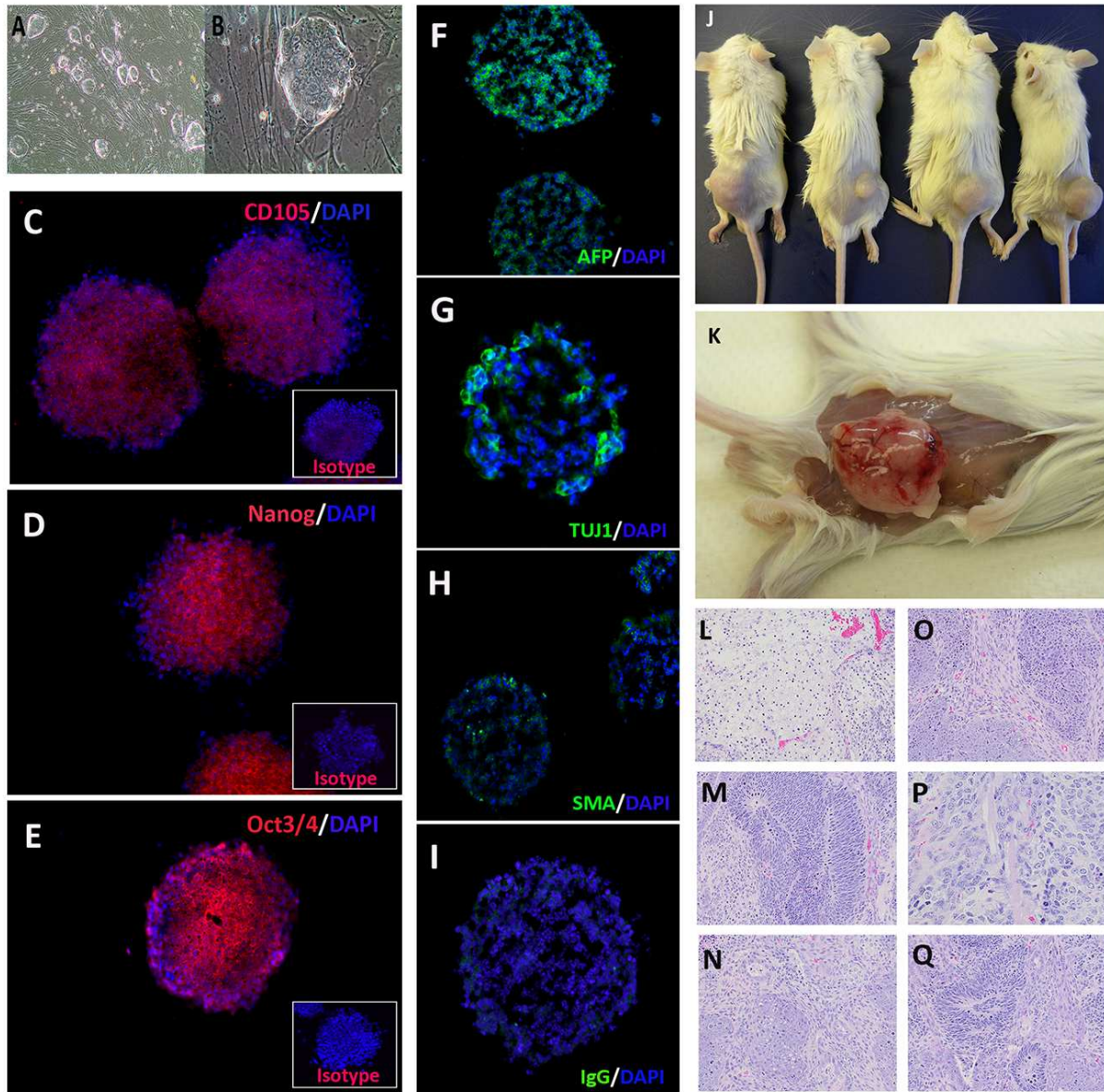


Figure 3.1 Characterization of canine induced pluripotent stem cells.

iPSC colonies derived from adult skin fibroblasts of a single dog, expanded from a single colony grown on MEF feeder layers, following induction by Sendai virus transfection with vectors containing OSKM factors (3.1A; 4X magnification). Single iPSC colony, demonstrating defined border and multinucleated center (3.1B, 40X magnification). Expression of pluripotency markers by iPSC colonies as evaluated by immunofluorescence imaging (3.1C- 3.1E; 20x magnification). iPSC colonies immunostained for detection of intracellular expression of stem cell antigens. Inset boxes depict staining with isotype control antibodies (3.1C- 3.1E). CD105 expression (3.1C). Nanog expression (3.1D). Oct-3/4 expression (3.1E). Germ line differentiation of embryoid bodies formed from canine iPS cells. (3.1F-1I). Expression of AFP (3.1F). Expression of β -tubulin (3.1G) and expression of SMA (3.1H) Negative isotype mouse IgG (1I). Teratoma formed in NOD/SCID mice 20 days after injection of iPSC (3.1J-3.1Q).

Gross image of euthanized NOD/SCID mice (n=4) with subcutaneous teratomas on right flank (**3.1J**). Gross image of an exposed, subcutaneous teratoma from one of the mice in figure 1J (**3.1K**). Photomicrographs of H&E stained tumor sections demonstrating the presence of white matter (ectoderm) formed within the tumor (**3.1L**); center rosette structures reminiscent of primitive neuroectoderm within the teratoma (**3.1M**); cartilage (**3.1N**) and smooth muscle tissue within tumor representative of mesoderm formation (**3.1O**); myotubes (**3.1P**) and endodermally-derived, ciliated pseudostratified columnar respiratory epithelium formation (**3.1Q**).

Inhibition of the TGF- β type I receptor promotes the rapid differentiation of iPSC cells to a mesenchymal lineage cell type

The TGF- β inhibitor SB431542 is known to induce differentiation of pluripotent cells by inhibiting SMAD2/3 phosphorylation^{24, 29}. To assess the ability of iPSC to differentiate into MSC like cells, iPSC colonies were plated on Matrigel substrate with the addition of TGF β inhibitor SB431542. Beginning at day 2, cellular outgrowth was observed from the periphery of the iPSC colonies. After 10 days, all cells were re-seeded at high density in tissue culture flasks. To enrich for mesenchymal like cells, the culture media was changed to MSC medium (KO-DMEM +10% FBS). By passage 1, cells resembled MSCs, with fibroblastic morphology and elongated spindle shaped edges (**Figure 3.2A**), which henceforth were referred to as induced MSC (iMSC). The iMSC generated were capable of differentiating into adipocytes (**Figure 3.2D**) osteocytes (**Figure 3.2E**), and chondrocytes (**Figure 3.2F**); iMSCs retained the MSC characteristic fibroblastic morphology beyond passage 15, and continued to proliferate in monolayer. The growth kinetics of iMSC were more rapid than that of Ad-MSC and BM-MSC when plated at low density, but growth became arrested when reaching approximately 80% well confluency (**Figure 3.2G**).

Safety evaluation of single iMSC line shows no tumorigenicity

The ability of iMSCs to generate teratomas was also evaluated in NOD/SCID mice, as noted above. Unlike the case with iPSC, iMSCs showed no evidence of induction of teratoma

formation during 6 months of observation in mice (**Figure 3. 2H, 3.2I**). Moreover, the skin at the site of iMSC injection did not contain residual detectable tumor cells, as noted by histopathology (data not shown).

Studies were conducted next to evaluate the safety of iMSC in adult dogs. These studies specifically addressed the issue of tumor-formation by iMSC following systemic administration, as this is the route by which these cells are likely to be administered for most clinical applications for suppression of inflammatory disorders. Three adult, purpose bred Beagle dogs were each injected i.v. with 2×10^6 iMSC per kg body weight. The dogs were then monitored for tumor formation (cutaneous and internal tumors), first by whole body CT evaluation at 3 months (compared to pre-treatment CT evaluations) and also by monthly evaluation by physical examinations. The CT evaluation did not reveal the presence of tumor nodules or other abnormal tissues in any body sites examined, compared to pre-injection whole body CT scans (**Figure 3.3**). At the completion of the 90-day study, the 3 dogs used in this study were adopted out to local owners and the dogs were monitored by periodic physical examinations for tumor formation. At follow up of 15 months after iMSC injection, all 3 injected dogs remained healthy and free of any obvious tumor formation.

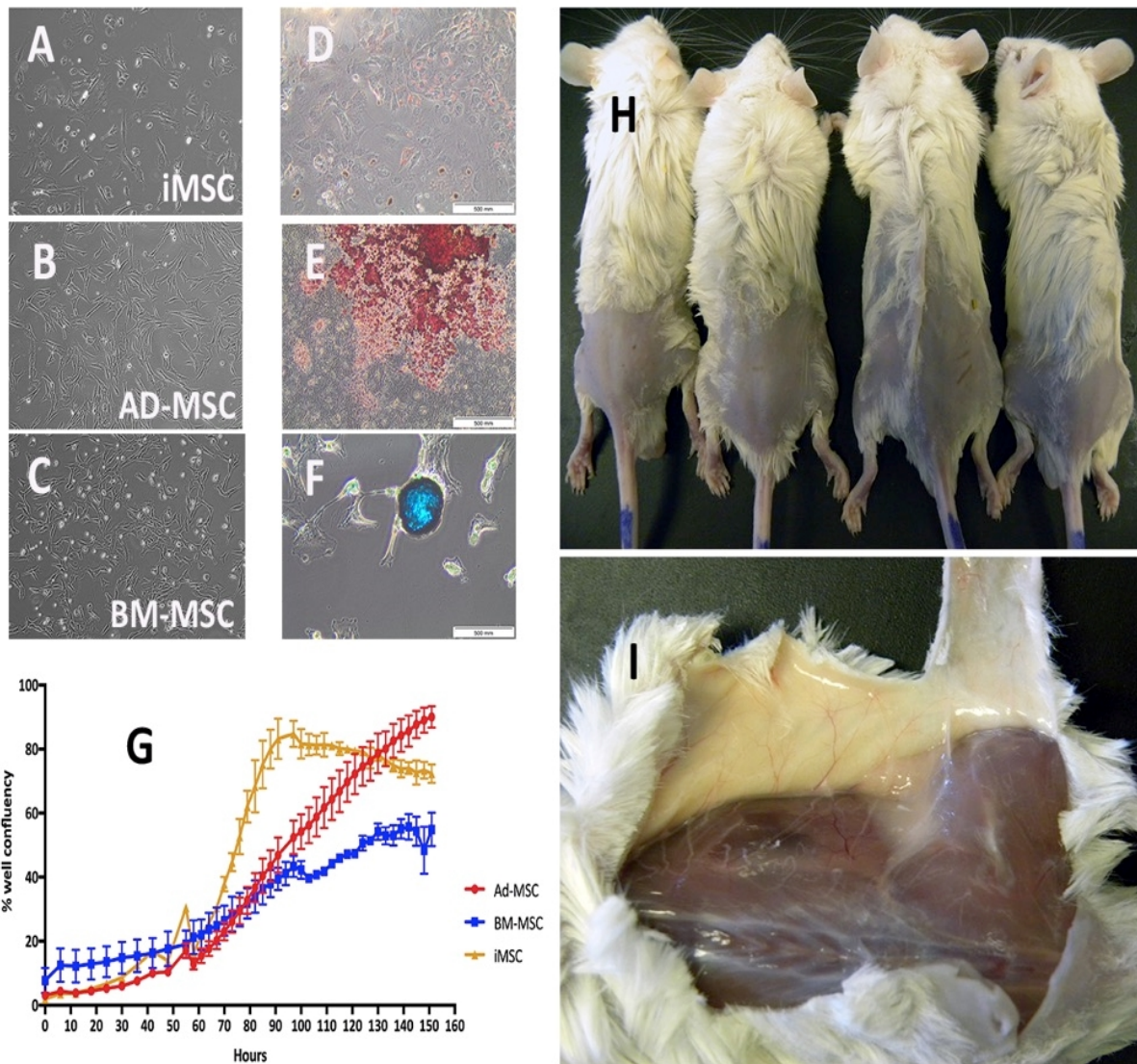


Figure 3.2 Generation of multipotent MSC from canine iPSC using TGF- β inhibitor. Induced MSC (iMSC) were generated from a single canine iPSC line following treatment with SB431542. Morphological comparison of Ad-MSC (3.2B) and BM-MSC (3.2C) and iMSC (3.2A) all obtained from the same donor dog. Tri-lineage differentiation of iMSC (3.2D- 3.2F). Oil Red O staining of lipid droplets differentiated from iMSC (3.2D). Alizarin Red staining of calcium deposits on osteocytes differentiated from iMSC (3.2E). Alcian blue staining of proteoglycans within chondrocyte cluster differentiated from iMSC (3.2F). Comparison of growth curves of iMSC, Ad-MSC, and BM-MSC, as determined using an IncuCyte® live cell imager. The X axis depicts time and the y axis percent cell confluency. Ad-MSC growth curve shown in red, BM-MSC in blue and iMSC in yellow (3.2G). NOD/SCID mice injected s.c. with 2×10^6 iMSC imbedded in Matrigel, demonstrating lack of teratoma formation at 6 months post injection (3.2H). Image of 1 euthanized NOD/SCID mouse from figure 3.2H with injection area exposed showing no teratoma formed (3.2)

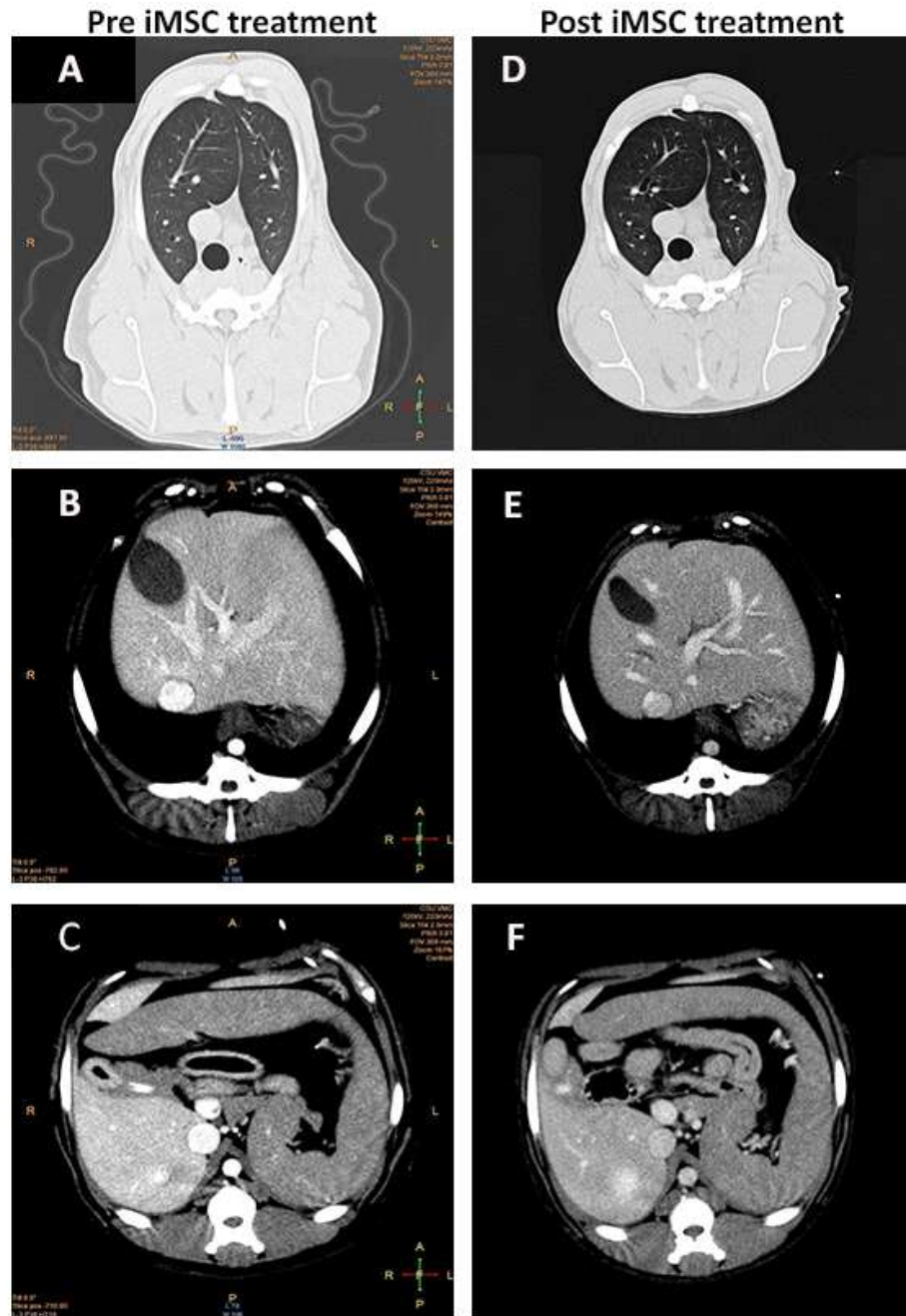


Figure 3.3 Evaluation of iMSC for tumor formation in purpose-bred dogs.

Three purpose-bred young adult Beagle dogs were injected i.v. with 2×10^6 iMSC (derived from a single line of canine iPSC) per kg body weight, and monitored for tumor formation by whole body CT imaging. Representative CT images from one treated dog. Transverse CT images were obtained just prior to cell injection (3.3A- 3.3C) and again 90 days later (3.3D- 3.3F). These figures show cross sectional images of major organs including lung (3.3A, 3.3D), liver (3.3B, 3.3E) and spleen (3.3C, 3.3F), each matched for the corresponding level of section.

Comparison of surface phenotype of iMSC and Ad-MSC and BM-MSC.

The immunophenotype of iMSC and Ad-MSC and BM-MSC derived from the same dog was assessed with flow cytometry, using a panel of cell surface antigens described previously^{25, 26, 30} (Figure 4). Canine Ad-MSC and BM-MSC shared a very similar surface phenotype for all markers evaluated, including positive expression of CD44, CD90, CD105 and lack of expression of CD24, CD34 and CD45. Analogous to the Ad-MSC and the BM-MSC, the iMSC did not express CD34 or CD45, and expressed uniform levels of CD105. In contrast however, the iMSC did not express CD90, had very low levels of CD44, and expressed CD24 on a subpopulation of iMSC (**Figure 3.4**). Moreover, iMSC expressed high levels of CD73, whereas the Ad-MSC and BM-MSC did not express CD73 by flow cytometry. iMSCs did not express the intracellular pluripotency marker Oct3/4 (POU5F1), in contrast to the parent iPSC, which were highly positive for this marker. The Ad-MSC and BM-MSC both expressed low levels of Oct3/4. Thus, iMSC shared some markers associated with Ad-MSC and BM-MSC in other species (CD73, CD105), but lost expression of pluripotency marker Oct3/4 compared to the parental iPSC.

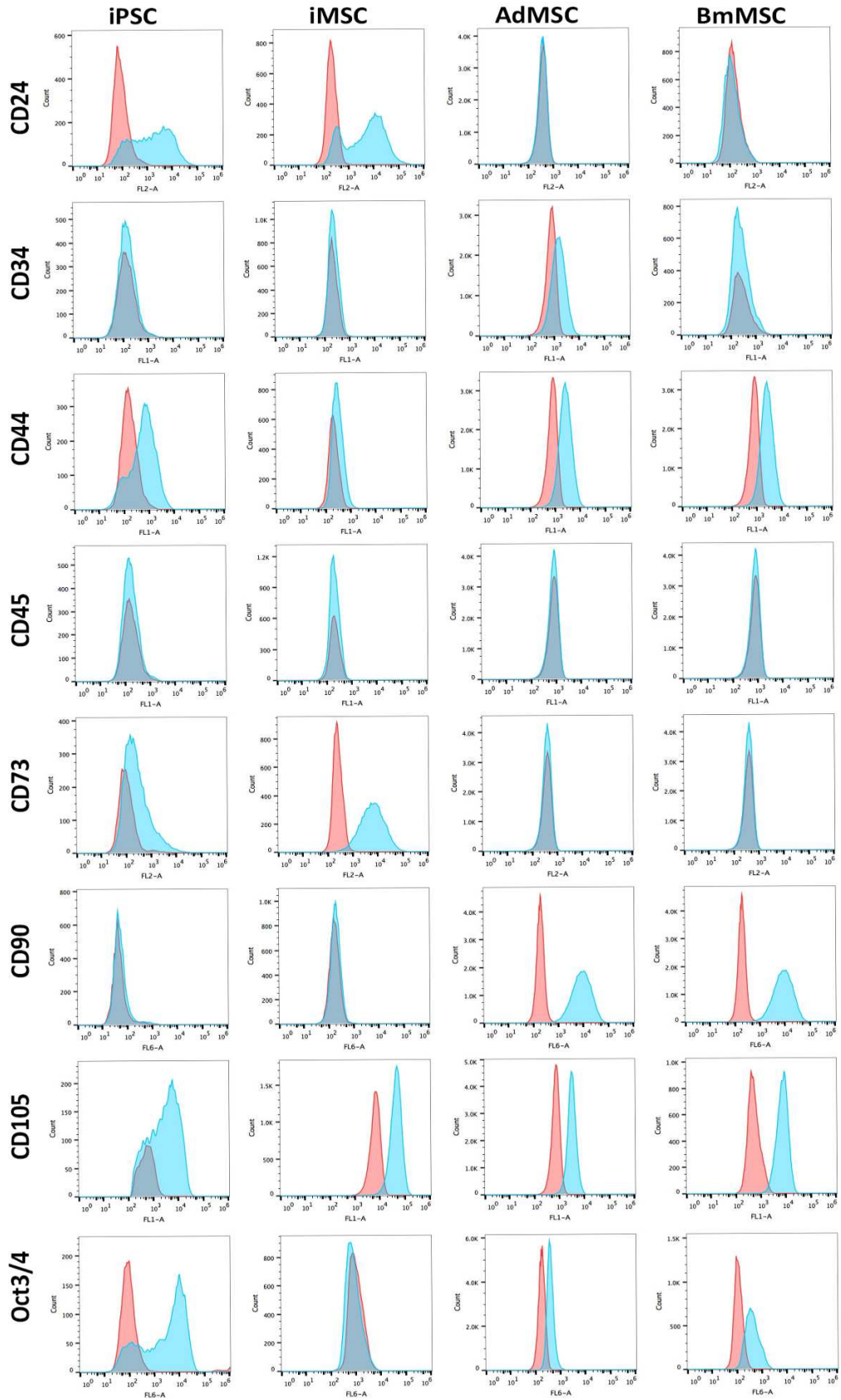


Figure 3.4 Immunophenotypic characterization of iPSC, iMSC, Ad-MSC, and BM-MSC by flow cytometry.

iPSC, iMSC, AD-MSC and BM-MSC derived from the same donor dog were immunostained with antibodies to CD24, CD34, CD44, CD45, CD73, CD90, and CD105 and Oct3/4 as noted in Methods, and analyzed by flow cytometry. Histograms (blue) were generated using Flowjo 9.0.8 software, with the x-axis representing florescence intensity and the y-axis representing cell count. Red histograms display isotype staining for each corresponding antibody. Phenotyping was repeated at 3 different passages for each cell line and showed the same results.

iMSC inhibit T cell proliferation and PBMC IFN- γ production.

To determine the relative potency of immune modulation exhibited by iMSCs, the ability of iMSC to suppress T cell proliferation and IFN- γ production was compared to that of Ad-MSC and BM-MSC. . We have previously reported that canine Ad-MSC and BM-MSC suppress both T cell and DC activation ^{25,26}. When iMSC and Ad-MSC and BM-MSC were compared, we observed that all 3 types of MSC significantly suppressed T cell proliferation, using PBMC obtained from 3 different unrelated dogs (**Figure 3.5**). The iMSCs generated an average of 54% decrease in T cell proliferation, while Ad-MSC induced an average 65% decrease in proliferation and BM-MSC induced average 58% decrease in T cell proliferation.

Co-culture of activated PBMC with iMSC also produced a significant suppression of IFN- γ release; with an average 67% suppression by iMSC, 65% suppression by Ad-MSC and 55% suppression by BM-MSC (none of these differences were statistically significant) (**Figure 3.5C**). These results indicated that iMSC were capable of inducing significant suppression of *in vitro* immune function, at roughly equivalent potency to Ad-MSC and BM-MSC.

iMSC inhibit DC maturation.

The impact of iMSC on DC maturation was assessed using co-culture assays with iMSC and monocyte-derived DC. Incubation of DCs obtained from 3 different, unrelated donor dogs with iMSCs (untreated or IFN- γ pre-activated iMSC) all produced a significant decrease in DC

expression of MHCII by LPS-activated DC (**Figure 3.5D**), consistent with suppression of activation by iMSC. In addition, expression of the co-stimulatory molecule CD86 was also significantly inhibited following co-culture with IFN- γ activated iMSCs (**Figure 3.5E**).

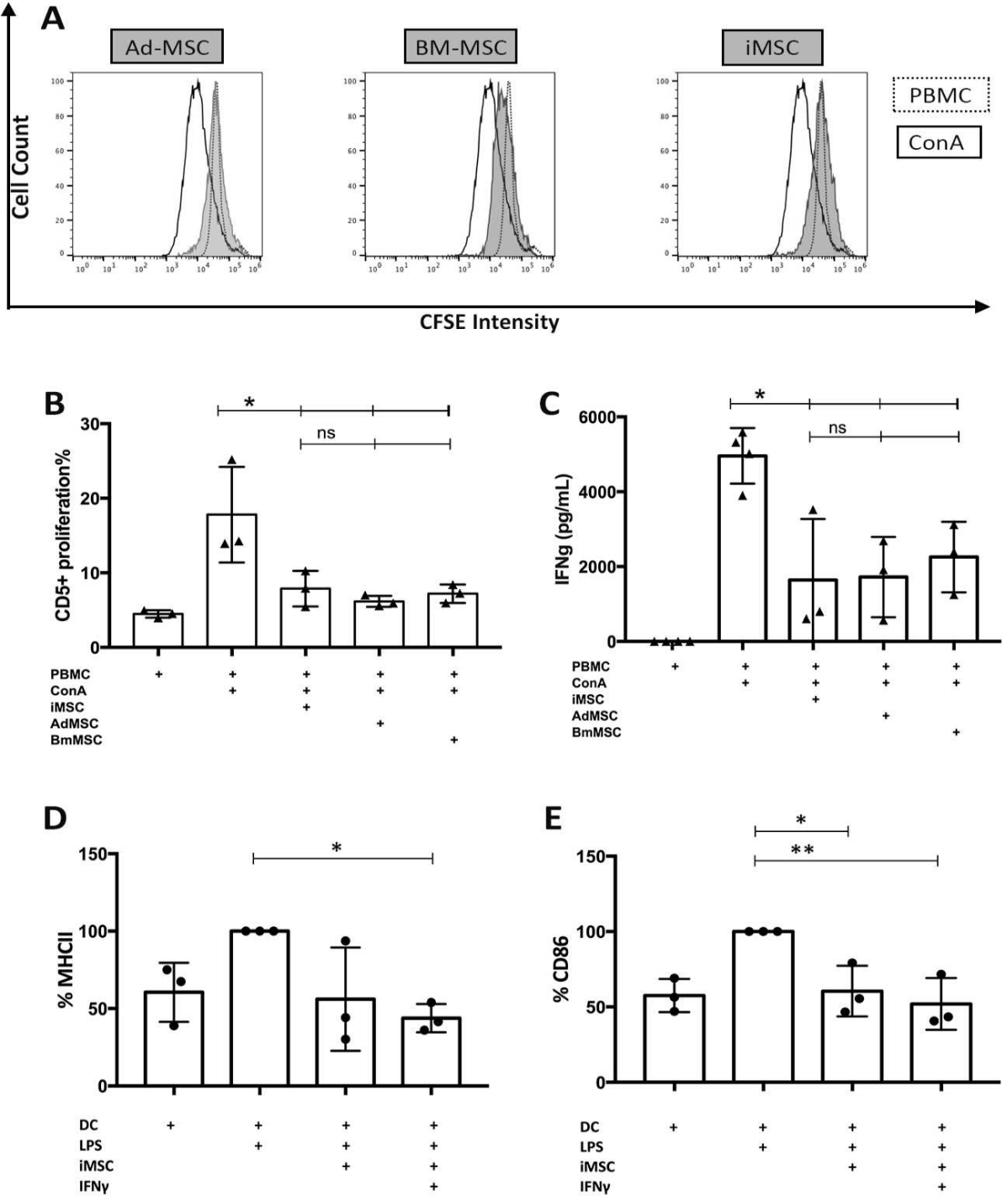


Figure 3.5 Effects of iMSC, Ad-MSC, and BM-MSC on T cell proliferation, PBMC IFN- γ production and DC maturation and activation.

Peripheral blood mononuclear cells (PBMC) from healthy donor dogs (n=3) were co-cultured with MSC at a ratio of 1:10 MSC:PBMC to assess the effects of MSC on T cell proliferation. Representative histograms of proliferating CD5⁺ T cells, either T cells alone, T cells co-cultured with iMSC, Ad-MSC or BM-MSC (the latter represented with shaded gray area) (**3.5A**). X-axis represents fluorescence intensity of CFSE (FITC) while the y-axis represents cell counts. Unstimulated, CFSE+CD5⁺ T cells shown in dotted line, while activated CFSE+CD5⁺ T cells are depicted in solid line, no shading. Effect of MSC on T cell cultures, each point represents average of technical replicates, using PBMC from 3 different unrelated donor dogs, and iMSC derived from a single iPSC line. Percent T cell proliferation depicted on the y-axis (**3.5B**). IFN- γ concentrations were measured in supernatants collected from co-culture experiments at 96 hours (**3.5C**). Statistical significance was evaluated using one-way ANOVA, with Tukey's multiple means comparison test (*p <0.05).

Immature canine DC were treated with LPS to induce maturation; and expression of co-stimulatory molecules MHCII and CD86 was compared with DCs incubated with untreated or IFN- γ activated iMSCs, was measured by flow cytometry (**3.5D**, **3.5E**). X axis represents normalized percentage mean fluorescence increase, with stimulated DC at 100%. MHCII expression differences between untreated DC (iDC), LPS-stimulated DCs, and DCs incubated with un-treated or IFN- γ activated iMSC (**3.5D**). CD86 expression (**3.5E**). Each point represents average of technical replicates of DC derived from 3 unrelated donor dogs. Statistical significance was determined using 1-way ANOVA with Tukey's multiple means comparison (* p <0.05).

Gene expression profiles of iMSC compared to iPSC and Ad-MSC and BM-MSC.

Microarray studies were done using Affymetrix canine OST 1.0 chips to compare gene expression patterns between the 3 different types of MSC, and between iMSC and iPSC, using cells all derived from the same adult dog. In the first comparison (iMSC versus iPSC), it was observed that the iMSC showed only approximately 1% difference out of 25,455 genes analyzed (**Figure 3.6**). Principle component analysis (PCA) revealed that inhibition of TGF β signaling created a distinct cell type different from the parent iPSC population (**Figure 3.6A**). In contrast, when comparing iMSC to Ad-MSC and BM-MSC, the PCA plot demonstrated closer clustering of Ad-MSC and BM-MSC to each other; whereas the gene expression profile of iMSCs was divergent from both Ad-MSC and BM-MSC (**Figure 3.7**).

Differential gene expression analysis revealed that the expression of 165 genes was up regulated with a fold change >2 when iMSC were compared to iPSC (**Figure 3.6B**), while the expression of 88 genes was downregulated. The pluripotency of the iMSC was decreased compared to that of the iPSC cells, with 69.6% downregulation of significant genes representing iPSC and ESC specific protein interactions³¹ (**Figure 3.6C**). Pathway enrichment analysis revealed that the TGF- β pathway was the most upregulated pathway when comparing iMSC vs. iPSC; with an enrichment score of 6.11, while the most downregulated pathway was the Fc gamma R-mediated phagocytosis pathway, with an enrichment score of -7.5 (**Figure 3.6D**).

The iMSCs exhibited a very different gene expression profile compared to both the Ad-MSC and the BM-MSC, with $>60\%$ differences in gene expression. (**Figure 3.7B, 3.7C**). We used the top 1000 differentially expressed genes to perform KEGG pathway analysis between iMSC and Ad-MSC and BM-MSC (**Figure 3.7E, 3.7F**). This comparison revealed that pathways including hedgehog signaling, pluripotency regulation, and cell adhesion molecule signaling were up regulated in iMSCs. Conversely, metabolic pathways such as carbon, purine, and pyrimidine pathways and ECM receptor interactions were down regulated in iMSCs. We then compared cytokine and chemokine gene expression between iMSC and Ad-MSC and BM-MSC, using gene lists from Immport.org (**Figure 3.7D**). This analysis revealed that iMSCs, relative to Ad-MSC and BM-MSC, overexpressed anti-inflammatory genes for cytokines such as IL-13, IL-22, IL-19, and IL-27, as well as IL-1 receptor antagonist and IL-36 receptor antagonist. iMSCs also expressed upregulated multiple anti inflammatory bone morphogenetic proteins BMP4, BMP6 and BMP10. Contrarily, iMSC exhibited up regulation of inflammatory genes including IFN- α and members of TNF (tumor necrosis factor) family. Many inflammatory interleukins such as IL-1A, IL-2, IL-16, and IL-7 were downregulated in iMSCs, as well as the

anti-inflammatory TGF- β family members such as TGF β 3, TGF β 2 and receptors. A comparison of the chemokine and receptor gene profile revealed that 85% of these genes were upregulated in iMSCs, compared to Ad-MSC and BM-MSC. In contrast, only a 7% difference in these genes was identified between Ad-MSC and BM-MSC.

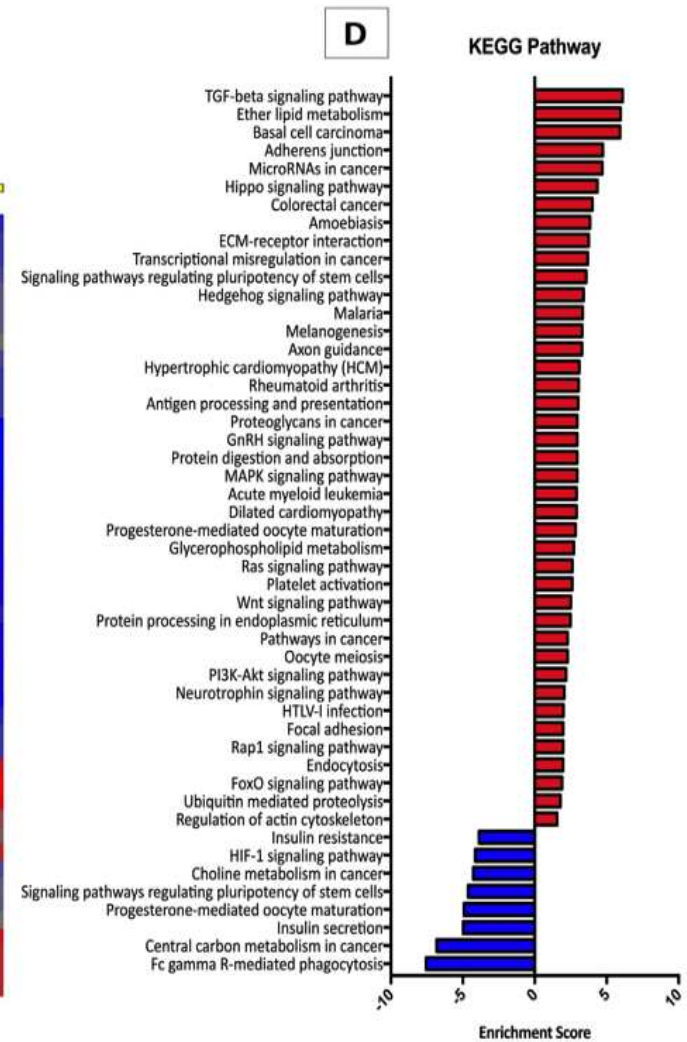
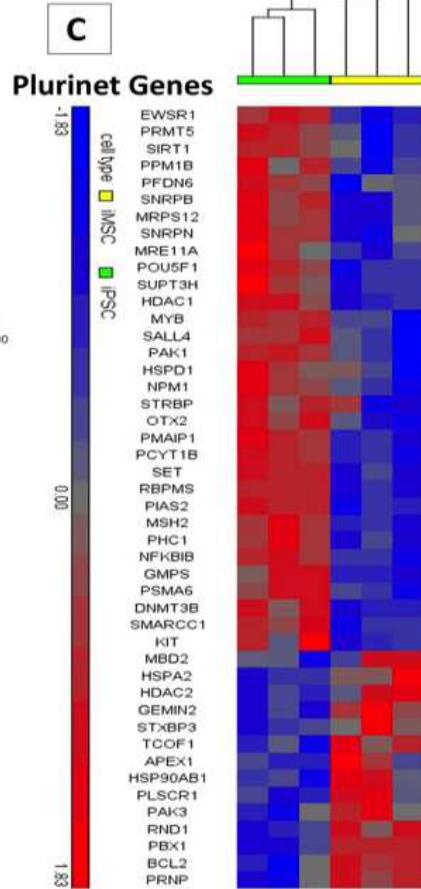
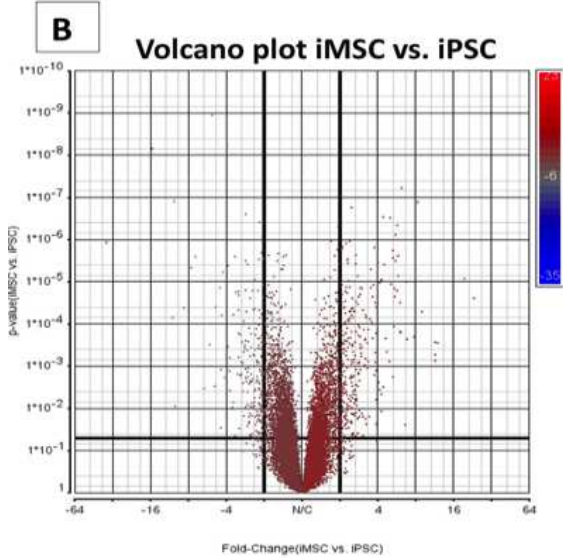
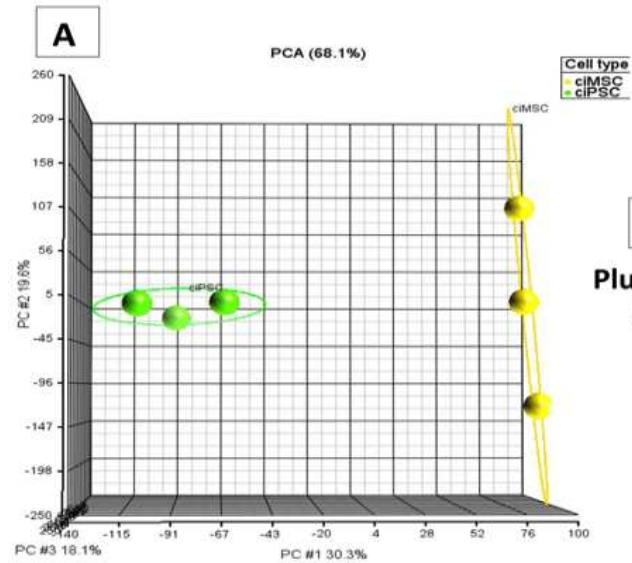


Figure 3.6. Gene expression profiles of canine iMSC and iPSC.

RNA was isolated from triplicate cultures of iMSC and iPSC and hybridized individually to Affymetrix Canine 1.0 chips. iPSC used were derived from a single clone, each in separate cultures at > 50 passages. Three iMSC lines were derived from different passage iPSC using the TGF- β inhibition method²⁴. Array data was analyzed using Partek Genomic Suite v6.6 software. Principle component analysis (PCA) plots of triplicate samples from iMSC (yellow) and iPSC (green) (**3.6A**). Ellipsoids were drawn around samples to demonstrate differences at the level of 2 standard deviations. PC1 depicts the highest variation of 30.1% between cell types, whereas PC2 depicts a variation of 19.6% and PC3 depicts a variation of 18.1%. Volcano plot of all differentially expressed genes from iMSC versus iPSC (**3.6B**). In this figure, the x-axis represents fold change, with thick axis lines drawn to depict fold changes of -2 and 2. The y axis represents *p*-values, with thick line marking $p = 0.05$. Color code shown in side bar represents fold change. In figure **3.6C**, hierarchal clustering heat map of iPS and ESC specific Mueller plurinet genes³¹ (from gene set GSE11508) is depicted. 46 genes out of 226 total Plurinet genes had a *p*-value <0.05. In Figure **3.6D**, KEGG pathway analysis of differentially expressed genes in iMSC vs. iPSC with a fold change <-2 or >2 is depicted. Red represents pathways over-expressed in iMSC relative to iPSC, while blue represents pathways under-expressed in iMSC. The x-axis delineates enrichment scores for each pathway with negative values for under-expressed pathways in iMSC.

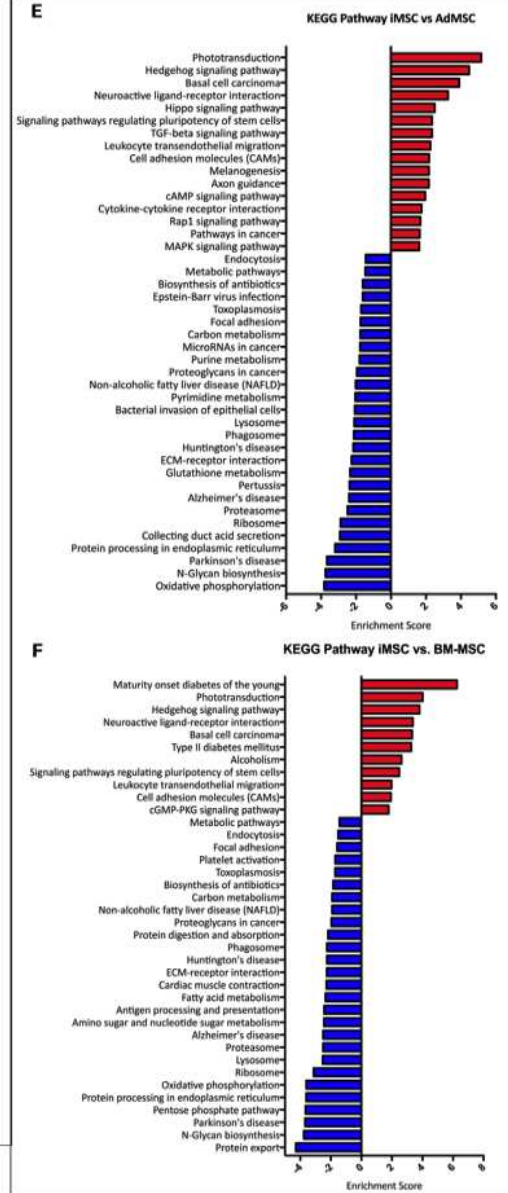
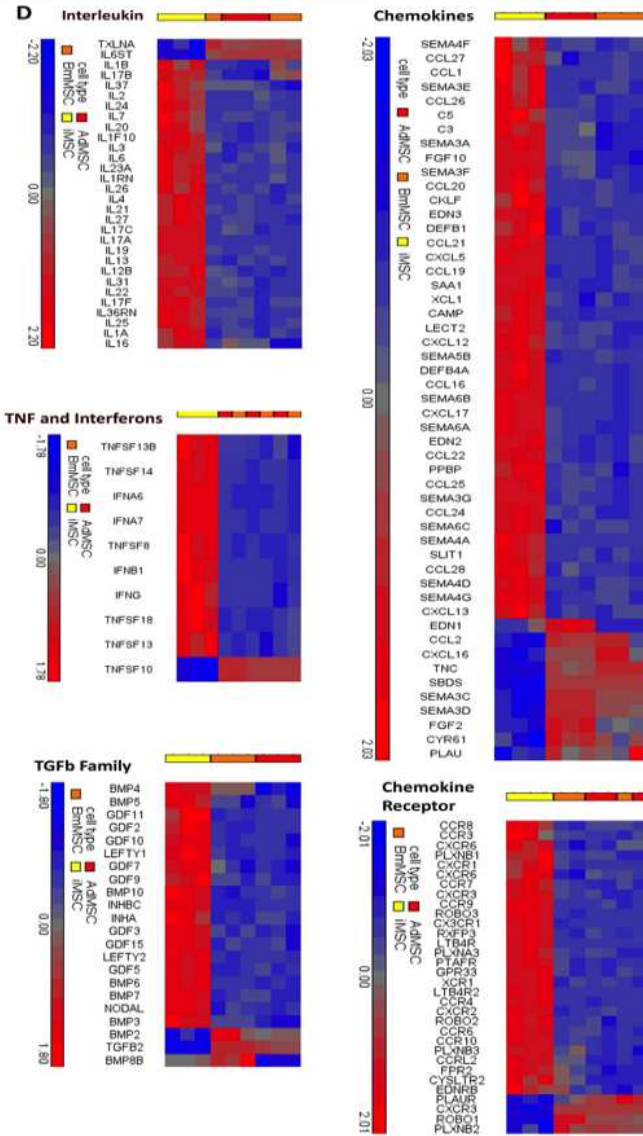
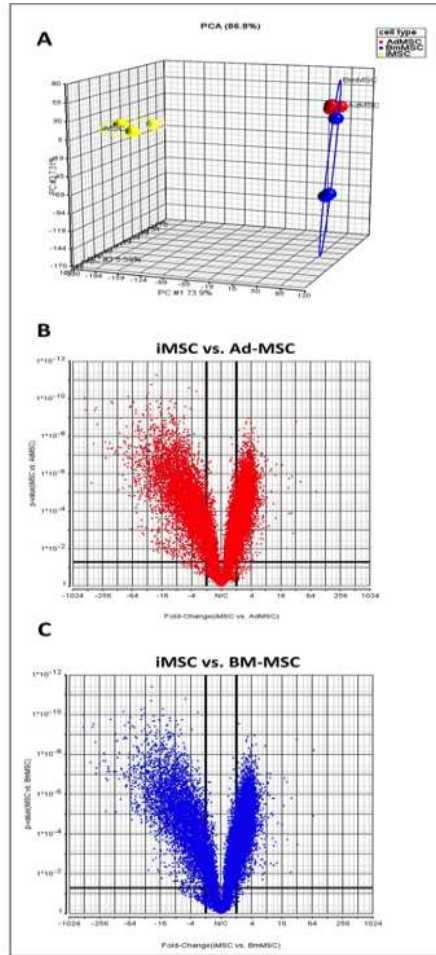


Figure 3.7 Global gene expression and cytokine gene profiles of canine iMSC compared to Ad-MSC and BM-MSC.

PCA plot of iMSC biological replicates (yellow), Ad-MSC (red) and BM-MSC (blue). Each iMSC was derived from 3 independent passages of iPSC, Ad-MSC and BM-MSC replicates are samples derived from the same dog and passaged independently, as described in Methods. Ellipsoids were drawn around samples to depict a standard deviation = 2 within cell types. PC1 depicts the highest variation of 73% between cell types, PC2 depicts a variation of 5.6% and PC3 depicts a variation of 27.3% (**3.7A**). Volcano plots of all differentially expressed genes in the analysis of iMSC versus Ad-MSC (**3.7B**) and iMSC versus BM-MSC (**3.7C**). X axis represents fold change, with thick axis lines drawn at fold changes of -2 and 2. Y axis represents p values, and the thick axis line denotes significance at $p = 0.05$. Five heat maps of significant ($p < 0.05$) immune-related molecule genes (**3.7D**). Cell types are color coded and listed on the side bar, with gene expression values normalized using Partek software and coded with red for high expression and blue for low expression with exact number scales shown in side bar. KEGG pathway analysis of iMSC versus Ad-MSC (**3.7E**). KEGG pathway analysis using the top 1000 over-expressed and top 1000 under-expressed genes in the differential gene expression analysis of iMSC versus BM-MSC (**3.7F**). The x-axis shows enrichment scores for each pathway. Red represents pathways over-expressed in iMSC with positive enrichment scores; blue represents pathways that are under-expressed in iMSC with negative enrichment scores.

Discussion

Current limitations to the use of iPSC-derived cells such as iMSC for treatment of diseases include the potential risk for tumor formation and the lack of effective spontaneous animal disease models for evaluation of iPSC-derived cell safety and efficacy¹¹. Advancing the use of iMSC for clinical therapy is dependent on safety and efficacy data generated from relevant clinical models. Therefore, in the present report we addressed the functional immune modulatory properties of iMSC, based in part on the relevance of the canine spontaneous disease model to stem cell translational research, especially with regards to immune modulation^{25, 26, 32-34}. Notably, the results of our studies indicated clearly that canine iMSC possessed equivalent functionality to conventional Ad-MSC or BM-MSC with regards to *in vitro* immune modulatory activity against both T cells and DC. These results are concordant with those found in human iPS derived MSC^{35, 36}, in that iMSC suppress lymphocyte proliferation and inflammatory cytokine production. In addition, like human iPS derived MSCs³⁵, canine iMSC significantly suppressed the maturation and up-regulation of co-stimulatory molecule expression by canine DC. Taken together, these results indicate that iMSC from dogs have the potential to be used for immune modulation in a clinical disease model.

One of the key defining properties of iPSC is their ability to form multiple different germ layers, as well as teratomas *in vivo*²⁷. The teratoma assay in immune deficient mice is very important for the verification of a successful transduction of iPS cells, and is considered the one of the most stringent tests for pluripotency³⁷. Indeed, we found that our canine iPSC line readily formed embryoid bodies *in vitro*, and also formed teratomas within 20 days of s.c. inoculation in immune deficient NOD/SCID mice. This has reportedly been difficult in the dog model, and only accomplished by half of the groups that reported canine iPS lines to date^{13, 15, 20, 38}, possibly due

to incomplete reprogramming, differences in lenti viral or retroviral packaging, or lack of canine specific OSKM vectors. Some groups also reported the use of small molecule inhibitors after colony formation to aid in reprogramming.

However, the tumorigenicity of iPSC leads to another major concern with use of iPSC-derived cells in the clinic, we found the canine iMSC failed to form teratomas in immune deficient mice, even during an extended observation period. Equally important, canine iMSC also did not form tumors in adult dogs; even following i.v. injection 2×10^6 cells/kg, and over an extended observation period of 1 year. This cell number used for injection is in accordance published canine safety test using Ad-MSC^{11,39}. It is also higher than the number of ESC derived cells used in a canine model of Crohn's disease³², and higher than several published clinical trials using human BM-MSC⁴⁰. These results are an important step in determining the safety of allogeneic iMSC for use in both veterinary and human patients.

Previous studies have found that iMSC derived from human and mouse iPSC exhibited a similar phenotype with respect to cell surface molecule expression as conventional Ad-MSC or BM-MSC⁴¹⁻⁴³. iMSC have previously been generated from dog iPSC by the use of TGF β pathway inhibitors²⁹ These canine iMSC were found to express typical MSC cell surface molecules. However, the dog iMSC in that report did not have reduced expression of the iPSC pluripotency markers. Our studies revealed a somewhat different phenotype for canine iMSC compared to canine Ad-MSC and BM-MSC (see Figure 4). There are several potential explanations for the observed discrepancies in surface molecule expression between iMSC and conventional MSC. For one, this may reflect species-specific differences. For example, we have also observed discordant surface molecule expression between iMSC and BM-MSC from horses (Colbath and Dow, et al, unpublished data). In contrast, previous studies have found much more

similar levels of expression for human and mouse iMSC and BM-MSC⁴³⁻⁴⁵. In addition, the iPSC in our studies were generated using a non-integrating viral OSKM transduction system, whereas previous canine studies have used retroviral or lentiviral transduction systems (which results in permanent chromosomal integration of the OSKM transcription factors) to generate iPSC. Unlike the intermediate MSC like populations found when using different techniques to generate MSC like cells⁴⁶, we observed the same phenotypic differences in iMSC versus Ad-MSC or BM-MSC when using serial passaging or EB intermediates (data not shown). Canine iMSC also proliferated much more rapidly than Ad-MSC or BM-MSC, a difference that was sustained even at very high passages for the iMSC. Thus, the differences in iMSC cell surface phenotype and proliferation capacity that we observed appear to be inherent to canine iMSC, and represent a key distinction from Ad-MSC and BM-MSC.

The studies reported here are the first to conduct an in-depth analysis and comparison of gene expression patterns between canine iPSC, iMSC, Ad-MSC and BM-MSC. Several important findings emerged from these genetic analyses. For one, it was apparent that iMSC much more closely resembled iPSC than either Ad-MSC or BM-MSC. These findings differ from the previously published full genome array comparison of human iMSC and MSC, which found that iMSC had a closer genotype to the primary MSC than the parent iPSC⁴⁷. However, the human iMSC in that report were generated by serial passaging of iPSC, and in addition the human iMSC were less effective in suppressing T cell activation *in vitro* than we observed with canine iMSC. The gene expression profile of canine iMSC was significantly different from that of both Ad-MSC and BM-MSC, which is also consistent with the cell surface phenotype differences we observed. Lastly, we observed that canine iMSC downregulated many pluripotency genes, which is concordant with the human literature^{44, 46}. This is an important

consideration for considering the use of these cells in clinical patients, since expression of pluripotency genes can lead to uncontrolled proliferation and possible tumor formation.

Examination of immune related gene expression patterns revealed important differences in cytokine gene expression between iMSC and Ad-MSC and BM-MSC. We observed that iMSCs had upregulated expression of Th-2 related or immune suppressive cytokines. Despite upregulation of several pro-inflammatory genes, on balance iMSC exhibited a more immune suppressive pattern of gene expression. This difference was also reflected in the functional immune cell suppression assays, where it was noted that iMSCs were generally more immune suppressive than Ad-MSC or BM-MSC. Taken together, these studies indicate that canine iMSC are fully functional in terms of immune suppressive gene pathways relative to conventional MSC, and capable of sustained proliferation and maintenance of their cell surface phenotype through multiple cell culture passages. Importantly, these studies also demonstrated that canine iMSC were safe *in vivo* with respect to induction of teratoma formation (mice) or tumor formation (dogs). Thus, the findings reported here are important preliminary studies that will pave the way for pre-clinical evaluation of canine iMSC in studies in pet dogs with spontaneous inflammatory diseases such as inflammatory bowel disease, osteoarthritis, and autoimmune diseases, and will also accelerate the use of these cells in clinical trials in humans.

REFERENCES

1. Takahashi K, Yamanaka S. A decade of transcription factor-mediated reprogramming to pluripotency. *Nat Rev Mol Cell Biol.* 2016;17:183-193.
2. Squillaro T, Peluso G Fau - Galderisi U, Galderisi U. Clinical trials with mesenchymal stem cells: An update. *Cell, Transplant.* 2016.
3. Mohd Ali N, Boo L, Yeap SK, et al. Probable impact of age and hypoxia on proliferation and microrna expression profile of bone marrow-derived human mesenchymal stem cells. *PeerJ.* 2016;4:e1536.
4. Choudhery Ms Fau - Badowski M, Badowski M Fau - Muise A, Muise A Fau - Pierce J, et al. Donor age negatively impacts adipose tissue-derived mesenchymal stem cell expansion and differentiation. *J. Transl Med.* 2014.
5. Zhang J, Huang X, Wang H, et al. The challenges and promises of allogeneic mesenchymal stem cells for use as a cell-based therapy. *Stem cell research & therapy.* 2015;6:234.
6. Reinders MEJ, Dreyer GJ, Bank JR, et al. Safety of allogeneic bone marrow derived mesenchymal stromal cell therapy in renal transplant recipients: The neptune study. *Journal of Translational Medicine.* 2015;13:344.
7. Jung Y, Bauer G, Nolta JA. Concise review: Induced pluripotent stem cell-derived mesenchymal stem cells: Progress toward safe clinical products. *Stem cells (Dayton, Ohio).* 2012;30:42-47.
8. Kimbrel EA, Lanza R. Current status of pluripotent stem cells: Moving the first therapies to the clinic. *Nat Rev Drug Discov.* 2015;14:681-692.
9. Zhang Y, Liang X, Liao S, et al. Potent paracrine effects of human induced pluripotent stem cell-derived mesenchymal stem cells attenuate doxorubicin-induced cardiomyopathy. *Scientific reports.* 2015;5:11235.
10. Jeon OH, Panicker LM, Lu Q, et al. Human ipsc-derived osteoblasts and osteoclasts together promote bone regeneration in 3d biomaterials. *Scientific reports.* 2016;6:26761.
11. Hoffman AM, Dow SW. Concise review: Stem cell trials using companion animal disease models. *Stem, Cells.* 2016.
12. Baird AEG, Barsby T, Guest DJ. Derivation of canine induced pluripotent stem cells. *Reproduction in Domestic Animals.* 2015;50:669-676.
13. Lee AS, Xu D Fau - Plews JR, Plews Jr Fau - Nguyen PK, et al. Preclinical derivation and imaging of autologously transplanted canine induced pluripotent stem cells. *J. Biol Chem.* 2011.

14. Koh S, Tsai S, Bischoff S, et al. Generation of putative induced pluripotent stem cells (ips) from adult canine fibroblast. *Biology of Reproduction*. 2011;85:783-783.
15. Whitworth DJ, Ovchinnikov Da Fau - Wolvetang EJ, Wolvetang EJ. Generation and characterization of lif-dependent canine induced pluripotent stem cells from adult dermal fibroblasts. *Stem Cells, Dev*. 2012.
16. Kwon HS, Oh HJ, Lee DH, et al. Generation of canine induced pluripotent stem cells from canine fetal fibroblast and adult fibroblast of cloned dog. *Reproduction, Fertility and Development*. 2012;25:290-290.
17. Shimada H, Nakada A, Hashimoto Y, et al. Generation of canine induced pluripotent stem cells by retroviral transduction and chemical inhibitors. *Molecular Reproduction and Development*. 2010;77:2-2.
18. Luo J, Suhr St Fau - Chang EA, Chang Ea Fau - Wang K, et al. Generation of leukemia inhibitory factor and basic fibroblast growth factor-dependent induced pluripotent stem cells from canine adult somatic cells. *Stem Cells, Dev*. 2011.
19. Nishimura T, Hatoya S Fau - Kanegi R, Kanegi R Fau - Sugiura K, et al. Generation of functional platelets from canine induced pluripotent stem cells. *Stem Cells, Dev*. 2013.
20. Koh S, Thomas R Fau - Tsai S, Tsai S Fau - Bischoff S, et al. Growth requirements and chromosomal instability of induced pluripotent stem cells generated from adult canine fibroblasts. *Stem Cells, Dev*. 2013.
21. Herberts CA, Kwa MSG, Hermsen HPH. Risk factors in the development of stem cell therapy. *Journal of Translational Medicine*. 2011;9:29-29.
22. Lian Q, Zhang Y Fau - Zhang J, Zhang J Fau - Zhang HK, et al. Functional mesenchymal stem cells derived from human induced pluripotent stem cells attenuate limb ischemia in mice. *Circulation*. 2010.
23. Takahashi M. Retinal cell therapy using ips cells. *Nippon Ganka Gakkai, Zasshi*. 2016.
24. Chen YS, Pelekanos Ra Fau - Ellis RL, Ellis RI Fau - Horne R, et al. Small molecule mesengenic induction of human induced pluripotent stem cells to generate mesenchymal stem/stromal cells. *Stem Cells Transl, Med*. 2012.
25. Chow L, Johnson V, Coy JW, et al. Mechanisms of immune suppression utilized by canine adipose and bone marrow-derived mesenchymal stem cells. *Stem Cells, Dev*. 2016.
26. Wheat WH, Chow L, Kurihara JN, et al. Suppression of canine dendritic cell activation/maturation and inflammatory cytokine release by mesenchymal stem cells occurs through multiple distinct biochemical pathways. Lid - 10.1089/scd.2016.0199 [doi]. *Stem Cells, Dev*. 2016.

27. Ohnuki M, Takahashi K, Fau - Yamanaka S, Yamanaka S. Generation and characterization of human induced pluripotent stem cells. *Curr Protoc Stem Cell, Biol.* 2009.
28. Gropp M, Shilo V, Vainer G, et al. Standardization of the teratoma assay for analysis of pluripotency of human es cells and biosafety of their differentiated progeny. *PloS one.* 2012;7:e45532.
29. Whitworth DJ, Frith JE, Frith TJ, et al. Derivation of mesenchymal stromal cells from canine induced pluripotent stem cells by inhibition of the tgfbeta/activin signaling pathway. *Stem cells and development.* 2014;23:3021-3033.
30. Al Delfi IR, Sheard JJ, Wood CR, et al. Canine mesenchymal stem cells are neurotrophic and angiogenic: An in vitro assessment of their paracrine activity. *Vet, J.* 2016.
31. Muller F-J, Laurent LC, Kostka D, et al. Regulatory networks define phenotypic classes of human stem cell lines. *Nature.* 2008;455:401-405.
32. Ferrer L, Kimbrel EA, Lam A, et al. Treatment of perianal fistulas with human embryonic stem cell-derived mesenchymal stem cells: A canine model of human fistulizing crohn's disease. *Regen, Med.* 2016.
33. Kang JW, Kang Ks, Fau - Koo HC, Koo Hc, Fau - Park JR, et al. Soluble factors-mediated immunomodulatory effects of canine adipose tissue-derived mesenchymal stem cells. *Stem Cells, Dev.* 2008.
34. Russell KA, Chow NH, Dukoff D, et al. Characterization and immunomodulatory effects of canine adipose tissue- and bone marrow-derived mesenchymal stromal cells. *PloS one.* 2016.
35. Gao W-X, Sun Y-Q, Shi J, et al. Effects of mesenchymal stem cells from human induced pluripotent stem cells on differentiation, maturation, and function of dendritic cells. *Stem cell research & therapy.* 2017;8:48.
36. Fu QL, Chow YY, Sun SJ, et al. Mesenchymal stem cells derived from human induced pluripotent stem cells modulate t-cell phenotypes in allergic rhinitis. *Allergy.* 2012;67:1215-1222.
37. Hentze H, Soong PL, Wang ST, et al. Teratoma formation by human embryonic stem cells: Evaluation of essential parameters for future safety studies. *Stem Cell Research.* 2009;2:198-210.
38. Gonçalves NJN, Bressan FF, Roballo KCS, et al. Generation of LIF-independent induced pluripotent stem cells from canine fetal fibroblasts. *Theriogenology.* 2017;92:75-82.
39. Perez-Merino EM, Uson-Casaus JM, Zaragoza-Bayle C, et al. Safety and efficacy of allogeneic adipose tissue-derived mesenchymal stem cells for treatment of dogs with inflammatory bowel disease: Clinical and laboratory outcomes. *Vet, J.* 2015.

40. Gao F, Chiu SM, Motan DA, et al. Mesenchymal stem cells and immunomodulation: Current status and future prospects. *Cell Death, Dis.* 2015.
41. Jung Y, Bauer G Fau - Nolta JA, Nolta JA. Concise review: Induced pluripotent stem cell-derived mesenchymal stem cells: Progress toward safe clinical products. *Stem, Cells.* 2012.
42. Villa-Diaz LG, Brown Se Fau - Liu Y, Liu Y Fau - Ross AM, et al. Derivation of mesenchymal stem cells from human induced pluripotent stem cells cultured on synthetic substrates. *Stem, Cells.* 2012.
43. Obara C, Takizawa K, Tomiyama K, et al. Differentiation and molecular properties of mesenchymal stem cells derived from murine induced pluripotent stem cells derived on gelatin or collagen. *Stem Cells International.* 2016;2016:9013089.
44. Hynes K, Menicanin D Fau - Mrozik K, Mrozik K Fau - Gronthos S, et al. Generation of functional mesenchymal stem cells from different induced pluripotent stem cell lines. *Stem Cells, Dev.* 2014.
45. Liu Y, Goldberg Aj Fau - Dennis JE, Dennis Je Fau - Gronowicz GA, et al. One-step derivation of mesenchymal stem cell (msc)-like cells from human pluripotent stem cells on a fibrillar collagen coating. *PLoS one.* 2012.
46. Diederichs S, Tuan RS. Functional comparison of human-induced pluripotent stem cell-derived mesenchymal cells and bone marrow-derived mesenchymal stromal cells from the same donor. *Stem cells and development.* 2014;23:1594-1610.
47. Froebel J, Hemedda H, Lenz M, et al. Epigenetic rejuvenation of mesenchymal stromal cells derived from induced pluripotent stem cells. *Stem Cell Reports.* 2014;3:414-422.
48. Gomes IC, Acquarone M Fau - Maciel RdM, Maciel Rde M Fau - Erlich RB, et al. Analysis of pluripotent stem cells by using cryosections of embryoid bodies. 2010.
49. Huang DW, Sherman BT, Lempicki RA. Systematic and integrative analysis of large gene lists using david bioinformatics resources. *Nat. Protocols.* 2008;4:44-57.

CHAPTER 4

Direct and Indirect Antimicrobial Activity of Human Mesenchymal Stem Cells

Summary

Human bone marrow derived MSC (BM-MS) have been shown to improve wound healing and suppress inflammatory immune responses. Newer research also indicates that MSC exhibit antimicrobial activity, though the mechanisms underlying this activity have not been fully elucidated. **Therefore, we designed in vitro and in vivo studies to investigate the hypothesis that human BM-MSs directly influence bacterial growth and secrete factors that influence phagocytic cells to increase bacterial uptake and killing.** These studies utilized assays of direct bacterial killing mechanisms, and assays to investigate the interaction of MSC with the host innate immune response to bacterial infection. Activity of human MSC against bacterial biofilm infections was also investigated in vivo. We found that MSC exhibited direct bacterial killing, and also inhibited the growth of *S. aureus* biofilm formation and disrupted the growth of already established biofilms. Moreover, conditioned medium (CM) from MSC cultures elicited synergistic killing of multi-drug resistant bacteria when combined with several major classes of antibiotics. Important interactions of MSC with the host innate immune response that were identified in these studies included triggering of neutrophil extracellular traps (NETs), increased phagocytosis of bacteria, and increased bacterial killing by macrophages. Moreover, activated MSC generated significant reductions in bacterial load at the infection site of chronically infected mice when combined with antibiotic therapy. These results indicate the MSC exert multiple mechanisms, including both direct and indirect actions, leading to control of chronic infections with drug-resistant bacteria.

Background

The increasing incidence of antibiotic resistant bacterial infections has prompted a search for more effective therapies, including alternatives to conventional antibiotic treatment ¹.

Methicillin-Resistant *Staphylococcus Aureus* (MRSA) in particular accounts high mortality worldwide ² and is responsible for many early term antibiotic resistant infections in prosthetic implants ³. The use of MSC to treat bacterial infections has received increasing attention in recent years. In part, MSC therapy is being evaluated based on in vitro studies documenting direct bacterial killing activity, and on recent studies indicating that the MSC interaction with the innate immune response can also trigger antibacterial responses ^{4,5}. Given the interest in the use of MSC to treat infections, it is important to elucidate more fully how these activities are mediated.

Biofilms provide an environment that favors bacterial persistence and evasion of the host immune response ⁶. Multiple factors associated with biofilms lead to a resistant population of bacteria that evade killing by the immune system and antibiotics and continued bacterial growth ⁷. For example, *S. aureus* biofilms influence macrophage polarization and inhibit phagocytosis ⁸. Biofilms also limit neutrophil recruitment and killing because of their compact three dimensional structure that decreases surface receptor recognition and protects the core of the biofilm from attack ⁹.

Previous studies have shown that MSCs have the ability to directly influence the immunological properties of macrophages and neutrophils, by secreting factors such as PGE₂ ¹⁰, IL-6, IL-8 or IFN- β ¹¹. After MSC conditioning, macrophages exposed to bacteria had increased phagocytic ability by enhancing the phagocytosis-induced NADPH oxidase activation ¹², while neutrophils exposed to MSC conditioned media experienced decreased apoptosis and increased

migration¹³. *In vivo*, human MSCs also have the ability to increase monocyte recruitment and decrease the excessive neutrophil influx and neutrophil elastase production in murine models of cystic fibrosis infected with *Pseudomonas aeruginosa*¹⁴.

In addition to influencing immune cells, MSC also produce antimicrobial peptides (AMPs), which kill bacteria directly by disrupting the integrity of the microbial membrane¹⁵. Human MSCs have been shown to produce cathelicidin antimicrobial peptide LL-37¹⁶, Hepsidin¹⁷, β - defensin 2 (hBD2), and lipocalin 2 (Lcn-2)¹⁸, which can be upregulated by exposure to bacteria. AMPs secreted by MSCs are thought to play a direct role in killing bacteria and are a critical component to clear infections.

Various *in vivo* mouse models explored the effect of MSCs on acute bacterial infections. For example, human MSC decreased bacterial burden in a mouse model of *E. coli* pneumonia.¹⁶ In another study, human MSCs also reduced mortality associated with *Pseudomonas aeruginosa* in a mouse peritonitis and sepsis model¹⁹. MSC have also been shown to augment antibiotic treatment effects in murine cystic fibrosis²⁰, in part by the secretion of LL-37¹⁴. Studies with explanted human lung tissue also suggest MSC antibacterial activity²¹. In that study, instillation of MSC into airways of explanted lungs caused a reduction in *Escherichia coli*, and ameliorated acute lung injury including alveolar fluid clearance and inflammation.

To date our research group has been the only group to investigate the use of activated MSC to treat chronic bacterial infections⁴. In studies done in a mouse model of implant infection, and in pet dogs with spontaneous drug resistant chronic infections, activated MSCs delivered systemically demonstrated strong antibacterial activity against multiple different bacterial pathogens, including MRSA and *P. aeruginosa* infections.

Based on these compelling data from realistic animal models of chronic bacterial biofilm infections, we have now investigated in greater detail the mechanisms by which human MSC may control or eradicate bacterial infections. In these studies, *in vitro* assays were used to investigate direct bacterial killing mechanisms, as well as indirect mechanisms involving host innate immune defense.. In addition, a mouse chronic implant infection model was used to assess the effectiveness of activated human MSC. These studies provided therefore a more complete understanding of the multiple mechanisms by which MSC may be used as adjunctive therapy along with antibiotics for treating highly drug-resistant infections in relatively inaccessible sites such as implant infections. This information will be valuable for the design of human clinical trials to investigate stem cell therapy as a new tool for managing drug resistant infections.

Materials and Methods.

Generation of bone marrow derived stem cells.

One mL of human bone marrow aspirate (Lonza, Boston, MA) from healthy donors (3 total used in this study) was plated in T75 tissue culture flasks (CellTreat Scientific Products, Pepperell, MA) with MSC media containing DMEM, 10%FBS, Glutamax 1x, Pen/Strep 1x, NEAA 1x (Thermo Fisher Scientific, Waltham MA), and 2 ng/mL of human Recombinant Human FGF-basic (PeproTech, Rocky Hill, NJ). Media change was first performed on day 5, and adherent cells were passaged starting day 12 using Trypsin-EDTA (Thermo Fisher Scientific, Waltham MA). BM-MSCs were then collected at low passage and stored in liquid nitrogen in freezing medium containing 9% DMSO and FBS for further use.

Bacterial culture.

The MRSA (Methicillin Resistant Staphylococcus aureus) strain USA300 was provided by Dr. H. Schweizer at the Colorado State University Infectious Disease Research Center.

Escherichia coli was purchased from American Type Culture Collection (ATCC Manassas, VA), FDA strain Seattle 1946 (DSM 1103, NCIB 12210). Bacteria were propagated in Lysogeny broth (LB) (BD Falcon). Overnight cultures were grown in MSC media without antibiotics prior to use in various assays. Sub cultures were grown to log phase OD₆₀₀= 0.6 prior to use.

Flow cytometric assessment of bacterial killing.

Determination of Bacterial killing by flow cytometry was performed according to manufacturer's instruction using LIVE/DEAD™ BacLight™ Bacterial Viability and Counting Kit (Thermo Fisher Scientific, Waltham MA). Histograms generated with flowjo 10.5 software.

Direct bacterial killing assay (BKA).

Conditioned medium (CM) from human BM-MSC was generated by plating 5×10^5 cells per well in a 24 well plate with 500 uL per well of antibiotic free media then incubating at 37°C in a 5% CO₂ incubator. CM was collected 24 hours post plating and immediately frozen at -80°C. CM was thawed prior to use and cellular debris was removed by centrifugation. CM was then inoculated with log phase *S. aureus* cultures in 24-well plates. Bacteria was used at a multiplicity of infection (MOI) of 10:1 (bacteria per cell). And up to 40:1 for titration experiments. Co-cultures of bacteria and CM were incubated at 37°C in ambient air for 3hr, then numbers of viable bacteria was determined by plating log₁₀ serial dilutions and manual counting of colonies 24 hours later. The ability of MSC CM to augment antibiotic activity was determined by BKA, with or without the addition of low concentrations of cefazolin 375ng/mL, Gentamicin 200ng/mL, Vancomycin 500ng/mL, Enrofloxacin 2ug/mL, Imipenem 30ng/mL or Daptomycin

50ng/mL (Sigma-Aldrich, St. Louis, MO). Synergy and additive statistical analysis was performed using interaction factor calculations with 2 way ANOVA.

Immunocytochemical and flow cytometry evaluation of AMP in MSC.

To determine protein expression of antimicrobial peptides (AMP) by MSC, cells were seeded in chamber slides overnight, and the cells were fixed and permeabilized. Slides were blocked with donkey serum and then incubated with primary antibody anti-cathelicidin, anti-surfactant protein D, anti-Lipocalin-2 / NGAL, anti-beta 2 defensin, anti-hepcidin, or corresponding rabbit or goat IgG control antibodies (Abcam, Cambridge, MA). After primary antibody incubation, chambers were washed and incubated with secondary antibody donkey anti rabbit or anti goat Cy3 (Jackson ImmunoResearch Laboratories, Inc. West Grove, PA) and counter stained with DAPI. Visualization of fluorescence staining was performed on Olympus IX83 spinning disk confocal microscope. Flow cytometry was performed using the same antibodies, using saponin (0.15% in PBS) (Sigma-Aldrich, St. Louis, MO) with a 2 hour permeabilization after fixation. Samples were run on a Beckman Coulter Gallios flow cytometer (Brea, CA), and histograms were generated using FlowJo Software (Ashland, OR) v10.5.

MSC activation.

MSC activation was performed in 15 mL filter top Bio-Reaction tubes (CellTreat Scientific Products, Pepperell, MA). MSC were detached from flask then re-suspended at 2.5×10^6 cells/mL in MSC growth media and treated with the following stimulants: NOD1 ligand γ -D-Glu-mDAP (iE-DAP) 10ug/mL and its negative control Muramyl dipeptide (MDP) 10 ug/mL, TLR ligand type B CpG oligonucleotide (CpG) 0.1 uM, TLR3 ligand Poly(I:C) 10 ug/mL (InvivoGen, San Diego, CA). TLR4 ligand Lipopolysaccharides from Escherichia coli (LPS) 10 ng/mL (Sigma-Aldrich, St. Louis, MO), and Recombinant Human IFN- γ 10 ng/mL (PeproTech,

Rocky Hill, NJ). MSC were stimulated for 2 hours at 37°C in a 5% CO₂ incubator with agitation every 30 minutes, then washed with PBS and plated in 24 well plates. Supernatants (for BKA) or cells (for RT-PCR) were collected 24 hours later.

Neutrophil bacterial phagocytosis assay.

Neutrophils were collected from human blood using the Lympholyte®-Poly (Cedarlane Peterborough, UK) separation gradient according to manufacture's instructions. Quantitative phagocytosis over time was performed using the IncuCyte ZOOM® system (Essen BioScience Inc. Ann Arbor, MI). Log phase *S. aureus* cultures were first fixed and stained using the pHrodo™ Red Phagocytosis Particle Labeling Kit (Thermo Fisher Scientific, Waltham MA) according to manufacture's instructions. 500,000 neutrophils were incubated in 24 well plate wells, and *S. aureus* was added at an MOI of 25:1 (bacterial to cells). 9 images per well were collected every 15 ~ 30 minutes using a 10x objective, and analyzed using IncuCyte® S3 Software (Essen BioScience Inc. Ann Arbor, MI).

Neutrophil extracellular trap (NET) assay.

Human neutrophils were plated on Poly-L Lysine (Sigma-Aldrich, St. Louis, MO) coated coverslips (Chemglass Life Sciences LLC, Vineland, NJ) in 24 well cell culture plates, then incubated with BM-MSC CM for 3 hours. After washing off the CM, *S. aureus* was added at an MOI of 1 for indicated time points in HBSS containing calcium, magnesium and autologous human serum. NET staining was performed according to published protocol²² using anti histone H3, and anti-neutrophil elastase (Abcam, San Francisco CA), with slight modifications for staining in a 24 well plate. Images were taken on Olympus IX83 spinning disk confocal microscope, 15 random fields per condition for 3 different neutrophil donors. NET area was

calculated using ImageJ ²³; NET area (in pixels) was determined by overlapping channel 2 and 3 pixels which represent Histone H3 and Neutrophil Elastase staining, then normalized to DAPI channel area.

Neutrophil intracellular bacterial killing

Fresh neutrophils were incubated with MSC-CM for 3 hours, then plated at 250,000 cells per well in a 96 well flat bottom plate (Thermo Fisher Scientific, Waltham MA) and infected with MRSA at an MOI of 1 in HBSS containing autologous adult human serum, magnesium and calcium. After a 30 minute incubation, surface bacteria was washed away with PBS, and neutrophils were then cultured at 37°C in ambient air for times ranging from 0 min to 2 hours. At the end of each time point neutrophils were lysed with 0.25% saponin (Sigma-Aldrich, St. Louis, MO) in DiH₂O, sonicated and then intracellular bacteria were plated on agar dishes. After 24 hours colonies were counted in each quadrant and converted to CFU.

RT-qPCR Analysis.

RT-qPCR was used to compare mRNA expression of antimicrobial peptides. RNA was isolated using the RNeasy kit (Qiagen, Hilden, Germany) per manufacturer's instructions. The QuantiTect Reverse Transcription Kit (Qiagen, Hilden, Germany) was then used to synthesize cDNA from 1 ug of RNA following the manufacture's protocol. Primers were designed using Primers Primer-BLAST (NCBI); concentrations of 100nM and 200nM were used for forward and reverse primers respectively. iQTM SYBR® Green Supermix (Bio Rad, Hercules CA) was used to detect florescence amplification on a Agilent Mx3000P QPCR System (Agilent Technologies, Santa Clara, CA). Fold change was calculated using ddCT method normalized to untreated controls and housekeeping gene GAPDH. See table 4.1. For Primer sequences

Table 4.1: RT PCR primer sequences		
Gene	Direction	Sequence 5'-3'
Cathelicidin (LL37)	Fwd	GAAGACCCAAAGGAATGGCC
	Rev	CAGAGCCCAGAAGCCTGAGC
Hepcidin	Fwd	CCCACAACAGACGGGACAAC
	Rev	CTCCTTCGCCTCTGGAACAT
Lipocalin (LCN2)	Fwd	GGAGCTGACTTCGGA ACTAAAGG
	Rev	TGTGGTTTTTCAGGGAGGCC
Beta Defensin2 (hBD2)	Fwd	CCAGCCATCAGCCATGAGGG
	Rev	GGAGCCCTTTCTGAATCCGC
Surfactant Protein D (SPD)	Fwd	ACAAAAAGAAACCTGCCATGCT
	Rev	TGGGCATTGTTCTGTGGGAG

S. aureus biofilm assays.

S. aureus (strain MRSA USA300) was grown to log phase in MSC media without antibiotics, then diluted to an optical density reading (O.D) of 0.1. 200 uL of bacteria was incubated at 37°C in ambient air for 72 hours in 96 well flat bottom cell culture plates (Thermo Fisher Scientific, Waltham MA). Inhibition of biofilm formation was tested with replacement of 100uL of MSC-CM at 24 and 48 hours for experimental groups. After 72 hours non-adherent bacteria was washed with PBS, and biofilms were stained with 0.05% crystal violet solution (Sigma-Aldrich, St. Louis, MO). Crystal violet was then dissolved with ethanol and O.D readings were obtained from a microplate reader at 570 nm. To determine if MSC-CM could disrupt fully formed biofilms, MSC-CM was added at 72 hours after initial plating of bacteria (350uL) on glass slides in 24 well plates, and incubated with the fully formed biofilm for times ranging from 2 hours to 24 hours. Live/dead visualization of biofilms was performed using the LIVE/DEAD™ BacLight™ Bacterial Viability and Counting Kit (Thermo Fisher Scientific, Waltham MA) according to manufacture's instructions, and visualized on a Olympus IX83 spinning disk confocal microscope. Ratios were calculated by counting total area of each channel using ImageJ software.

Detection of cytokines by ELISA.

Supernatants were collected from BM-MSC after 24 hours in culture; IL-8 and MCP-1 concentrations were measured according to manufacture's instructions using human DuoSet ELISA (R&D Systems, Minneapolis, MN).

Mesh implant biofilm model.

S. aureus mesh was implanted in nude mice (Charles River Laboratories Japan (CRLJ)) as previously described⁴. Mice were imaged on IVIS in vivo imaging system (Caliper Life

Sciences) every 3 days following tail vein injection of 2×10^6 Poly(I:C) activated MSC mixed with heparin (100 IU/ml). Photon flux was calculated with IVIS Living Image Software. For quantification of bacteria in mouse subcutaneous wounds, the infection site was excised, weighed and homogenized by sonication in PBS. Homogenates were then plated on LB agar 4 quadrant plates (Sigma-Aldrich, St. Louis, MO) in log₁₀ serial dilutions. *S. aureus* colonies were counted and quantified to CFU, 24 hours later.

Statistical analyses.

Statistical comparisons between those data sets with two treatment groups were done using nonparametric t-tests (Mann-Whitney test). Comparisons between 3 or more groups were done using one-way ANOVA, followed by Tukey multiple means post-test. Tests for synergy were performed using a two-way ANOVA. Analyses were done using Prism7 software (GraphPad, La Jolla, CA). For all analyses, statistical significance was determined for * $p < 0.05$.

Results

Human BM-MSc inhibit common wound infection causing bacterial growth in vitro

Methicillin-resistant *Staphylococcus aureus* (MRSA) is a common source of contamination in chronic wounds. MSC produce soluble factors that significantly inhibit MRSA and *E. coli* growth *in vitro* up to 1.5 fold (**Figure 4.1A**). Incubation of 10,000 CFU MRSA with MSC-CM induced a 1.4 fold significant decrease in total bacterial colony count, with a titratable effect (not shown). Undiluted MSC-CM was also able to inhibit MRSA growth at up to 40 MOI (**Figure 4.1B**). In addition to inhibition of MRSA, this killing activity was observed from 3 donor MSCs (male and female), (data not shown). Passage of MSC did not impact killing

activity. Supernatants produced from BM-MSC up to passage 9 also significantly inhibited colony formation of MRSA, with no significant differences between passage 1~9 (**Figure 4.1C**).

MSC act synergistically with antibiotics to enhance in vitro bacterial killing

To test the augmentation of bacterial killing, six different antibiotics at low concentrations as described in the methods were tested in combination with MSC-CM. The results show that 4 of the 6 antibiotics including Cefazolin (Cephalosporin class), Enrofloxacin (fluoroquinolone), Daptomycin (cyclic lipopeptide) and Gentamicin (aminoglycoside) worked in synergy with MSC-CM to produce increased killing of MRSA (**Figure 4.1D**). The two remaining antimicrobial agents, Vancomycin (glycopeptide) and Imipenem (Carbapenem) have an additive killing effect with BM-MSC instead of synergism. (**Figure 4.1E**).

Protein level expression of human BM-MSC

To determine the mechanisms utilized by MSC to directly inhibit bacterial growth, we first examined the expression of AMPs LL37, beta defensin (hBD2), Heparin, Surfactant protein D (SPD) and Lipocalin (LCN) by ICC (immunocytochemistry) and flow cytometry, as these are the most commonly explored AMPs expressed by human stem cells⁵. ICC shows that the expression of these peptides is present in the cytoplasmic region (**Figure 4.2A**). All the AMPs aside from SPD were uniformly expressed as shown by histograms of mean fluorescence intensity (MFI) using flow cytometry. SPD was only present in a few cells and did not show an increased MFI compared to isotype (**Figure 4.2B**).

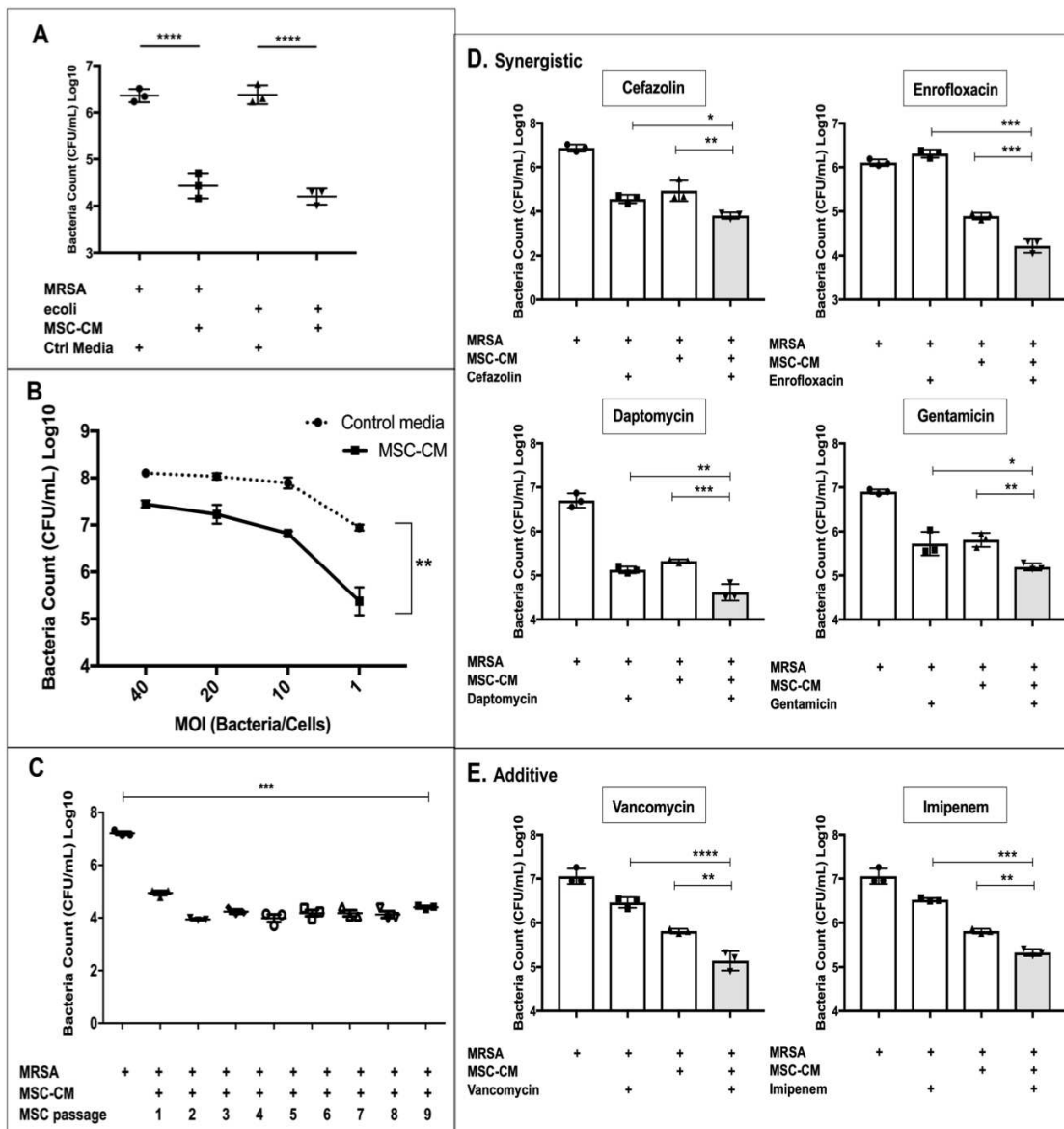


Figure 4.1: Direct Antimicrobial activity of human BM-MSc and interaction with antibiotics in vitro

BKA using supernatant collected from MSC (4.1A) Decreased CFU of *S. aureus* and *E. coli* incubated with MSC conditioned media (CM) Y axis depicts bacterial colony counts (CFU/mL) represented in log scale. (4.1B) MSC-CM incubated with increasing MOI of *S. aureus*. X axis shows decreasing MOI of bacteria/cells, dotted line represents bacterial growth when incubated with control media alone, solid line represents *S. aureus* incubated with MSC-CM. (4.1C) Comparison of bacterial killing on log scale between CM collected at passages 1 to 9 of BM-MSc. (4.1D) Antibiotics that show synergistic activity with MSC-CM. Y axis shows bacterial colonies (*S. aureus*) converted to log scale. Tests for synergy were performed using a 2 way ANOVA, with interaction factor $p < 0.05$ *. (4.1E) Antibiotics that have an additive effect on bacterial killing when combined with MSC-CM. For all figures * denotes $p < 0.05$ as assessed by ANOVA and Tukey multiple means post-test.

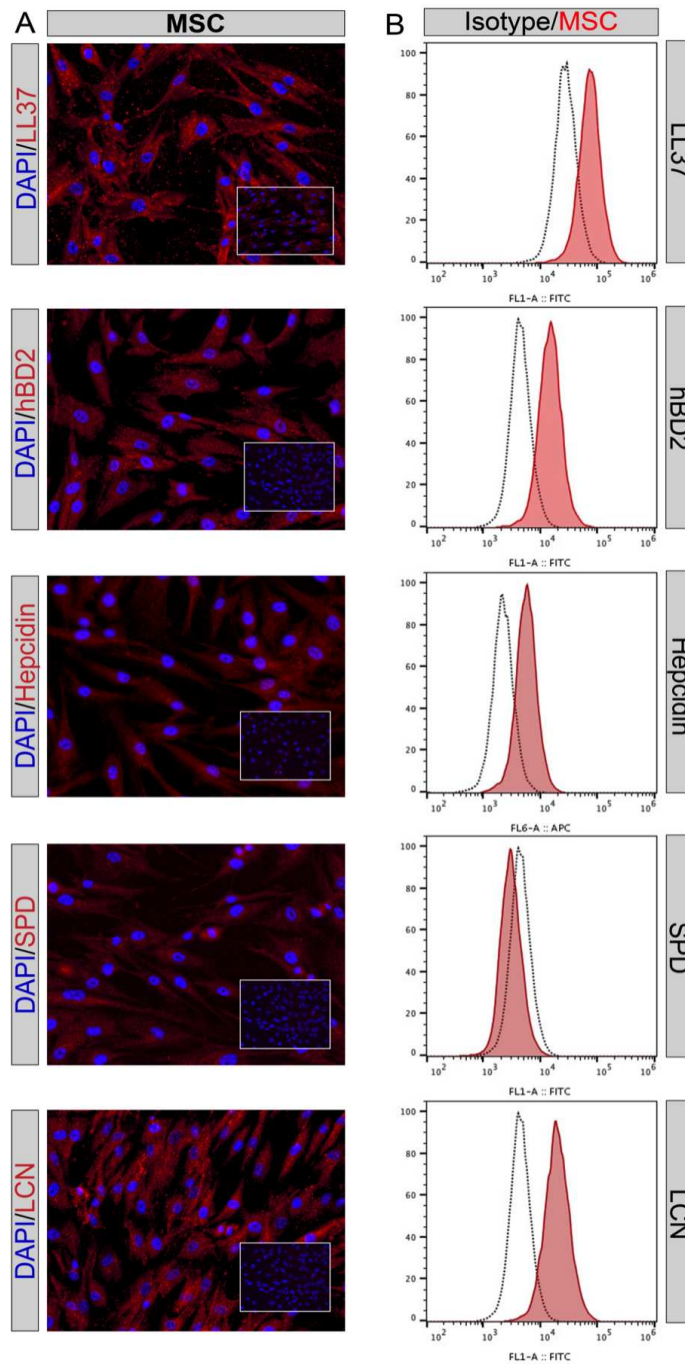


Figure 4.2: Protein expression of antimicrobial peptide by ICC and flow cytometry
(4.2A) Resting BM-MSC stained with AMP antibodies as described in methods. Red shows positive staining for each AMP. Matched concentration negative isotype staining shown in bottom right inset box. **(4.2B)** Histograms of AMP expression by flow cytometry showing mean fluorescence intensity on x axis; isotype control antibody (black dotted line), resting BM-MSC (red). Figures are representative of results seen in 3 donor MSCs.

Activation of TLR signaling pathways changes AMP gene expression and cytokine production

Previous studies have shown that pre-conditioning MSCs increases their immune modulation ability²⁴. To increase the bacterial killing ability as well as AMP production, MSCs were stimulated with various TLR agonists, as well as inflammatory mediators. Upon comparison of all the AMPs tested, including LL-37 (**Figure 4.3A**), beta-defensin 2 (**Figure 4.3B**), Hecpidin (**Figure 4.3C**), surfactant protein D (SPD) (**Figure 4.3D**), and lipocalin (**Figure 4.3E**), we found that CpG oligodeoxynucleotides (CpG ODN), a TLR9 agonist produced the most overall up-regulation of AMPs for 3 MSC donors. The best AMP stimulator CpG was followed by LPS (lipopolysaccharide), a TLR4 agonist. The third most effective AMP stimulator was Poly(I:C) (polyinosinic-polycytidylic acid or PIC), a synthetic analog of double-stranded RNA which activated TLR3 pathways. Incubation of MSC with IFN γ (interferon gamma), an inflammatory cytokine also produced up-regulation in the expression of AMPs, though to a lower degree. We also stimulated MSCs with NOD1 agonist γ -D-Glu-mDAP (iE-DAP); which activates the NF- κ B pathway. However, IE-DAP did not up-regulate AMP expression compared to the negative control isomer (MDP) uramyl-dipeptide (**Figure 4.3F**). In addition to AMPs, we also tested the supernatant for Monocyte chemoattractant protein-1 (MCP-1/CCL2)²⁵ and IL-8, an important regulation factor for macrophage/ monocyte and neutrophil activation/ recruitment respectively.. Over a 24 hour period, un-stimulated MSC produced an average of 449 pg/mL of IL-8, while Poly(I:C) stimulated MSC had the most increase in IL-8 production up to an average of 4089 pg/mL (**Figure 4.3G**). MCP-1 production was also increased the most with Poly(I:C) stimulation, producing an average of 4968 pg/mL compared to un-stimulated 807 pg/mL (**Figure 4.3H**). None of the pre-conditioning measures caused an increase in bacterial killing *in vitro* (data not shown)

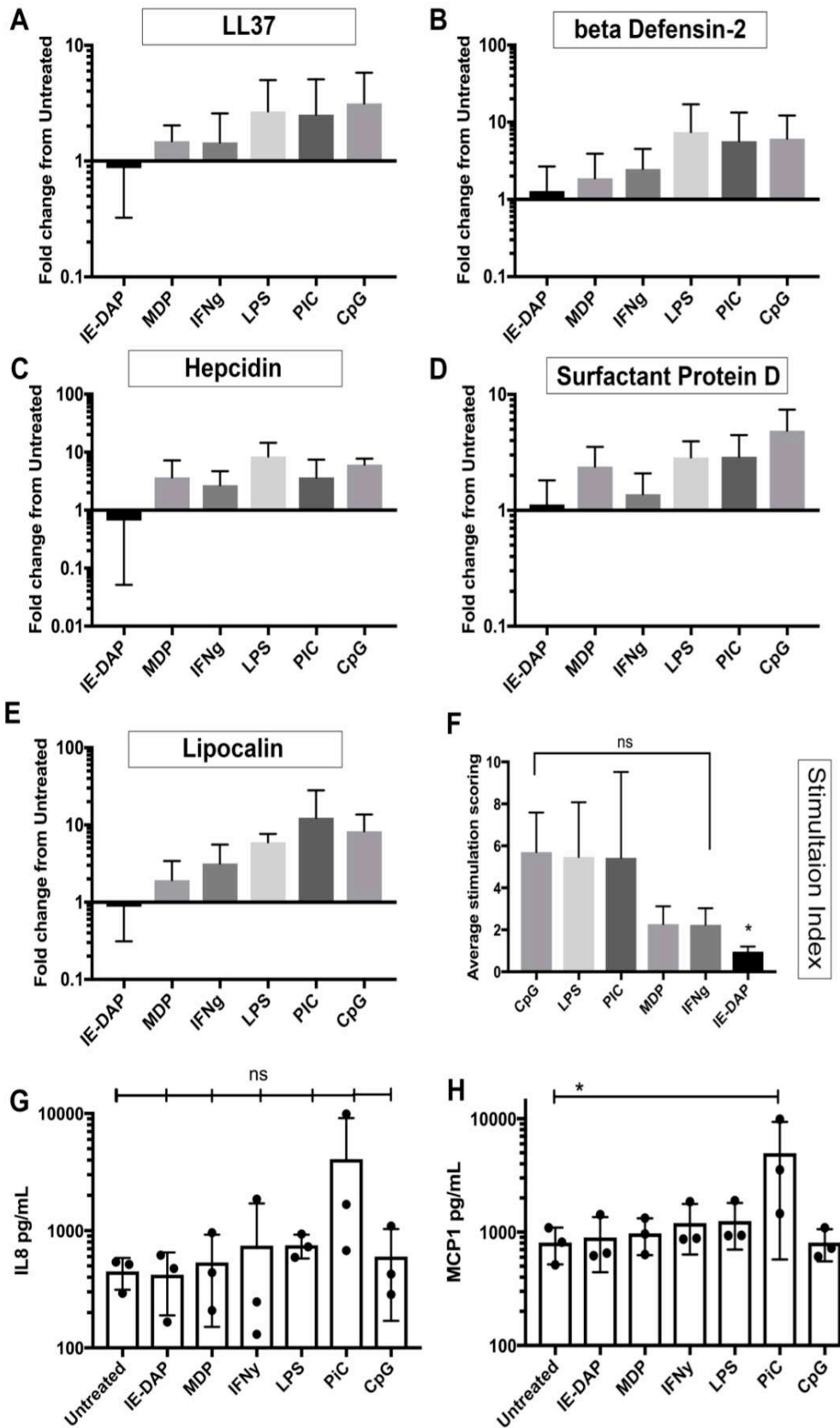


Figure 4.3: Expression of antimicrobial peptides and cytokines after pre-conditioning

Expression of antimicrobial peptides in MSC activated with different ligands as described in methods. Y axis shows fold change in expression, calculated using ddCT method normalized to un-stimulated MSC and housekeeping gene GAPDH. **(4.3A)** Increase in LL37 expression **(4.3B)** beta Defensin2. **(4.3C)** Hecpudin. **(4.3D)** Surfactant protein D. **(4.3E)** Lipocalin. Figures shows average fold change in log scale of 3 technical replicates repeated in 3 donor MSCs **(4.3F)** Simulation index showing average fold changes of 5 AMPS combined, ranked in order of best to least up regulation. **(4.3G)** MSC supernatant collected after 24 hours measured for IL-8 production. **(4.3H)** Supernatant collected measured for MCP-1. Each point on all graphs in represent averages of 3 technical replicated from 3 different donor MSCs.

Secreted molecules by MSC exert killing effect on MRSA within 15 min of co-incubation

In order to examine the bacterial killing mechanisms, flow cytometry was used to stain live and dead bacteria in a time course assay from time 0 (prior to addition of MRSA) to three hour of co-incubation time. Bacterial death was evident at around 15 minutes after addition of MSC-CM **(Figure 4.4A)**. Percentage of dead bacteria continued to increase until reaching a plateau at 2.5 hours, at which time 98% of the culture consisted of dead bacterial fragments. The difference in membrane stain permeability (CYTO9 and PI) was used to visualize the decrease in live bacteria over three hours **(Figure 4.4B)**, as compared to antibiotic free cell culture media, which had greater than 90% viability at the end of the 3 hour co-incubation.

BM-MSC secrete soluble factors that prevent and disrupt biofilm formation in vitro

In addition to killing planktonic bacteria, factors secreted by MSCs also have the ability to disrupt biofilm formation when added continuously to biofilm cultures. Addition of MSC-CM prevented adhesion and formation of MRSA biofilm in culture plates **(Figure 4.4D)**; with a 42% decrease in crystal violet O.D. We also sought to determine if MSC-CM would disrupt pre-formed (72 hours), mature MRSA biofilms. Addition of MSC-CM caused a significant decrease in the live bacteria present in fully formed biofilms **(Figure 4.4E)** as evidenced by the decrease in live/dead florescent ratio from 6.5 to 1.2 and 2.1, respectively. The effects of the MSC-CM persisted up to 24 hours from the time of addition, with a 79% significant decrease in live/dead

florescent ratio (**Figure 4.4E**). The effect of MSC-CM is also apparent visually (**Figure 4.4C**), using the SYTO9 (green) for live bacteria, and PI (red) for dead populations, which when merged becomes a yellow color.

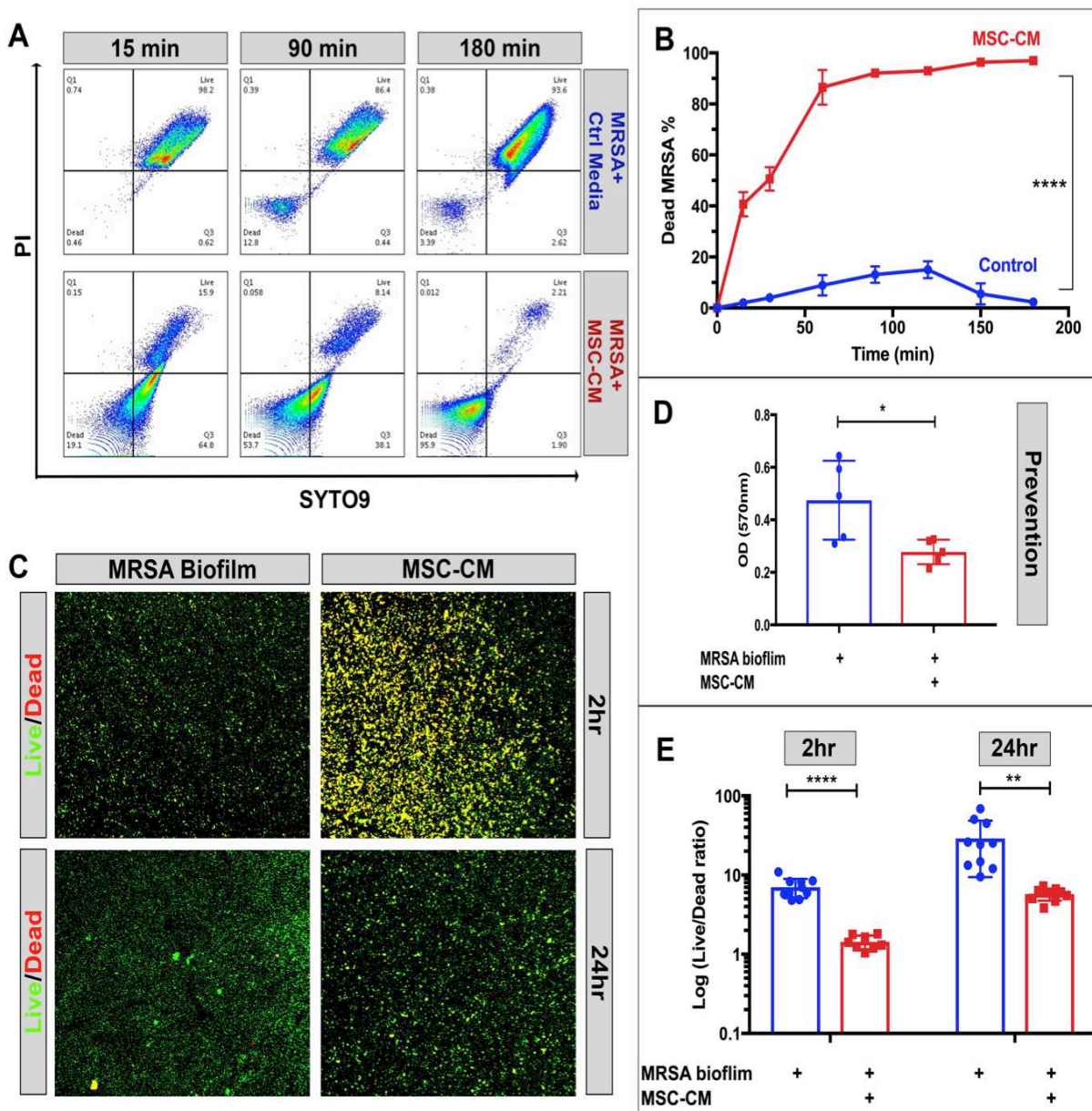


Figure 4: Assessment of planktonic and biofilm bacterial killing

(4.4A) Bacterial killing measured with LIVE/DEAD™ BacLight™ kit by flow cytometry. Representative flow plots from time points 15, 90 and 180 minutes. Dead and live quadrants labeled in bottom left and top right. (4.4B) Percentage of dead MRSA by flow cytometry at different time points, MSC-CM incubated bacteria shown in red, control with media only shown

in blue **(4.4C)** MRSA biofilm stained with LIVE/DEAD™ BacLight™ kit as described in methods. Green (SYTO9) represents live bacterial clusters and yellow represents dead colonies which membrane are penetrated by PI (red) staining. **(4.4D)** Prevention of biofilm adhesion by MSC. Y axis shows Optical density readings of crystal violet stained MRSA biofilms formed in 72 hours, with addition of MSC-CM (red) at 24 and 48 hours. **(4.4E)** Disruption of biofilm by MSC after fully formed for 72 hours. MSC-CM was added after 72 hours and incubated for 2 or 24 hours. Bars show ratio of live vs. dead staining calculated by image J. * denotes $p < 0.05$ as assessed by one way ANOVA and Tukey multiple means post-test. Each test was conducted using supernatants from 3 different donor MSCs, figures are representations of results seen in all 3 donors.

Activated MSC conditioned supernatant increase neutrophil phagocytosis

MSCs decrease neutrophil apoptosis. However, previous reports have not focused on phagocytosis, an important part of bacterial killing mechanisms as well. Using pH dependent fluorescent dye **(Figure 4.5C)**, we show that over a two hour time period, neutrophils exposed to Poly(I:C) activated MSC-CM (PIC treated CM), but not un-activated MSC-CM were significantly augmented in their ability to phagocytize bacteria, with an increase in AUC (area under curve) of 5.3 million uM/well to 8.3 million uM/well red fluorescence of phagocytized bacteria **(Figure 4.5A, 4.5B)**.

Treatment with activated MSC-CM increases neutrophil extracellular trap area

NETs are naturally produced upon contact with bacteria, which traps bacterial particles and increases killing activity. After neutrophils were exposed to Poly(I:C) activated MSC conditioned media, the area of NET increased significantly as shown by double staining of histone H3 and neutrophil elastase **(Figure 4.6B)**. Under high magnification, thin strands of NETs extended between clumps of neutrophils **(Figure 4.6C)**. Significant differences were observed between the control groups and the poly(I:C) pre-conditioned MSC supernatant groups at thirty minutes and two hours after exposure to MRSA. this effect was however not seen in neutrophils treated with un-stimulated MSC-CM **(Figure 4.6A)**

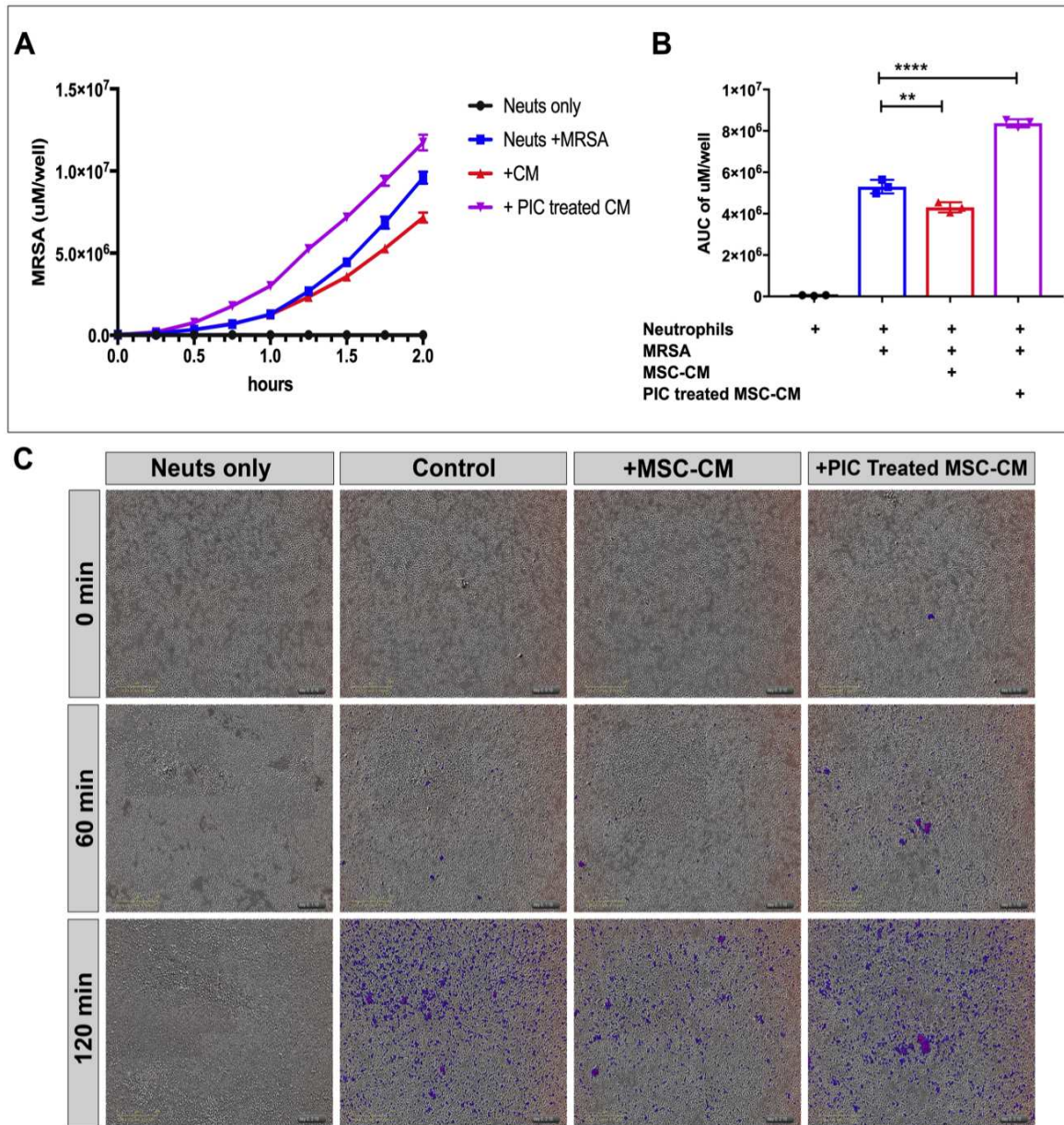


Figure 4.5: Effects of MSC-CM on neutrophil phagocytosis

(4.5A) Neutrophil phagocytosis of MRSA stained with pH red dye, x axis shows time up to 2 hours after addition of bacteria, y axis shows the amount of phagocytosed bacteria represented by an average uM per image as described in methods **(4.5B)** Area under curve calculations of total phagocytosed bacteria over a 2 hour time period. Neutrophils only with no bacteria shown in black, with the addition of bacteria in blue, addition of MSC-CM shown in red, and addition of poly(I:C) treated MSC-CM shown in purple. AUC calculated using Prism 7 column statistics, * denotes $p < 0.05$ as assessed by ANOVA and Tukey multiple means post-test. **(4.5C)** Representative photos from IncuCyte ZOOM® system of 0, 1 hour, and 2 hours after addition of bacteria in each of 4 conditions. Blue color shows pseudo coloring MRSA stained with pH dependent dye which was phagocytosed by neutrophils as analyzed by IncuCyte® S3 Software.

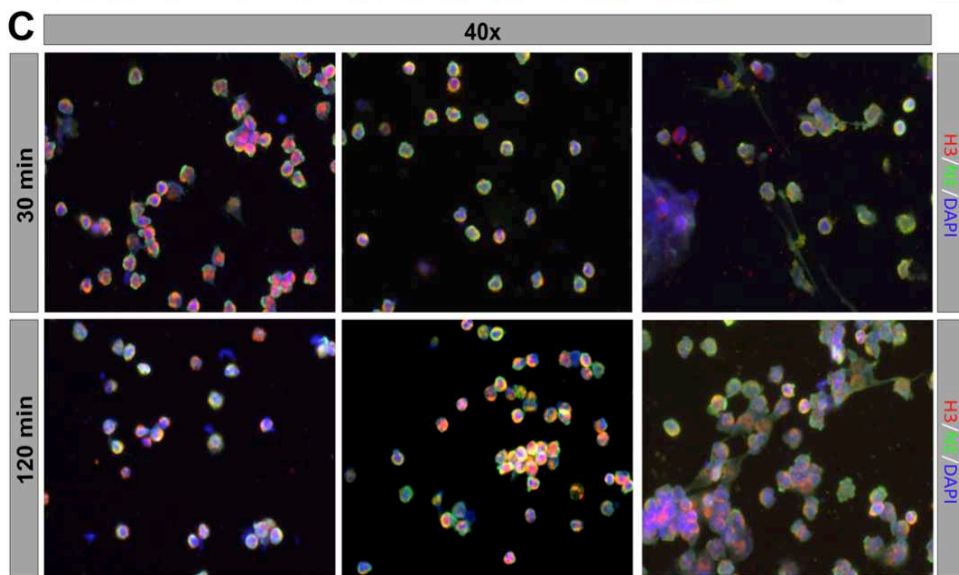
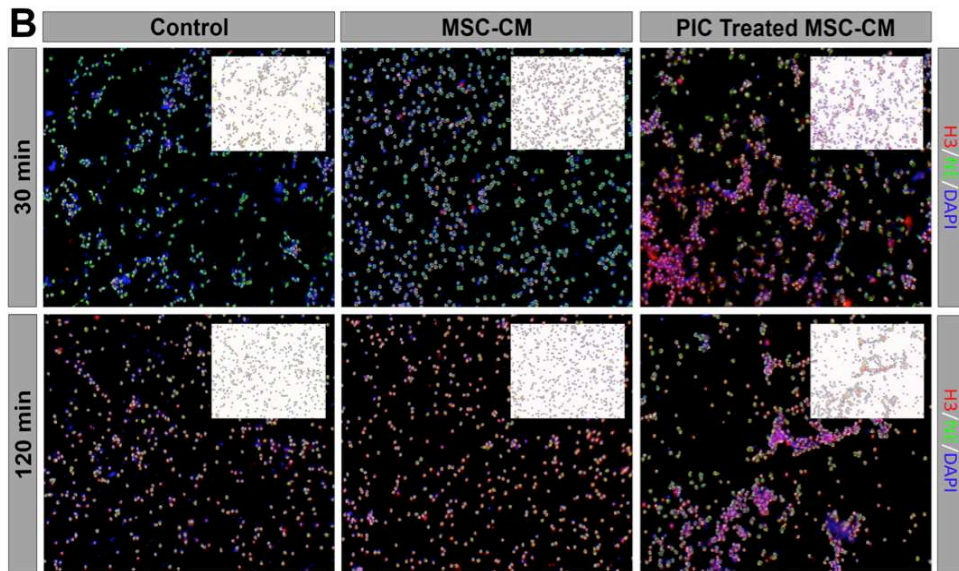
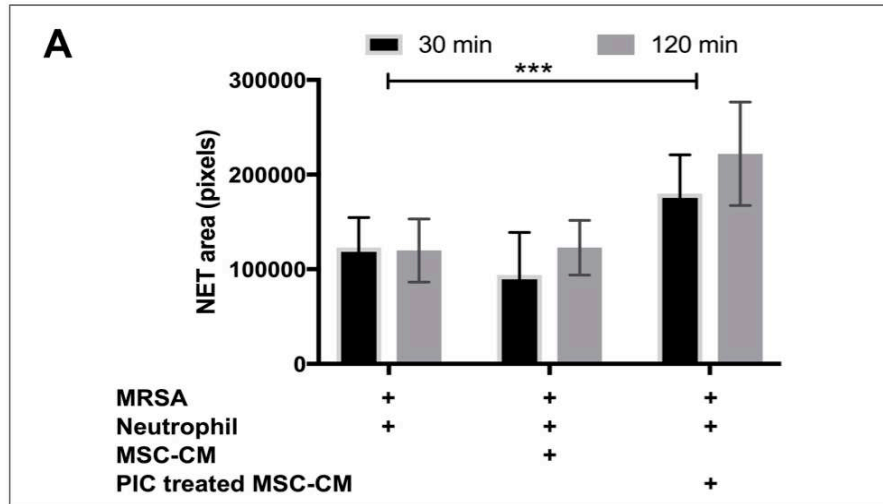


Figure 4.6: Effects of MSC-CM on neutrophil extracellular trap

(4.6A) Total NET area normalized to DAPI cell count, analyzed by image J. Bars show total area at 30min (black) or 2 hours (gray) after exposure to *S. aureus*, *** denotes $p < 0.0005$ as assessed by ANOVA and Tukey multiple means post-test. **(4.6B)** 10x magnification images of release of neutrophil extracellular trap after 30 min (top row) or 2 hours (bottom row) of exposure to MRSA Red, green and blue depict Histone H3, neutrophil elastase, and DAPI staining respectively. Upper right corner shows representative areas of total area of NETs calculated by Image J software, with colors inverted for clarity. **(4.6C)** Representative 40x magnification images of neutrophils under same conditions as described above.

Treatment with activated MSC decrease bacterial burden in a mouse model of chronic biofilm infection.

To determine the efficacy of MSC in an *in vivo* infection model, immune deficient nude mice were implanted with *S. Aureus* coated mesh as previously described ⁴. The bacterial burden at the end of the study was significantly less in the BM-MSc treated group (**Figure 4.7A**). Photon flux of *S. aureus* bacterial luminescence was also significantly lower when comparing AUC for the 14-day trial (**Figure 4.7B**). In addition to the decrease in bacterial colonies and luminescence, the wound area was also smaller in the treated group (**Figure 4.7C**), decreasing from an average of 37.9 mm² to 26.7 mm². There was also less pus within the abscess and more visible mesh outline underneath the skin (**Figure 4.7D**). Visible differences can be seen in representative photos from Poly(I:C) activated MSC treated mice groups as well as control groups

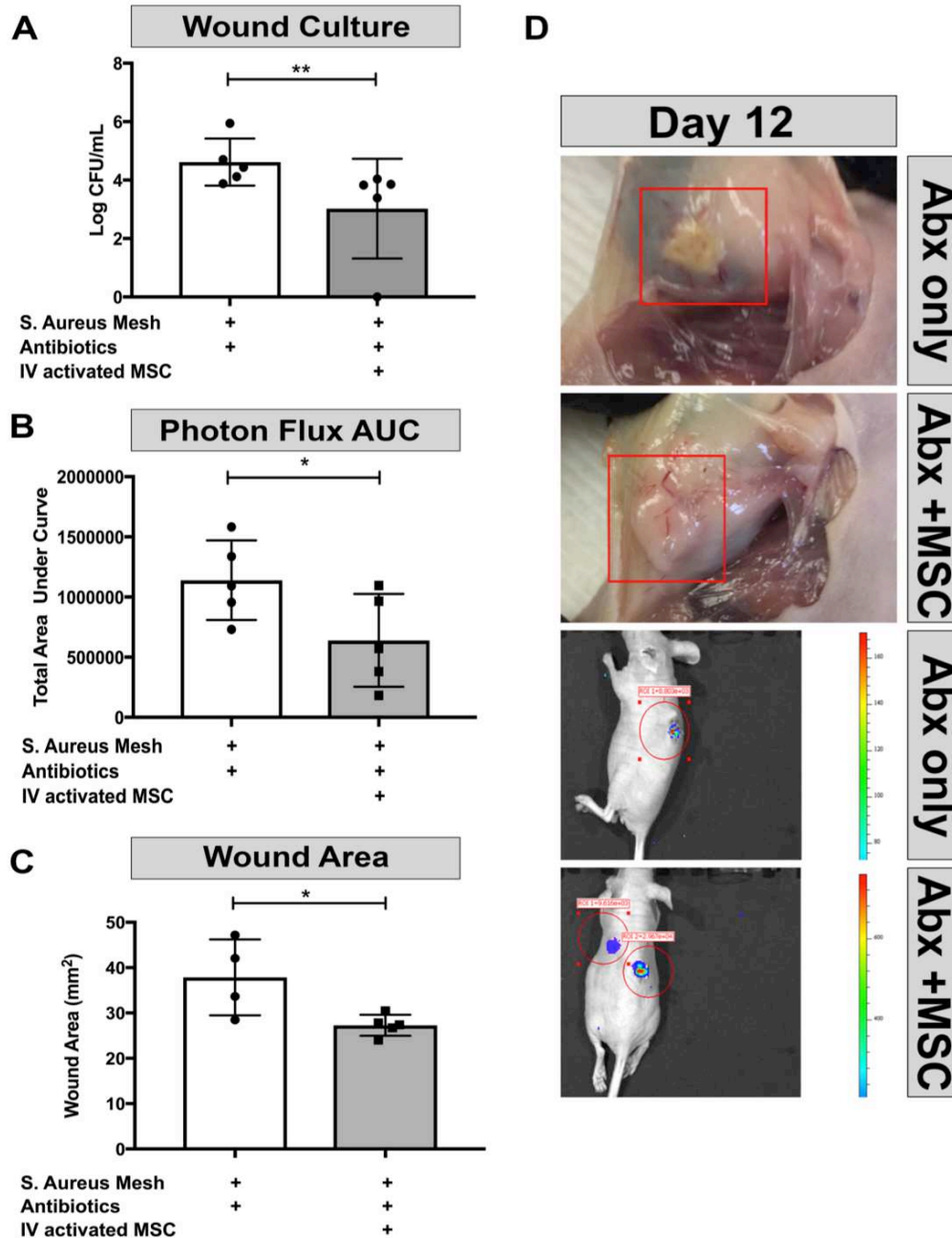


Figure 4.7: Effect of human BM-MSC on chronic biofilm infection in nude mice

Nude mice were implanted with surgical mesh soaked in *S. aureus* as described in methods, with n=5 for each group including antibiotics only and Poly(I:C) activated MSC with the addition of antibiotics (4.7A) Amount of bacteria cultured from implant wounds after 14 day trial, colony counts converted to log (CFU/mL) as described in methods. (4.7B) AUC calculations from photon flux MFI (luminescent bacteria) over a 14 day period. (7C) Wound area (mm²) measured using a caliper, at the end of the 14 day study period. (4.7D) Representative images taken from 1 of 5 mice per group, digital camera pictures shown on top prior to removal of abscess. IVIS imaging (bottom 2) showing photon flux MFI of luminescent bacteria on right bar. * denotes p < 0.05 as assessed by ANOVA and Tukey multiple means post-test.

Discussion

Human primary tissue derived MSCs have been utilized for their anti-inflammatory and regenerative properties for many years²⁶; however, many questions remain open about the mechanisms as well as the variability in donor response. There is also limited knowledge or clinical trials using MSCs in antibiotic resistant biofilm infections, as well as chronically infected implants. In this study, we explored both direct and indirect mechanisms that MSCs utilized to inhibit bacterial growth; our *in vitro* findings support what others have found in multiple species^{5, 27, 28}, soluble molecules secreted by MSCs killed gram positive and negative bacteria. Our novel experiments with *in vitro* biofilms show important implications for clinical studies, where chronic infections are accompanied by mature biofilms that cannot be eliminated with antibiotics. The direct killing ability persisted up to a high passage, which is important due to the limitations of primary tissue derived stem cell life time; the ability to expand MSCs further will allow for multiple patients to be treated from the same donor cells, limiting the treatment variability to produce more consistent improvements in clinical parameters. Chronic infections due to biofilm formation on implants are often treated with high doses of antibiotics²⁹; which are often ineffective due to metabolic and growth phase changes in the deeper layers of the biofilm³⁰. To address the ineffectiveness of antibiotics in chronic infections, Sutton et al.²⁰ showed positive interactions between MSC-CM and Aminoglycosides, as well as Cephalosporins using a mouse Cystic Fibrosis (CF) model. In addition to these two classes of antimicrobials, we also show synergistic interaction between factors produced by MSC and Lipopeptides, Fluoroquinolones, as well as additive bacterial killing ability with Glycopeptides and Carbapenems. Although this *in vitro* data does not fully represent chronic infections in a

biological system, it is still important to recognize the beneficial effects, and the possibility of augmenting antibiotics when treating resistant infections.

One of the most explored direct antimicrobial mechanisms in MSCs are the production of AMPs^{5, 18, 28, 31, 32}. Previous studies have shown the utility of pre-conditioning MSCs with TLR agonists (TLR priming) prior to treatment to ramp up MSC immune modulation for a maximum response²⁴, which triggers enhanced migration and cytokine production³³. Therefore, we sought to investigate the effect of TLR priming on AMP production. We found that although there was an overall up-regulation in gene expression when comparing multiple donors, the protein expression as detected by ICC and flow cytometry was not significant. Priming with TLR ligands also failed to increase bacterial killing, both in suspension and the biofilm model (data not shown). However, the clinical trials in dogs point to increased efficacy when exposing MSCs to TLR-3 ligand Poly(I:C) prior to treatment⁴. Along with previous reports^{24, 34}, this alludes to indirect mechanisms of MSCs that are activated upon priming to enhance bacterial killing *in vivo*. To this end, we investigated the effect of Poly(I:C) primed MSC on neutrophil activity. Increased phagocytosis was apparent in neutrophils only after exposure to activated MSC-CM, not resting MSCs. This was easily visualized and quantified using fixed *S. aureus* stained with a pH sensitive dye that changes color upon internalization. Similar to our results, Brandau et al. showed that neutrophil phagocytosis was enhanced with LPS (a TLR-4 ligand) activated BM-MSC supernatants³⁵, albeit with manual staining and visualization methods. In addition to the reported changes in phenotype and increased survival of neutrophils³⁶, we also found increased NET area after treating with activated MSC-CM, this may be beneficial to skin or implant infections³⁷ since biofilms adhered to implants have the ability to inhibit NET formation and AMP production by neutrophils^{3, 38}. IL-8 which is increased in Poly(I:C) simulated MSC, has

been shown to be responsible for driving NET formation ³⁹, which could possibly be one of the key mediators of the increased NET area. With the increased NET area, we also found that activated MSCs enabled neutrophils to kill more bacteria *in vitro*. However, since neutrophils have a short life span once extracted, the incubation time with MSC-CM was limited to a period of only up to 4 hours. Although this was sufficient to increase phagocytosis and NET area, the bacterial killing was not consistent between multiple donors.

In addition to indirect mechanisms, we also showed an important direct effect of human MSC-CM on fully attached biofilms, an area of study that is lacking in both the treatment of infected medical implant devices, and multidrug resistant bacterial infections. Not only did MSC-CM kill planktonic bacteria within 15 minutes of co-incubation, MSC-CM also prevented the adhesion of bacteria, thus decreasing biofilm load. This has been shown using the same crystal violet assays in the equine model ²⁸.

Furthermore, *S. aureus* biofilms that have already undergone adhesion and colonization can also be disrupted by MSC-CM with inhibition of growth lasting up to 24 hours. Lastly, we showed the efficacy of I.V administered poly(I:C) activated MSCs in a Foxn1^{nu} (nude) mouse chronic implant infection model. The effect of mouse MSC administration has been well documented in this model ⁴; yet, this is the first study to show that human MSCs are also able to promote clearance of infection and bacterial burden. And although we have yet to examine the indirect effects MSCs have on immune cells *in vitro* during chronic infections; the studies mentioned in this manuscript are the first step to gaining the recognition that MSCs might have a beneficial treatment effect for people suffering from long-term antibiotic resistant infections.

REFERENCES

1. Ventola CL. The antibiotic resistance crisis: Part 1: Causes and threats. *Pharmacy and Therapeutics*. 2015;40:277-283.
2. McGuinness WA, Malachowa N, DeLeo FR. Vancomycin resistance in staphylococcus aureus. *The Yale Journal of Biology and Medicine*. 2017;90:269-281.
3. Arciola CR, Campoccia D, Montanaro L. Implant infections: Adhesion, biofilm formation and immune evasion. *Nature Reviews Microbiology*. 2018.
4. Johnson V, Webb T, Norman A, et al. Activated mesenchymal stem cells interact with antibiotics and host innate immune responses to control chronic bacterial infections. *Sci, Rep*. 2017.
5. Alcayaga-Miranda F, Cuenca J, Khoury M. Antimicrobial activity of mesenchymal stem cells: Current status and new perspectives of antimicrobial peptide-based therapies. *Frontiers in Immunology*. 2017;8:339.
6. Bjarnsholt T. The role of bacterial biofilms in chronic infections. *APMIS Suppl*. 2013.
7. Hanke ML, Kielian T. Deciphering mechanisms of staphylococcal biofilm evasion of host immunity. *Frontiers in Cellular and Infection Microbiology*. 2012;2:62.
8. Scherr TD, Hanke ML, Huang O, et al. Staphylococcus aureus biofilms induce macrophage dysfunction through leukocidin ab and alpha-toxin. *Mbio*. 2015.
9. Hirschfeld J. Dynamic interactions of neutrophils and biofilms. *Journal of Oral Microbiology*. 2014;6:10.3402/jom.v3406.26102.
10. Vasandan AB, Jahnavi S, Shashank C, et al. Human mesenchymal stem cells program macrophage plasticity by altering their metabolic status via a pge2-dependent mechanism. 2016.
11. Maqbool M, Vidyadaran S Fau - George E, George E Fau - Ramasamy R, et al. Human mesenchymal stem cells protect neutrophils from serum-deprived cell death. 2011.
12. Rabani R, Volchuk A, Jerkic M, et al. Mesenchymal stem cells enhance nox2-dependent reactive oxygen species production and bacterial killing in macrophages during sepsis. *European Respiratory Journal*. 2018;51.
13. Raffaghello L, Bianchi G Fau - Bertolotto M, Bertolotto M Fau - Montecucco F, et al. Human mesenchymal stem cells inhibit neutrophil apoptosis: A model for neutrophil preservation in the bone marrow niche. *Stem, Cells*. 2008.
14. Sutton MT, Fletcher D, Episalla N, et al. Mesenchymal stem cell soluble mediators and cystic fibrosis. *Journal of stem cell research & therapy*. 2017;7:400.

15. Mahlapuu M, Håkansson J, Ringstad L, et al. Antimicrobial peptides: An emerging category of therapeutic agents. *Frontiers in Cellular and Infection Microbiology*. 2016;6:194.
16. Krasnodembskaya A, Song Y, Fang X, et al. Antibacterial effect of human mesenchymal stem cells is mediated in part from secretion of the antimicrobial peptide Il-37. *Stem cells*. 2010;28:2229-2238.
17. Alcayaga-Miranda F, Cuenca J, Martin A, et al. Combination therapy of menstrual derived mesenchymal stem cells and antibiotics ameliorates survival in sepsis. *Stem cell research & therapy*. 2015;6:199.
18. Gupta N, Krasnodembskaya A, Kapetanaki M, et al. Mesenchymal stem cells enhance survival and bacterial clearance in murine escherichia coli pneumonia. *Thorax*. 2012;67:533-539.
19. Krasnodembskaya A, Samarani G, Song Y, et al. Human mesenchymal stem cells reduce mortality and bacteremia in gram-negative sepsis in mice in part by enhancing the phagocytic activity of blood monocytes. *American Journal of Physiology - Lung Cellular and Molecular Physiology*. 2012;302:L1003-L1013.
20. Sutton MT, Fletcher D, Ghosh SK, et al. Antimicrobial properties of mesenchymal stem cells: Therapeutic potential for cystic fibrosis infection, and treatment; 2016: 12.
21. Lee JW, Krasnodembskaya A, McKenna DH, et al. Therapeutic effects of human mesenchymal stem cells in ex vivo human lungs injured with live bacteria. *American Journal of Respiratory and Critical Care Medicine*. 2013;187:751-760.
22. Brinkmann V, Laube B, Abu Abed U, et al. Neutrophil extracellular traps: How to generate and visualize them. *Journal of Visualized Experiments : JoVE*. 2010:1724.
23. Schneider CA, Rasband Ws Fau - Eliceiri KW, Eliceiri KW. Nih image to imagej: 25 years of image analysis. *Nat, Methods*. 2012.
24. Najar M, Krayem M, Meuleman N, et al. Mesenchymal stromal cells and toll-like receptor priming: A critical review. *Immune Network*. 2017;17:89-102.
25. Deshmane SL, Kremlev S, Amini S, et al. Monocyte chemoattractant protein-1 (MCP-1): An overview. *Journal of Interferon & Cytokine Research*. 2009;29:313-326.
26. Galipeau J, Sensebe L. Mesenchymal stromal cells: Clinical challenges and therapeutic opportunities. 2018.
27. Johnson V, Webb T, Dow S. Activated mesenchymal stem cells amplify antibiotic activity against chronic staphylococcus aureus infection (p5056). *The Journal of Immunology*. 2013;190:180.111.

28. Harman RM, Yang S, He MK, et al. Antimicrobial peptides secreted by equine mesenchymal stromal cells inhibit the growth of bacteria commonly found in skin wounds. *Stem cell research & therapy*. 2017;8:157.
29. Connaughton A, Childs A, Dylewski S, et al. Biofilm disrupting technology for orthopedic implants: What's on the horizon? *Frontiers in Medicine*. 2014;1:22.
30. Hughes G, Webber MA. Novel approaches to the treatment of bacterial biofilm infections. *Br. J. Pharmacol*. 2017.
31. Krasnodembskaya A, Song Y, Fang X, Fang X, Gupta N, et al. Antibacterial effect of human mesenchymal stem cells is mediated in part from secretion of the antimicrobial peptide α -defensin-1. *Stem Cells*. 2011.
32. Sung DK, Chang YS, Sung SI, et al. Antibacterial effect of mesenchymal stem cells against *Escherichia coli* is mediated by secretion of α -defensin-2 via toll-like receptor 4 signalling. *Cellular Microbiology*. 2016;18:424-436.
33. Kaundal U, Bagai U, Rakha AA, Ohoo. Immunomodulatory plasticity of mesenchymal stem cells: A potential key to successful solid organ transplantation. *J. Transl Med*. 2018.
34. Salami F, Tavassoli A, Mehrzad J, et al. Immunomodulatory effects of mesenchymal stem cells on leukocytes with emphasis on neutrophils. *Immunobiology*. 2018.
35. Brandau S, Jakob M, Bruderek K, et al. Mesenchymal stem cells augment the antibacterial activity of neutrophil granulocytes. *PloS one*. 2014;9:e106903.
36. Cassatella MA, Mosna F, Micheletti A, et al. Toll-like receptor-3-activated human mesenchymal stromal cells significantly prolong the survival and function of neutrophils. *Stem Cells*. 2011;29:1001-1011.
37. Johnson CJ, Kernien JF, Hoyer AR, et al. Mechanisms involved in the triggering of neutrophil extracellular traps (NETs) by *Candida glabrata* during planktonic and biofilm growth. *Scientific reports*. 2017;7:13065.
38. Dapunt U, Hänsch GM, Arciola CR. Innate immune response in implant-associated infections: Neutrophils against biofilms. *Materials*. 2016;9:387.
39. Brinkmann V, Reichard U, Goosmann C, et al. Neutrophil extracellular traps kill bacteria. *Science*. 2004;303:1532.

CHAPTER 5

Final Conclusions and Future Directions

Stem cell therapy has been used in clinical trials since the 1950's. In the 1940's hematopoietic stem cells (HSC) were first used in mouse tests in preparation of treating patients exposed to radiation from atomic bombing ¹. The first human bone marrow transplant was performed in 1957, in attempt to treat leukemia patients after extensive chemotherapy ². It was not until much later that other stem cell populations, and more specifically the term "mesenchymal stem cells" was born from the clonal expansion culture studies of HSCs ³. Following many studies in immunodeficient mice using human MSCs, the first clinical trial using culture expanded MSCs was carried out in 1995 ⁴ on patients who had previously undergone bone marrow transplants. By 2011 there were already more than 200 registered clinical trials using MSC for a larger range of conditions ⁵. Yet how is it that, more than 20 years later there are still only a small number of "success" cases. This is restricting the wide spread use of MSCs for cellular therapy that could be advantageous to so many more patients.

In order to benefit more patients who have failed all traditional therapies, there are several directions to take to improve stem cell therapy. The first solution is to target the input cells, which means extensive study of the mechanisms that are involved in how stem cells influence biological systems, and to determine how to improve or select for the best type or donor MSCs. Consequently in chapter 1, we explored immune suppression mechanisms, and studied how different types of MSCs influence T cells and DCs. Using the canine model, which has historically been a very valuable preclinical model for the study of stem cells ^{6,7}, we discovered new pathways such as the adenosine, as well as TGF β signaling and PGE₂ production

that are essential to suppressing T cell activation. We also confirmed that the mechanisms of immune suppression differ between the origins of the MSCs, which is important when determining the most effective type of stem cells based on disease. Although we did discover new MSC pathways that regulate T cell response, cause T cell apoptosis and also discovered that IFN γ production is critical for immune suppression; there are more areas that should be expanded upon to ultimately advance knowledge of MSC cellular therapy. Over the last decade full transcriptome sequencing has become high throughput and much more affordable, along with the development of many new methods of analysis that can accurately detect transcripts with low expression ⁸. In Chapter 2 and 3, we used arrays to explore the differences in transcriptomes between various types of stem cells. To develop *in vitro* models of how MSCs affect immune cells, many functional assays have been completed which look at phenotype, cytokine expression and differentiation of immune cells ^{9, 10}. Therefore, to improve upon our current study, I would propose first an *in vitro* transcriptomics study of a purified T cell population after exposure to MSCs, much like what has been done using *in vitro* systems to explore cross talk between MSCs and endothelial cells ¹¹, or RNA sequencing studies investigating macrophages exposed to MSCs ¹². With the addition of expression and network data, we would be able to discover exactly what is happening to the T cells on a transcription level.

After potentially examining the transcriptome of T cells exposed to MSCs, the functional data that we collected, as well as the transcriptomic data from AD-MSC and BM-MSCs as described in Chapter 2, there would then be a complete picture of how MSCs regulate T cells at a transcript level. With advancements in gene editing technology ^{13, 14}, and the development of high throughput systems to study gene knockouts both in cell lines and live mice ¹⁵, it is possible

to further build upon the pathways discussed in Chapter 2 by conducting a systematic search of protein coding genes that are essential for immune suppression by MSCs. Therefore, the next step after investigating the transcriptome of immune cells exposed to MSCs would be to define a complete list of soluble molecules or ligands that are responsible for functional suppression and bactericidal activity. Currently the complete list of effector molecules include mostly soluble factors TGF- β , NO, IDO PGE₂, HGF, IL-6, IL-8, LIF, MMPs, VEGF, adenosine, TSG6, HO, Gal1, PDGF, ligands and receptors for Notch, HLA-G, CCL2, Fas, PD-L1, and PDL-2; also adhesion molecules ICAM and VCAM ^{16, 17}, and the list is getting more extensive every year. Although a systematic knockout experiment would be lengthy and require large amounts of technical support and financial backing, it would be beneficial for not only advancing the knowledge of stem cell mechanisms, but also for the selection of the optimal donor or cell lines to use for immune mediated diseases.

After completing the mechanistic and transcriptome studies suggested above, the next step would be to select or “engineer” an optimal cell type for immune mediated diseases. Many studies have been done to try and improve the functional properties of MSCs, first by developing optimal culture conditions such as media formulation, oxygen concentration, growth substrate and seeding density ¹⁸; and then also by pre-conditioning MSCs with inflammatory stimuli such as IFN γ ¹⁹, pharmacological agents or cytokines ²⁰, as well as priming with TLR agonists ²¹. In addition to improving primary cell derived MSCs, it would also be possible to forgo the inconvenience of a constant selection of new donors, and the possibility of not being able to derive the optimal homogeneous cell population. To this end, in Chapter 3 we explored a pluripotent cell line, canine iPSCs that not only have functions and phenotypic similarities to primary cell derived stem cells; they are also capable of unlimited expansion ²². All of these

characteristics, along with others discussed in Chapter 1 make using iPS cells seem like the holy grail of stem cell therapy. After the derivation of iPS cells in 2006²³, Japan now has several ongoing clinical trials. The first trial was performed in 2014 using iPS derived retinal pigment epithelial sheets in patients with age related macular degeneration²⁴. The transplant was successful in this patient, with no adverse events; the graft was functional after one year, however the overall visual acuity was not improved. The review boards pointed out a multitude of risks for using iPS derived cells in humans including tumorigenicity, genetic mutations, and other contaminations that could arise from the derivation and culturing process²⁵. Ultimately the trial was allowed to proceed, and paved the way for defining guidelines on any future quality control and regulatory procedures when using iPS derived cells. The second trial is also now approved, this time using iPS derived nerve cells to treat Parkinson's disease²⁶. The USA is far behind in this regard, and although the National Institutes of Health have published guidelines on using iPS cell line for research²⁷ clinical trials are not foreseeable in the next few years.

With the advent of yet another iPSC clinical trial on hand in Japan, this makes our studies in the canine model even more valuable for the progress of engineered cellular therapy. In order to advance the understanding of iPS cells with the ultimate goal of replacing primary tissue derived stem cells, in Chapter 3 we explored preliminary *in vitro* immune suppression tests and safety testing on canine iPS derived MSCs (iMSC). Indeed, gene expression data shows that iMSCs might even be superior to primary cell derived MSCs in immune modulation properties. As reviewed in Chapter 1, when comparing data available on iMSCs to adipose or bone marrow MSCs, the clinical trials and experimentation in large animal models is still considerably lacking. In order to advance the knowledge of iMSCs, and also moving towards eventual clinical trials; in Chapter 3 we first performed transcriptomics studies on the iPS and their derived iMSCs, then *in*

vitro functional studies, followed by preliminary safety testing in purpose breed dogs ²².

Although the preliminary studies were thorough, we were only able to generate a single canine iPS cell line. This is mostly due to the low efficiency of transfection rates using the Sendai virus transfection ²⁸, as well as the difficulties in growth factor and early detection antibody cross reactivity to canine cells.

To improve upon the iPS studies in Chapter 3, we have taken some measures in an attempt to address the shortcomings of the iPS derivation and the use of only a single cell line. First, various small molecule inhibitors and growth factors were added to the cocktail during the early stages of transfection; such as ALK5 inhibitor, GSK3 β inhibitor, Histone deacetylase inhibitor, 5-HT receptor agonist and MAPK/ERK signaling pathway inhibitor ²⁹. None of these alone nor the combination of several was successful at generating additional iPS lines. We then experimented with increasing concentrations of growth factors bFGF and LIF, neither increasing the concentration of bFGF up to 10 ng/mL or doubling the LIF concentration generated any colonies from fibroblasts of different donors. We also tested early detection antibodies (SSEA1, SSEA4, Tra-1-81, Tra-1-61³⁰) for cross reactivity, in the hope that iPS colonies were not manually selected for expansion early enough. We determined that unfortunately alkaline phosphatase live staining was the only canine cross-reactive stain that could be used. Failure to generate more iPS cell lines with the Sendai virus system then led us to experiment with non integrating plasmids that could be delivered using electroporation ^{31, 32}.

Around the time of these failed attempts, several reports emerged about using small amounts of peripheral blood to generate iPS cells ^{33, 34}; if successful, blood is a much more accessible source than skin biopsies, and can be routinely collected from any dogs entering the hospital for routine examinations. Therefore, using plasmids containing OSKM factors³⁵ we

transfected fresh PBMCs, along with erythroid and myeloid progenitor cells expanded from collected blood. After multiple failed trials, we determined first that the expansion of erythroid and myeloid progenitor cells in canine PBMCs is inefficient and causes cell death. Next, it is also possible that the canine OSKM factors and human gene sequences do not have enough similarity to activate pluripotency pathways. Consequently, future studies aiming to derive multiple iPSC lines will need plasmids designed specifically to the canine genome. Yet despite these setbacks, the canine model is still a very valuable clinical model that can be used to test iPS cell derived MSCs for immune modulation. For example, we have recently shown in a mouse inflammatory bowel disease model that iMSCs are just as effective as Ad-MSCs in ameliorating inflammation, lesions, and regulating the microbiome ³⁶. Canine IBD shares many pathological similarities with human inflammatory bowel conditions such as immune cell infiltration, gene expression and cytokine production ³⁷; therefore, canine IBD would be a very fitting model to perform the first clinical testing of iMSCs. Once additional canine iPS cell lines are generated, and *in vitro* testing is completed, this could be a major step forward in the direction of using iPS cells in human clinical trials.

In addition to canine MSC studies, we also explored mechanisms of human MSCs in this body of work. Building on the success of clinical trials using MSCs to heal antibiotic resistant wounds in dogs ³⁸; we discussed in Chapter 4 several direct as well as indirect mechanisms of bacterial killing by human bone marrow derived stem cells, in preparation for using MSCs in human patients suffering from chronically infected wounds. Human MSCs have already been shown to increase wound closure, angiogenesis, regulate extracellular matrix and decrease inflammation in wounds ³⁹. Chronic wounds often contain multiple bacterial species that form biofilms and are no longer susceptible to antibiotics ⁴⁰, which makes the healing process more

difficult and often leads to sustained infections for years⁴¹. In order to combat biofilm infections, both on skin surface and on medial implant devices, we first tested human bone marrow derived MSCs and their conditioned media on *S. aureus* biofilms *in vitro*. Although we did find that human MSCs do not have to contact bacteria to inhibit their growth, as well as synergistic interaction with several common classes of antibiotics; there are many more areas that can be expanded upon to understand the direct interaction between MSCs and bacteria. First, we know that MSCs produce AMPs, but there might be other soluble molecules capable of damaging bacterial membranes. For example, Monsel et al. showed that administration of micro vesicles produced by human MSCs significantly reduced bacterial load in mice with *E.coli* induced pneumonia⁴², and increased macrophage phagocytosis. Exosomes produced by MSCs have yet to be used in any *in vitro* biofilm killing assays or implant infection models such as the mesh biofilm infection discussed in Chapter 4.

In addition to exosomes, we could also investigate other soluble proteins produced by BM-MSCs that contribute to bacterial killing. Full proteomic studies have shown that there are at least one thousand proteins that are shared when comparing multiple donor BM-MSCs⁴³, with over 30% residing in the cytoplasm or plasma membrane. Mammalian phagocytic cells produce a class of soluble proteins called peptidoglycan recognition proteins (PGRPs)⁴⁴, which kill bacteria by concurrently causing oxidative, thiol, and metal stress responses in bacteria. To further direct mechanistic studies, we could look for PGRPs in the conditioned MSC media, or perform protein fractionation studies followed by bacteria killing assays to discover additional proteins capable of inducing bacterial death.

After improving upon the direct mechanistic studies, there are many areas that are still ambiguous, most of which involve the influence on immune cells. In Chapter 4, functional *in*

in vitro neutrophil assays were limited to phagocytosis; however increased bacterial killing was never consistently observed between different donor neutrophils incubated with MSC-CM. Other studies investigating neutrophil killing use neutrophils directly extracted from peripheral blood^{45, 46}; however, our studies required pre incubation with MSC-CM prior to exposure to bacteria. The lifetime of extracted neutrophils limits the incubation time before excessive apoptosis occurs, and this may be one of the reasons we did not observe consistent increases in bacterial killing even though an incubation of 2 to 4 hours was sufficient to achieve increased phagocytosis and NET area. It has also been reported that biofilms have the ability to evade immune detection and cause impaired neutrophil activity⁴⁰; therefore we also attempted several *in vitro* experiments to determine if MSC-CM increased neutrophil killing of mature biofilms. However, these experiments also showed no significant effects of MSC-CM, which points to the utility of using *in vivo* systems to investigate neutrophil activity. To build upon the mouse model of chronic biofilm infection study, there are plans to include additional parameters in the next study. For example, Hanke et al. used a Mouse model of *S. aureus* catheter-associated biofilm infection⁴⁷ to investigate how macrophage activation influences the persistence of biofilm on implants. They describe how the administration of M1 microbicidal macrophages attenuate MRSA biofilm infection; however MSCs traditionally induce a M2 phenotype⁴⁸, and yet still promote bacterial clearance in our mouse model of biofilm infection even though M2 macrophages are said to exacerbate the formation of fibrotic capsules that protect the biofilm environment⁴⁹. Therefore, we plan to investigate more thoroughly not only neutrophils *in vivo* but also the effect MSC administration has on resident macrophages in our chronic biofilm infection mesh implant model: including polarization, phagocytic ability, tissue infiltration, and cytokine production.

In summary, these studies describe mechanisms of immune modulation by canine adipose, bone marrow, and also iPS derived MSCs; as well as valuable preclinical safety testing using canine iMSCs. In addition, this work demonstrates novel mechanisms of an indirect antimicrobial activity by human BM-MSCs on neutrophils and also proves the utility of using activated MSCs to treat biofilm infections. These studies add to the existing repertoire of knowledge on the miraculous properties of stem cells, with the hope that in the near future stem cell therapy will become readily available to veterinary patients as well as humans for a variety of immune mediated as well as degenerative or infectious diseases; with the ultimate goal of promoting a prolonged and better quality of life.

REFERENCES

1. Prockop DJ, Prockop SE, Bertoncello I. Are clinical trials with mesenchymal stem/progenitor cells too far ahead of the science? Lessons from experimental hematology. *Stem Cells* (Dayton, Ohio). 2014;32:3055-3061.
2. Thomas Ed Fau - Lochte HL, Jr., Lochte HI Jr Fau - Lu WC, Lu Wc Fau - Ferrebee JW, et al. Intravenous infusion of bone marrow in patients receiving radiation and chemotherapy. *N Engl J Med*. 1957;257:491-496.
3. Caplan AI. Mesenchymal stem cells. *J Orthop Res*. 1991.
4. Lazarus HM, Haynesworth Se Fau - Gerson SL, Gerson SI Fau - Rosenthal NS, et al. Ex vivo expansion and subsequent infusion of human bone marrow-derived stromal progenitor cells (mesenchymal progenitor cells): Implications for therapeutic use. *Bone Marrow, Transplant*. 1995.
5. Wang S, Qu X, Zhao RC. Clinical applications of mesenchymal stem cells. *Journal of Hematology & Oncology*. 2012;5:19-19.
6. Lupu M, Storb R. Five decades of progress in hematopoietic cell transplantation based on the preclinical canine model. *Veterinary and comparative oncology*. 2007;5:14-30.
7. Hoffman AM, Dow SW. Concise review: Stem cell trials using companion animal disease models. *Stem, Cells*. 2016.
8. Kukurba KR, Montgomery SB. Rna sequencing and analysis. *Cold Spring Harbor protocols*. 2015;2015:951-969.
9. Gao F, Chiu SM, Motan DA, et al. Mesenchymal stem cells and immunomodulation: Current status and future prospects. *Cell Death, Dis*. 2016.
10. Kaundal U, Bagai U, Rakha AA-Ohoo. Immunomodulatory plasticity of mesenchymal stem cells: A potential key to successful solid organ transplantation. *J. Transl Med*. 2018.
11. Li J, Ma Y, Teng R, et al. Transcriptional profiling reveals crosstalk between mesenchymal stem cells and endothelial cells promoting prevascularization by reciprocal mechanisms. *Stem cells and development*. 2015;24:610-623.
12. Bouchlaka MN, Moffitt AB, Kim J, et al. Human mesenchymal stem cell-educated macrophages are a distinct high il-6 producing subset that confer protection in graft-versus-host-disease and radiation injury models. *Biology of blood and marrow transplantation : journal of the American Society for Blood and Marrow Transplantation*. 2017;23:897-905.
13. Peng J, Zhou Y, Zhu S, et al. High-throughput screens in mammalian cells using the crispr-cas9 system. *Febs, J*. 2015.

14. Klann TS, Black JB, Chellappan M, et al. Crispr-cas9 epigenome editing enables high-throughput screening for functional regulatory elements in the human genome. *Nat, Biotechnol.* 2017.
15. Brommage R, Liu J, Hansen GM, et al. High-throughput screening of mouse gene knockouts identifies established and novel skeletal phenotypes. *Bone Research.* 2014;2:14034.
16. Nishizawa KS, R. Mechanisms of immunosuppression by mesenchymal stromal cells: A review with a focus on molecules. *Biomed Res Clin Prac* 1. 2016.
17. Poggi A, Giuliani M. Mesenchymal stromal cells can regulate the immune response in the tumor microenvironment. *Vaccines.* 2016;4.
18. Lee MW, Ryu S, Kim DS, et al. Strategies to improve the immunosuppressive properties of human mesenchymal stem cells. *Stem cell research & therapy.* 2015;6:179.
19. Kim DS, Jang IK, Lee MW, et al. Enhanced immunosuppressive properties of human mesenchymal stem cells primed by interferon- γ . *EBioMedicine.* 2018;28:261-273.
20. Hu C, Li L. Preconditioning influences mesenchymal stem cell properties in vitro and in vivo. *Journal of Cellular and Molecular Medicine.* 2018;22:1428-1442.
21. Najjar M, Krayem M, Meuleman N, et al. Mesenchymal stromal cells and toll-like receptor priming: A critical review. *Immune Network.* 2017;17:89-102.
22. Chow L, Johnson V, Regan D, et al. Safety and immune regulatory properties of canine induced pluripotent stem cell-derived mesenchymal stem cells. *Stem Cell Research.* 2017;25:221-232.
23. Takahashi K, Yamanaka S. Induction of pluripotent stem cells from mouse embryonic and adult fibroblast cultures by defined factors. *Cell.* 2006;126:663-676.
24. Mandai M, Watanabe A, Kurimoto Y, et al. Autologous induced stem-cell-derived retinal cells for macular degeneration. *New England Journal of Medicine.* 2017;376:1038-1046.
25. Takashima K, Inoue Y, Tashiro S, et al. Lessons for reviewing clinical trials using induced pluripotent stem cells: Examining the case of a first-in-human trial for age-related macular degeneration. *Regen, Med.* 2018.
26. IWAI J. Parkinson's treatment using stem cells enters trials. Available at: <https://asia.nikkei.com/Life-Arts/Life/Parkinson-s-treatment-using-stem-cells-enters-trials>.
27. Barker RA, Carpenter MK, Forbes S, et al. The challenges of first-in-human stem cell clinical trials: What does this mean for ethics and institutional review boards? *Stem Cell Reports.* 2018;10:1429-1431.

28. Ban H, Nishishita N, Fau - Fusaki N, Fusaki N, Fau - Tabata T, et al. Efficient generation of transgene-free human induced pluripotent stem cells (ipscs) by temperature-sensitive sendai virus vectors. *Proc Natl Acad Sci, U. S. A.* 2011.
29. Ma X, Kong L, Zhu S. Reprogramming cell fates by small molecules. *Protein & Cell.* 2017;8:328-348.
30. Pomeroy JE, Hough SR, Davidson KC, et al. Stem cell surface marker expression defines late stages of reprogramming to pluripotency in human fibroblasts. *Stem Cells Translational Medicine.* 2016;5:870-882.
31. Okita K, Hong H, Fau - Takahashi K, Takahashi K, Fau - Yamanaka S, et al. Generation of mouse-induced pluripotent stem cells with plasmid vectors. *Nat, Protocol.* 2010.
32. Narsinh KH, Jia F, Robbins RC, et al. Generation of adult human induced pluripotent stem cells using non-viral minicircle DNA vectors. *Nature protocols.* 2011;6:78-88.
33. Zhou H, Martinez H, Sun B, et al. Rapid and efficient generation of transgene-free ipsc from a small volume of cryopreserved blood. *Stem Cell Reviews.* 2015;11:652-665.
34. El Hokayem J, Cukier HN, Dykxhoorn DM. Blood derived induced pluripotent stem cells (ipscs): Benefits, challenges and the road ahead. *Journal of Alzheimer's disease & Parkinsonism.* 2016;6:275.
35. Chou B-K, Gu H, Gao Y, et al. A facile method to establish human induced pluripotent stem cells from adult blood cells under feeder-free and xeno-free culture conditions: A clinically compliant approach. *Stem Cells Translational Medicine.* 2015;4:320-332.
36. Soontarak S, Chow L, Johnson V, et al. Mesenchymal stem cells (msc) derived from induced pluripotent stem cells (ipsc) equivalent to adipose-derived msc in promoting intestinal healing and microbiome normalization in mouse inflammatory bowel disease model. *Stem Cells Transl, Med.* 2018.
37. Cerquetella M, Spaterna A, Laus F, et al. Inflammatory bowel disease in the dog: Differences and similarities with humans. *World Journal of Gastroenterology : WJG.* 2010;16:1050-1056.
38. Johnson V, Webb T, Norman A, et al. Activated mesenchymal stem cells interact with antibiotics and host innate immune responses to control chronic bacterial infections. *Sci, Rep.* 2017.
39. Lee DE, Ayoub N, Agrawal DK. Mesenchymal stem cells and cutaneous wound healing: Novel methods to increase cell delivery and therapeutic efficacy. *Stem cell research & therapy.* 2016;7:37.
40. Bjarnsholt T. The role of bacterial biofilms in chronic infections. *APMIS Suppl.* 2013.

41. Han G, Ceilley R. Chronic wound healing: A review of current management and treatments. *Advances in Therapy*. 2017;34:599-610.
42. Monsel A, Zhu Y-g, Gennai S, et al. Therapeutic effects of human mesenchymal stem cell-derived microvesicles in severe pneumonia in mice. *American Journal of Respiratory and Critical Care Medicine*. 2015;192:324-336.
43. Mindaye ST, Ra M, Lo Surdo JL, et al. Global proteomic signature of undifferentiated human bone marrow stromal cells: Evidence for donor-to-donor proteome heterogeneity. *Stem Cell Research*. 2013;11:793-805.
44. Dziarski R, Gupta D. How innate immunity proteins kill bacteria and why they are not prone to resistance. *Current Genetics*. 2018;64:125-129.
45. Green JN, Winterbourn CC, Hampton MB. Analysis of neutrophil bactericidal activity. In: Quinn MT, DeLeo FR, Bokoch GM, eds. *Neutrophil methods and protocols*. Totowa, NJ: Humana Press; 2007:319-332.
46. Lu T, Porter AR, Kennedy AD, et al. Phagocytosis and killing of staphylococcus aureus by human neutrophils. *Journal of innate immunity*. 2014;6:639-649.
47. Hanke ML, Heim CE, Angle A, et al. Targeting macrophage activation for the prevention and treatment of s. Aureus biofilm infections. *Journal of immunology (Baltimore, Md. : 1950)*. 2013;190:2159-2168.
48. Carty F, Mahon BP, English K. The influence of macrophages on mesenchymal stromal cell therapy: Passive or aggressive agents? *Clinical and Experimental Immunology*. 2017;188:1-11.
49. Hanke ML, Kielian T. Deciphering mechanisms of staphylococcal biofilm evasion of host immunity. *Frontiers in Cellular and Infection Microbiology*. 2012;2:62.